MCNARR SCHOLARS PROGRAM



Montana State University

2016 McNair Scholars Research Journal

Volume III (McNair research conducted between 2013-2016)

Ronald E. McNair Postbaccalaureate Achievement Program Montana State University 405 Reid Hall, PO Box 172560 Bozeman, MT 59717



Production of this manual was made possible through funding by the U.S. Department of Education. Grant # P217A130148



The McNair Scholars Program is a TRiO Program.



McNair Research Journal Montana State University

Volume III Spring 2016

Table of Contents

McNair Program Staff	i
Acknowledgements	ii
Isaac Christensen	1
Optimization of a Protein Purification Process	
Mentor: Edward Schmidt, Ph.D.	
Katie DesLauriers	25
Grandparents Raising Grandchildren: Perceptions on healthy eating, access and	
affordability of healthy foods.	
Mentor: Dawn Tarabochia, Ph.D.	
Josh Gosney	29
Numerical Prediction of Microbubble Attachment in Biological Flows	
Mentor: Jeffery Heys, Ph.D.	
Heidi Hanson	43
A Sustainable Model for Health Programs: A Case Study in Zambia	
Mentor: Wendy Bianchini-Morrsion	
Erica Latorre	54
Effects of Anthocyanin AOX Supplementation on ROS Markers & Metabolic Flexibility	
After a Low-Intensity, Treadmill Exercise	
Mentor: Mary Miles, Ph.D.	
Jaycie Loney	62
Strengths Based Exercise Prescription in the Cancer Community	
Mentor: Lynn Owens, Ph.D.	
Amanda Parsons	83
Formation and Magnetic Resonance Imaging of Alginate Gels	
Mentor: Joseph Seymour, Ph.D.	
Arielle Richard	97
The Kinematics of Slope Style Skiing: Dominant vs. Non-Dominant	
Rotations in Professional, Intermediate & Beginner Level Athletes	
Mentor: John Seifert, Ph.D.	

Michael Ruiz	105
A Test of the Effectiveness of Undiluted Beach Method in Defleshing Human Remains	
Mentor: John Fisher, Ph.D.	
Kelly Walls	110
Characterization of a High Temperature Chlorosilane Corrosion System for Improved	
Polysilicon Production	
Mentor: Paul Gannon, Ph.D.	
Amanda Williams	116
Jacques-Louis David: Classical Forms and Iconography from Rome and Paris	
Mentor: Todd Larkin, Ph.D.	

McNair Program Staff

Principal Investigator David Singel, Ph.D. Associate Provost

Program Director, Co-PI Shelly Hogan, Ph.D.

Administrative Associate Kate Delaney

Acknowledgements

The McNair staff would like to commend the scholars on their pursuit of academic excellence. We would like to express a grateful and sincere thank you to the faculty mentors for supporting the McNair Scholars Program at Montana State University (MSU). Thank you to the Office of the Provost and the Office of the President at MSU.

Optimization of a Protein Purification Process

Isaac Christensen

McNair Scholars Program Montana State University

Mentors: McNair Research Faculty Mentor Edward Schmidt, PhD

ABSTRACT

The goal of the experiment was to express three proteins, Txnip, Txdcn17, and Keap1, in Escheria coli (E.coli) and purify these to use for production of antibodies. The proteins of interest are involved in the Glutathione and Thioredoxin pathways found in nearly all cells, which participate in maintenance of redox homeostasis. Protein purification proved to be difficult for the redox active proteins in this project. The methodology that was used in the effort to obtain these proteins was, first the transformation of E. coli bacteria with DNA plasmids that encode for the expression of three mouse proteins of interest fused to a cleavable affinity tag to support subsequent purification. The second step was the lysis of the bacteria under different conditions to attempt to maintain the proteins of interest in a soluble state. Then the third step involved the use of affinity binding chromatography to "fish" the proteins out of the lysate. The fourth step used dialysis and proteolytic cleavage of the affinity tag to enable purification. The fifth step was the removal of the cleaved tag and concentration of the protein. The final method step was the use of analytical polyacrylamide gel electrophoresis. The results of this project were the purification of two of the proteins, Txndc 17 and Keap 1, as well as progress on optimizing purification of the third protein, Txnip. These proteins were then sent to a commercial facility where they were used to create antibodies in rabbits. These antibodies are currently being analyzed and evaluated such that they can be used for studies on the biology and physiology of these proteins in mice.

INTRODUCTION

The purpose of this research is to express and purify recombinant proteins in bacteria. The three proteins of interest are Thioredoxin Interacting Protein (Txnip), Thioredoxin-like Protein 17 (Txndc 17), and Kelch-like ECH-associated Protein 1 (Keap 1). These proteins will be purified so that they can be used in the creation of antibodies, which will be utilized as an identifier of the respective proteins in mouse cells. Txnip, Txndc17, and Keap1 are involved in regulation of redox homeostasis pathways. Mice currently studied in the Schmidt laboratory contain mutations in key pathways that regulate redox homeostasis including Thioredoxin (Trx1), Thioredoxin Reductase (TR1), and Glutathione Reductase (GR). Previously, it was thought that the absence of these pathways in mouse livers would result in nonviable animals. However, mice with livers lacking TR1, GR, or both TR1 and GR are viable and fertile. In future experiments, identification of expression levels and activities of other redox proteins, including Txnip, Txndc17, and Keap1 will be necessary to be able to better understand the phenotype of these mutant mice. Thus, the antibodies that will be raised against Txnip, Txndc17, and Keap1 will be useful as an identification tool and perhaps in the future allow for better understanding of oxidation/reduction pathways that have been altered in mouse livers lacking Glutathione and Thioredoxin proteins. In the current stage of this experiment, the proteins are being purified either in a native or denatured conformation. Future experiments will cleave and remove protein purification tags before proteins are used for antibody generation.

Materials and Methods

For expression and purification of recombinant proteins, we used the auto-induction technique that was explained in Gustafsson, T.N. et al (2012) "*Bacillus anthracis* Thioredoxin Systems, Characterization and Role as Electron Donors for Ribonucleotide Reductase." J. Biol. Chem. 287, 39686-39697, with the exception that arabinose was omitted from the medium because of the absence of an autolysis strain that was used in the original paper. The reagents used in the experiments were of Molecular Biology or a higher grade.

Auto-induction medium preparation and the start of overnight cultures

The auto induction medium was created according to the recipe for 2A-medium (auto induction, auto –lysis medium) except for the use of arabinose since the autolysis strain was not available (Gustafsson, T.N., et.al.). The first reagent made was the medium base (10g peptone (Difco, cat. No. 0118-05, Sparks, MD, USA), 20g yeast-extract (EMD, cat. No. 1.03753.0500; Jaffery, New Hampshire), 0.5g MgSO₄ (Fisher Biotech, cat. No. BP213-1; Waltham, MA) x7H₂O (final concentration. 2mM)), these components were dissolved with distilled H₂O and the volume adjusted to 900ml then autoclaved and stored. The second reagent was the 20x Auto-induction mix (23.5g (85%) glycerol (Macron Fine Chemicals, cat. No. 56-81-5; Center Valley, PA), 12g α-lactose (Fisher, cat. No. L5-500; Waltham, MA), 0.3g glucose (Sigma-Aldrich, cat. No. 207-756-2; Lenexia, KS), which had its components dissolved in distilled H₂O and the volume adjusted to 100ml and then autoclaved. A 20x neutralized aspartic acid solution with phosphate-buffer [(8 g L-Aspartic acid (Sigma- Aldrich, cat. No. A93100; Lenexia, KS) and 20g K₂HPO₄ (Fisher Biotech, cat. No. BP362-1)] was created per 100ml of medium with distilled H₂O, the medium was adjusted to the pH of 7.5 with NaOH (J.T. Baker Chemical Company, cat.

No. 5635-02; Center Valley, PA). Equal amounts of neutralized aspartic acid and auto-induction mix were mixed to form 10x auto-induction mix and 10x neutralized aspartic acid+ phosphate, which was then autoclaved.

BL21 (DE3) chemically competent *E. coli* cells were transformed with expression plasmids encoding mouse Txnip (clone#11), mouse Txndc17 (clone#13), or mouse KEAP1 (clone#45). These bacteria had their entire open reading frame preceded by TEV cleavage site sequence of each protein- coding cDNA inserted into the PET 30 B plasmid. Colonies from each plate were used to inoculate 25mL overnight cultures grown at 30°C overnight with 50µg/ml of Kanamycin (Amresco, cat. No. 0408-10G; Solon, OH).

Start of Expression

Two cultures of each of the three protein targets were inoculated with a 50 times dilution of their respective overnight culture. These cultures were grown for 1.5 hours at 37 °C before the temperature was shifted to either 30°C or 20°C. Growth was then allowed to continue overnight while shaking at 220 rpm. MKeap 1 was expressed at a scale of 150ml in a 1-L flask at 20°C and 35 ml in a 250ml flask at 30°C. Then mTxnip and mTxndc17 were both expressed at 35-ml in 250ml flasks at both 30°C and 20°C.

Harvest of cultures

An OD_{600nm} measurement was taken before the cultures were harvested after a 20x dilution in Phosphate Buffer Solution (PBS) [(4g K₂HPO₄ (Fisher Biotech, cat. No. BP362-1), 4g KCl (Sigma-Aldrich, cat. No. P9333; Lenexia, KS), 160g NaCl (EMD, cat.No. sx0420-5; Jaffery, New Hampshire), 23g Na₂HPO₄ (Sigma-Aldrich, cat. No. S7907; Lenexia, KS)]. The amount of culture needed to get the equivalent of 1ml culture OD of 20 was calculated and small-

scale aliquots of each culture was taken to allow for small-scale expression tests and micro scale purification. The small scale cultures were centrifuged and the pellets drained of supernatant and stored at -20°C. The rest of the cultures were harvested by centrifugation in 50-ml Falcon tubes at 5000 rpm for 15 minutes. The pellets were then resuspended in lysis buffer [50mM Tris-HCl pH 8.0 (Sigma-Aldrich, cat. No. 80526; Lenexia, KS), 0.5mg/ml Lysozyme (Sigma-Aldrich, cat. No. L6876; Lenexia, KS), and 1000x dilutions of DNAse1 (Sigma-Aldrich, cat. No. D5025-15K4; Lenexia, KS) and RNAse A (Sigma-Aldrich, cat. No. R6513; Lenexia, KS)] and were stored at -20°C.

Small-scale analysis of expression and micro-scale purification

The expression and solubility of the proteins was checked with an expression test and a micro- scale purification. One pellet from each culture was thawed and 0.7xVolume (700μl) of lysis buffer was used to resuspend the pellets. These cultures were then re-frozen and thawed again. Sonication was then used, after sonication, glycerol, imidazole (Alfa Aesar, cat. No. 288-32-4; Ward Hill, MA), and NaCl were added to yield final concentrations of 5%, 25mM, and 250mM, respectively and samples were taken for analysis of total lysate (T). The volumes were then adjusted to 1000μl. Then the lysates were centrifuged at 13000 rpms at 4°C for 10 minutes. Samples of the soluble (S) fraction were transferred to a new tube and the pellets discarded, these samples of the soluble fraction were saved. Each of the soluble fractions was mixed with 100μl of 50% washed Nickle- NTA agarose (McLAB, cat. No. NINTA-400; San Francisco, Ca) and incubated with inversion for 10 minutes. The agarose beads were then spun down and washed 3 times in 500μl washing buffer (50 mM Tris-HCl pH 8.0, 250mM NaCl, 5% glycerol, 25mM Imidazole). Proteins were then eluted from the columns using 100μl of the above buffer with 10 times more Imidazole (250mM); samples were taken from these eluted fractions. Samples were

obtained from these respective fractions by mixing them 1 to 1 with 2x SDS loading buffer. Finally, the samples were analyzed on a 12% SDS-PAGE gel (BioRad cat. No. 4561049; Hercules, California) with a 20 well comb. The samples consisted of 7µl of (T) and (S) that were loaded in each well, whereas 12µl of Immobilized Metal Affinity Chromatography (IMAC)-elution fractions were loaded.

A new attempt at expression of mouse Txnip, Txndc17, and Keap1

This attempt was very similar to the before mentioned methods. This experiment was done to retry expression at 20°C for all three proteins. Cultures were grown at 30°C in TBG (1% Tryptone (10g/100ml) (Fisher Biotech, cat. No. BP1421-2; Fairtown, NJ), 0.5% yeast extract [(10g/1L), 3.0% glycerol] media with 50µg/ml Kanamycin. 2A medium was inoculated with a 50 times dilution of the respective overnight cultures. MTxnip and mTxndc17 were both used to inoculate 330ml culture in a 2L flask. Then mKeap1 was used to inoculate 3 times 330 ml cultures in 2L flasks with Kanamycin being added at 100µg/ml. The cultures were then grown at 37°C for 1.5 hrs., until they became turbid. The temperature of the incubator was then shifted down to 20°C and set at 230 rpm and growth was allowed for overnight. Frozen stocks were also obtained by transferring 1.5 ml of each culture to another Eppendorf tube and were spun down at 5000 rpm for 5minutes. Each of these pellets was resuspended in 400µl fresh TBG and were mixed with 600µl of 50% sterile-filtered glycerol (final concentration 30% glycerol). These cultures were then incubated on ice for 10 minutes and then were placed at -80°C. The harvesting stage of this experiment was very similar with the use of OD600nm, but a 25-x dilution with medium was used. The other difference was the cultures were harvested via centrifuge and (50mM Tris-HCl pH 8.0, 250mM NaCl, and 5% glycerol) was used as a wash. Then the rest of the harvest was similar to the previous methods.

Preparation of cultures for analysis and test of different conditions for more efficient extraction

Keap1 was found to be in the insoluble fraction and was inefficiently extracted so a variety of extraction conditions was required: Normal extraction, addition of 20mM dithiothreitol (DTT) to the normal buffer, 1% Triton X-100 with 1.5M Urea, and Triton X-100 (Sigma-Aldrich, cat. No. X100-1L; Lenexia, KS), urea, and DTT (Fisher Biotech, cat.No. BP172-25; Waltham, MA). The pellets were removed from the freezer and lysozyme was added to a final concentration of 0.5 mg/ml for each solution. The cultures were mixed with each condition, left at room temperature for 15 minutes, and then frozen again. Once these steps had been finished, the procedure received no changes and analysis could be completed.

Purification and analysis of mouse Txndc17 and Keap1

The purification of mouse Txndc17 and Keap1 were similar in the purification process besides the use of centrifugation and filtration through the use of 1.2µm syringe filters (PALL Corporation, cat. No. DN4618; Port Washington, NY) to clear lysate. The other difference was the use of a Bradford test (Thermoscientific, cat. No. 1856210; Rockford, IL) (30µl Bradford solution mixed with 10µl eluted fraction) that was run on the eluted fractions and fractions were pooled based on these results. The pooled IMAC-elution fractions were stored at 4°C until dialysis.

Dialysis and concentration of mouse Txndc17 and Keap1

The proteins Txndc17 and Keap1 were dialyzed overnight against 2.5 liters of (50mM Tris-HCl, pH 8.0; 5% glycerol; 250mM NaCl) to remove the imidazole. Both of the proteins

were concentrated by using spin-concentrators (Sigma-Aldrich, cat. No. CLS431479; Lenexia, KS) and the concentrations were estimated by using A_{280nm}. The concentrations were found by dividing the absorbance (A) by the extinction coefficients (E) of the proteins.

Test-cleavage of Txndc17 and Keap1 with TEV (Tobacco etch virus) protease

A test digest with TEV-protease was completed. All of the reactions were set up in duplicate with one being incubated at 4° C and room temperature. TEV-protease was then added at final concentrations of $1.7\mu M$ to the Txndc17 sample and $0.71\mu M$ to the Keap1 sample. These samples were mixed with the conditions of: normal buffer, normal buffer with 20mM DTT, and buffer with 0.65M Urea. These samples then were analyzed via SDS-PAGE gel.

Purification of mTxnip and mKeap1

The following methods focused on the purification of previously expressed mTxnip and mKeap1. Extraction of the proteins was attempted in the presence of 1.5M Urea and 1% Triton X-100. The Keap1 sample had Tris (2-carboxyethyl) phosphine hydrochloride (TCEP (Sigma-Aldrich, cat. No. C4706-10G; Lenexia, KS)) added as a reductant because of DTT's effectiveness, but it causes issues when combined with Nickel-columns. Tubes of the two proteins were removed from the -20°C freezer. The contents of the tubes were allowed to thaw just enough to allow the content to be placed in a flask. Each flask had an equal volume (50 ml) of sample and 2x lysis solution (50mM Tris-HCl, pH 8.0, 3M Urea, 2%Triton X-100) were added together. The flask containing Keap1 had a final concentration of TCEP added to it. Once these additions had been made to these cultures, they were sonicated. These lysates were then centrifuged at 15000 rpm for 15 minutes. The lysates soluble fraction was then filtered through a 1.2μm filter and each lysate was divided into two 50ml Falcon tubes. The Ni-NTA agarose was

prepared with an H₂O wash in order to remove ethanol. The agarose was then added to the cleared lysate (1.5ml packed bed volume per 50ml lysate). These mixtures were then incubated at 4°C for 30 minutes with 30-rpm inversion. This agarose slurry was then poured into a column. The column was first washed 10 times with column volumes of (50mM Tris-HCl pH 8.0, 25mM Imidazole, 250mM NaCl, 5% glycerol, 1M Urea, 1% Triton X-100). The second washing step was 30 column volumes of the same buffer without Triton X-100. The proteins were then eluted with the previous buffer with 250mM Imidazole (50mM Tris-HCl pH 8.0, 250mM Imidazole, 250mM NaCl, 5% glycerol, 1M Urea). The elution fractions were collected and a Bradford analysis was conducted in order to pool the fractions. The majority (10ml) of the pools was kept at 4°C and 1.5ml of each was kept at -20°C. The samples were then analyzed through SDS-PAGE gel.

Dialysis and TEV cleavage

Txndc17 was thawed out for TEV-cleavage. While, Txnip and Keap1 were dialyzed for 2 hours against a buffer (containing 50mM Tris-HCl pH 8.0, 0.5M Urea, 250 mM NaCl, 5% glycerol and 0.1mM Ethylenediaminetetraacetic acid (EDTA (Sigma-Aldrich, cat. No. E6758; Lenexia, KS). Then Txndc 17 had additions made to it rather than undergo dialysis. TEV-protease was then added to each dialysis bag to give a final TEV: substrate ratio of 1:25. After an additional 2 hours, the dialysis reaction was moved to 4°C because of precipitation and Txndc17 was left at room temperature. The reactions were allowed to proceed overnight.

<u>Subtractive IMAC and analysis of the whole purification of Txnip, Txndc17, and Keap1</u>

Once overnight dialysis had occurred, it was observed that the bag containing Txnip contained some precipitate. Whereas, Keap1 was almost free of precipitate. Txnip was

centrifuged and the pellet was resuspended in a 1/10 volume (100µ1) 8M urea. Then concentration was attempted on the soluble fraction by mixing equal amounts of 20% Trichloroacetic acid [TCA (EMD Millipore, cat. No. TX1045-1; Jaffery, NH)] in 50% Acetone (Sigma-Aldrich, cat. No. 179124; Lenexia, KS). The mix was allowed to sit on ice for 5 minutes and was then centrifuged. The pellet was then washed once with 100% cold acetone and was resuspended in 100µ1 8M urea. When the sample was mixed with, the loading buffer there was a color change so a few drops of 2M tris-buffer pH 8.0 was added to restore the proteins color. Txndc17 and Keap1 were washed with Ni-NTA agarose equivalent to 0.5 and 0.75 ml packed bed respectively was added to the tubes with the dialyzed proteins. Gentle inversions for 15 minutes at 4°C were used to incubate the mixtures. The next step involved the washing of Txnip and Txndc17 with dialysis buffer. Once extensive washing with dialysis buffer had been completed an elution buffer containing 250 mM Imidazole was applied, with the first 4ml's being collected. The samples were then analyzed through SDS-PAGE gel.

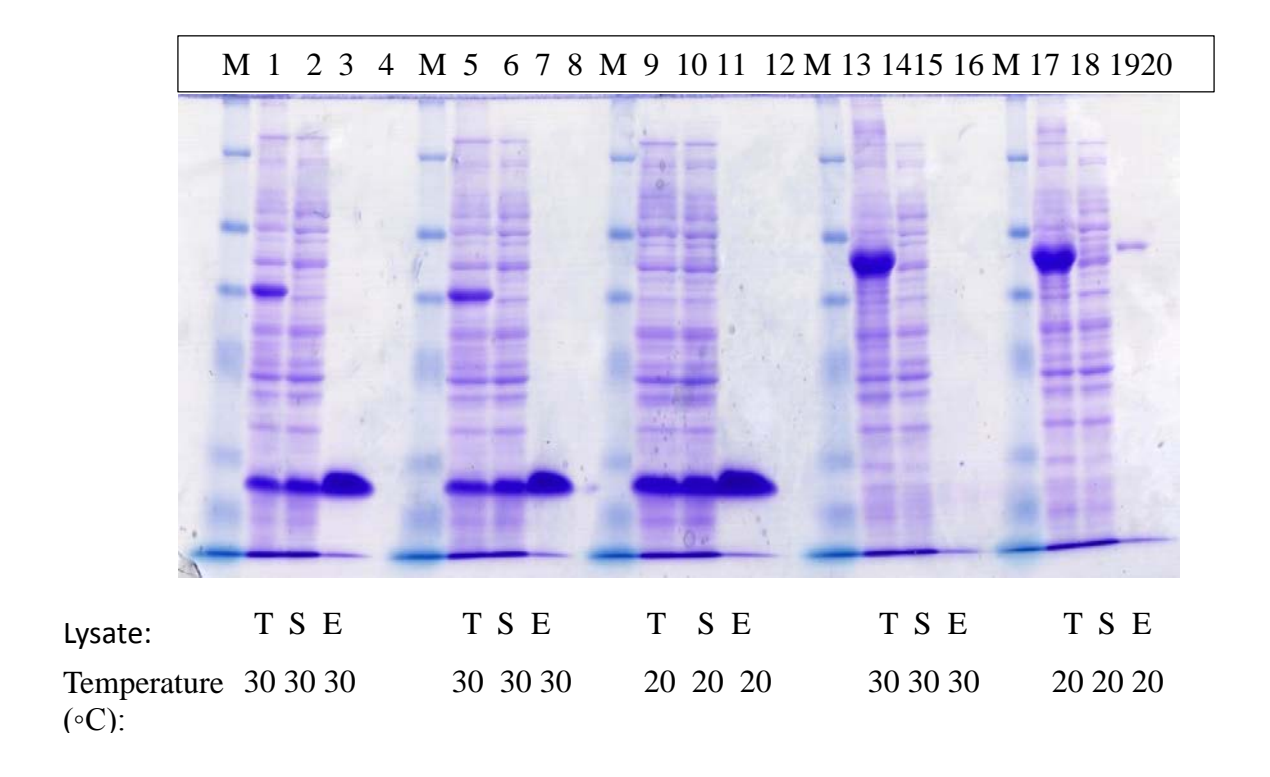


Figure 1.) Analysis of Expression and Solubility in Micro-scale Purification. The gel illustrates an attempt at expression and analysis through micro-scale purification of the mTxnip, mTxndc17, and mKeap1 proteins. Columns (1-4, 7-9, 12-14) contained the protein mTxndc 17, in this analysis mTxnip was lost prior to analysis so Txdcn17 replaced the columns that mTxnip would have occupied. Columns (17-19, 22-24) contained samples of the protein mKeap1. Each protein was separated by their growth under the temperatures of either 20°C or 30°C. Three samples were used for each protein analysis [total lysate (T), soluble fractions (S), eluted fraction (E), and molecular size marker (M)].

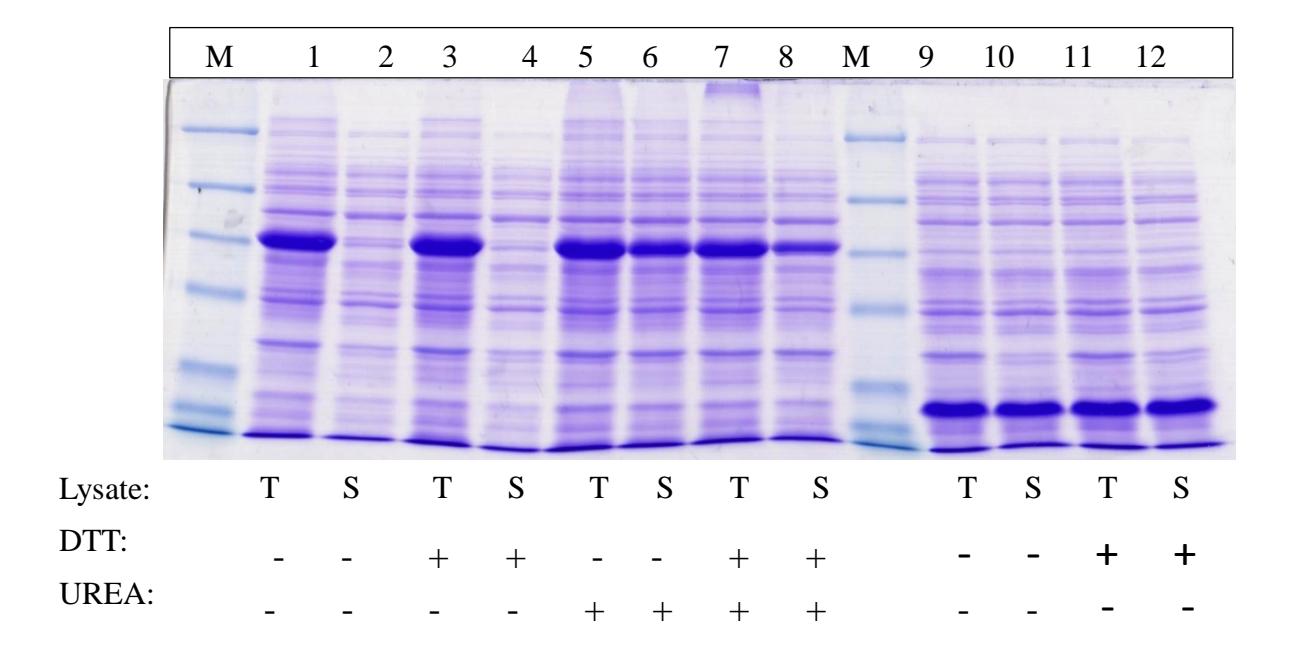
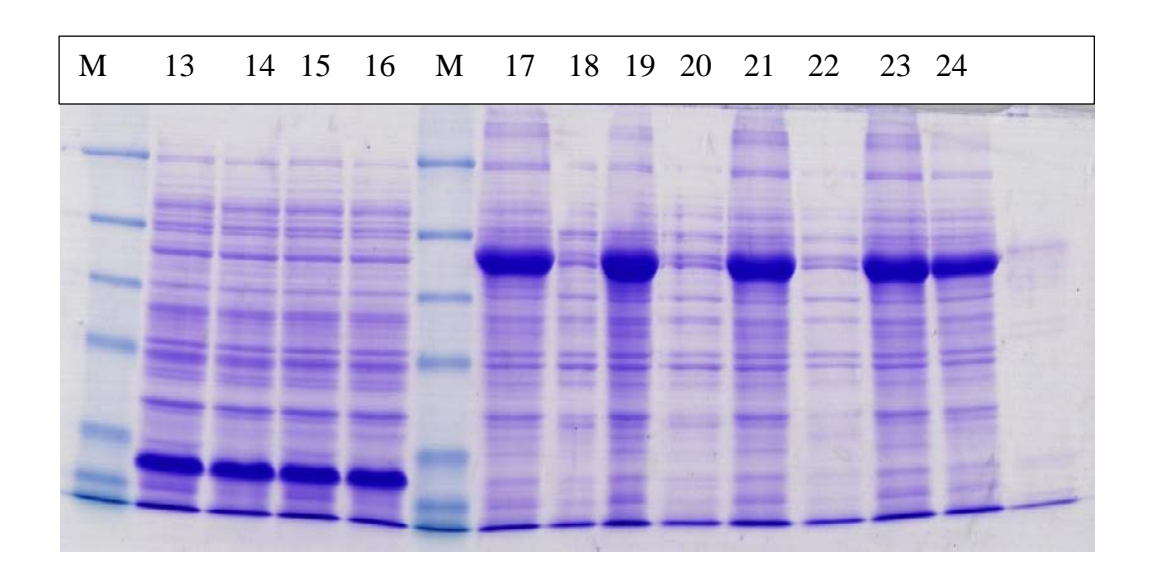


Figure 2.1) **Test of Expression and Solubility of mTxnip, mTxdcn17, and mKEAP1**. Both figure 2.1 and 2.2 is representative of the test solubility of mTxnip, mTxndc17, and mKeap (figure 2.2). The columns containing the specific proteins were Txnip (1-8), Txndc 17 (9-12, 13-16), and Keap1 (17-24). Samples were produced through *E. coli* bacterial expression of the before mentioned mouse proteins. These proteins were pelleted, the re-suspended pellets were then lysed by sonication in lysis buffer (50mM Tris HCl pH 8.0, 1000x-diluted DNAse1 and RNAse A, 0.5mg/ml Lysozyme), and insoluble debris was removed by centrifugation. A sample of the bacterial pellet (T) and of the soluble fraction (S) were boiled with SDS- loading buffer and separated by polyacrylamide gel electrophoresis. Proteins in the gels were visualized by Coomassie staining. The sizes of the three recombinant proteins are indicated by molecular size marker (M). Conditions of the addition of DTT, UREA, both, or no additions were also tested.



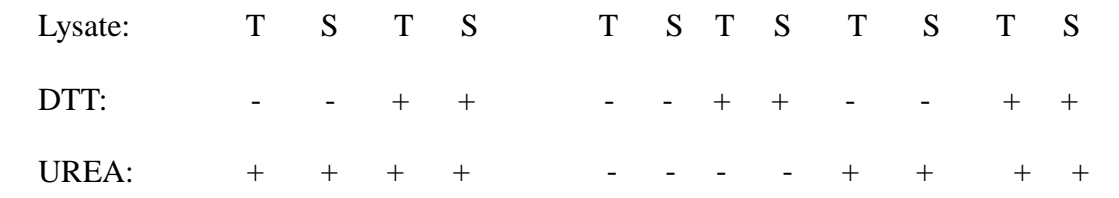


Figure 2.2.) This figure is a continuation of figure 2.1.

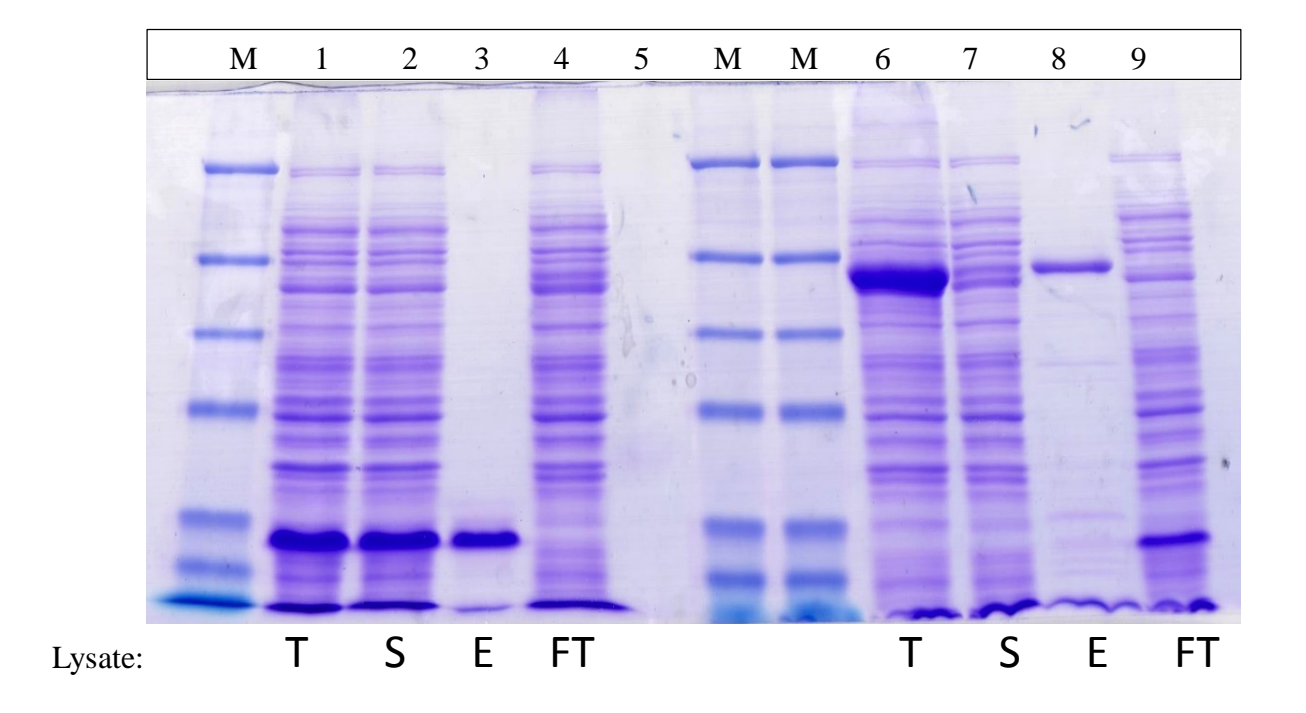


Figure 3.) **Purification of mTxndc 17 and mKeap1.** The proteins represented were mTxndc17 and mKeap1 with samples of the total lysate (T), soluble fraction (S), elution fractions pooled together via results of Bradford Assay (E), and the Immobilized Metal Affinity Chromatography flow through (FT). The samples were oriented mTxndc17 (1-4) and mKeap1 (6-9) and finally two protein markers (M). Once the cultures were sonicated additions of: 50mM Tris-HCl pH 8.0, 250mM NaCl, 5% Glycerol, 25mM Imidazole; were used to bring the final concentrations of the proteins up. The lysates were cleared via centrifugation and 1.3um syringe filter. The cleared lysates were introduced to a 50% slurry of Ni-NTA and then washed with washing buffer (50mM Tris-HCL pH8.0, 250mM NaCl, 5% Glycerol, 25mM Imidazole). After the usage of an elution buffer the eluted fractions underwent a Bradford assay (30µl Bradford solution mixed with 10µl eluted fraction). The fractions were then pooled based on these results.

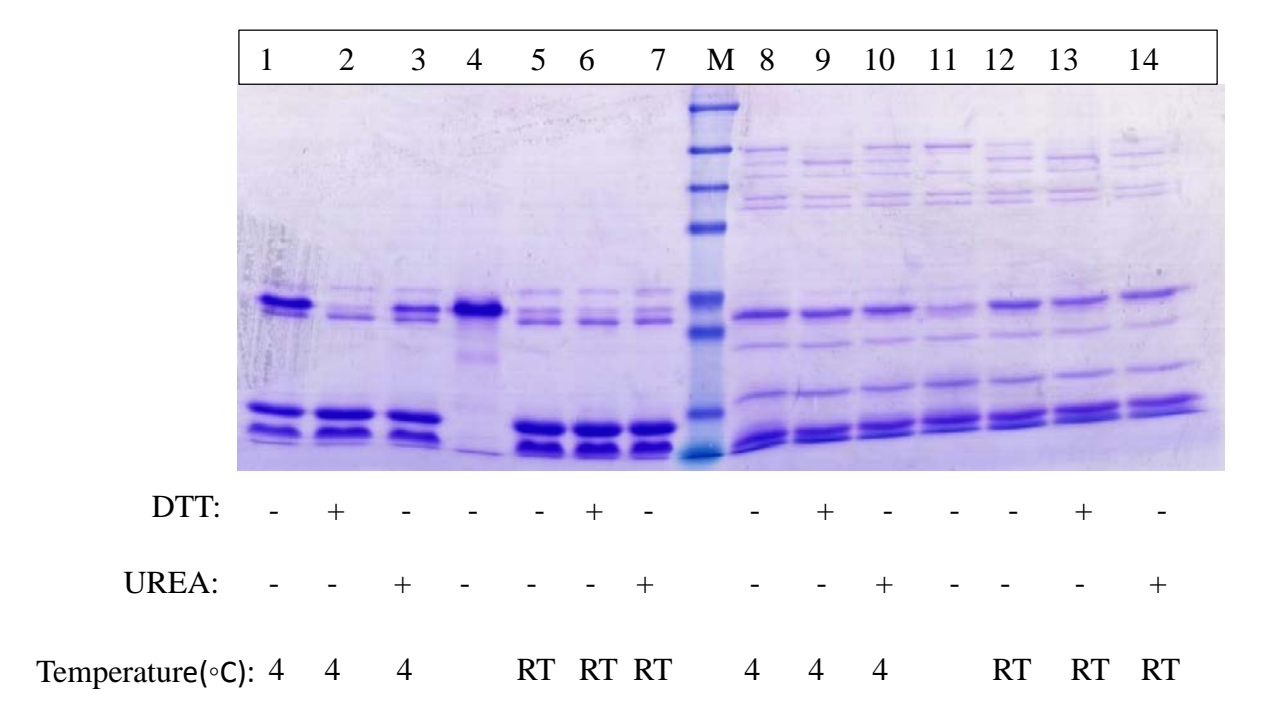


Figure 4.) **TEV-protease test-cleavage of mTxndc17 and mKeap1.** The proteins that were contained in each column were mTxndc17 (1-7) and mKeap1 (8-14). The samples involved the addition of either no addition, Urea, or DTT, while columns 4 and 11 were separate in the use of pure protein un-cleaved and Immobilized Metal Affinity Chromatography- purified protein after concentration respectively. The samples were also varied in the temperature condition they received either 4°C or at room temperature. These samples all underwent dialysis to remove imidazole and were concentrated with the use of spin- concentrators. Then TEV protease was added to these samples and their varied conditions in order to test the digest of these new proteins.

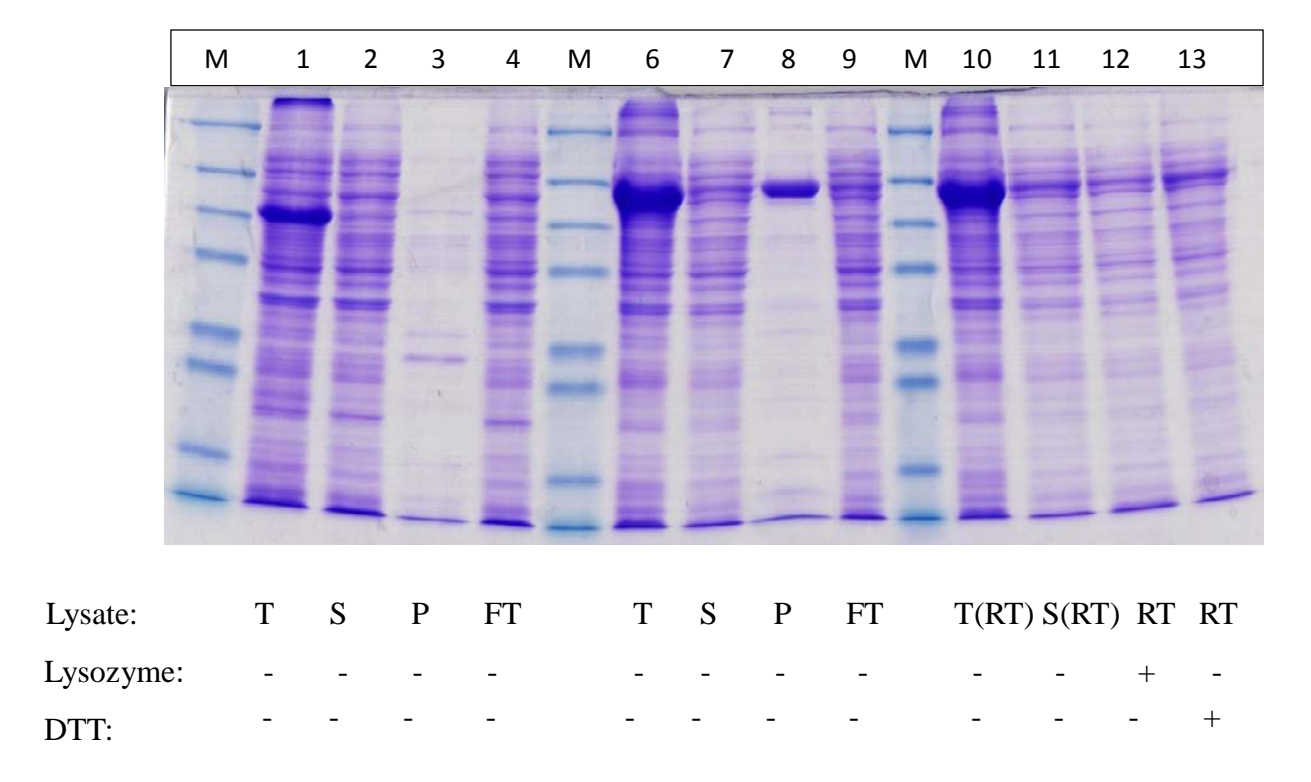


Figure 5.) **Purification of mTxnip and mKEAP1.** The figure shows that protein analysis of the mTxnip and mKeap1 proteins in a larger scale purification process. The difference was some samples were rethawed, some received lysozyme or DTT instead of TCEP. The columns containing mTxnip were (1-4) and mKeap1 were in (7-10). In the gel a total lysate (T), soluble fraction (S), IMAC pool (P), flow through (FT), and re-thawed (RT) samples were used. The RT samples had either no additions or received Lysozyme or DTT.

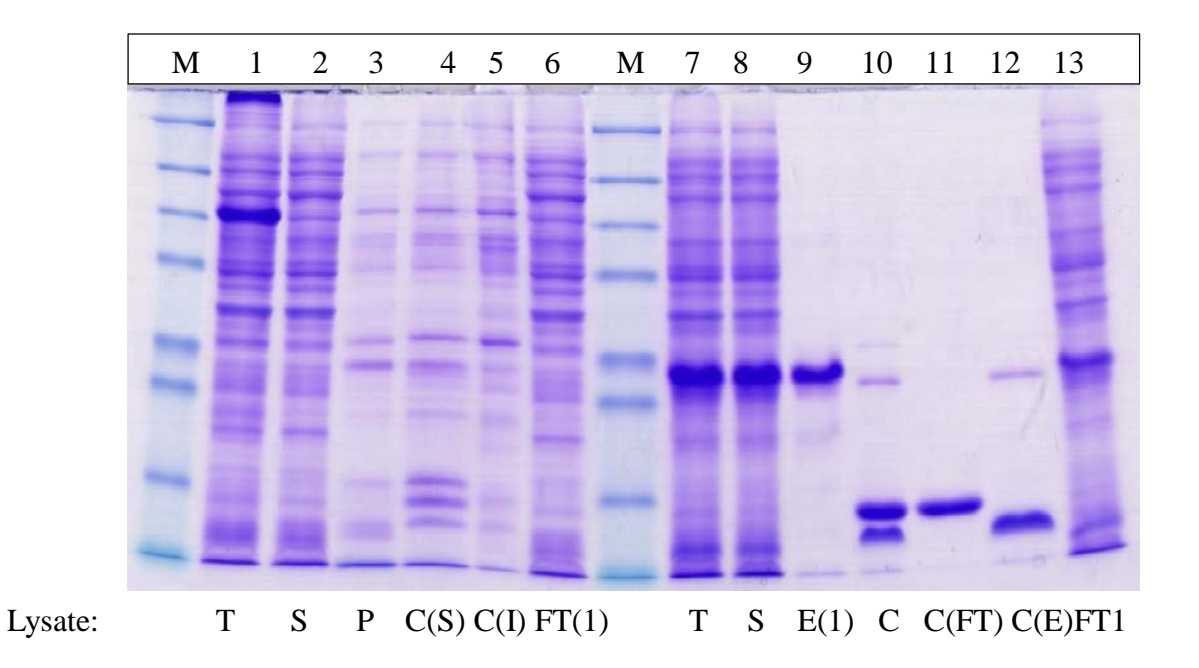


Figure 6.) **Re-analysis of mTxnip and mTxndc17.** The columns were made up of mTxnip (1-6) and mTxndc17 (7-13). The gel shows the use of total lysate(T), soluble fraction (S), IMAC first elution pool row 3 (P), cleaved (soluble) concentrated 5X by TCA precipitation [C(S)], cleaved (insoluble) concentrated 10X by Urea resuspension [C(I)], Flow through first IMAC [FT(1)], Elution from first IMAC[E(1)], cleaved (C), cleaved flow through from subtractive IMAC [C(FT)], cleaved elution from subtractive IMAC [C(E)].

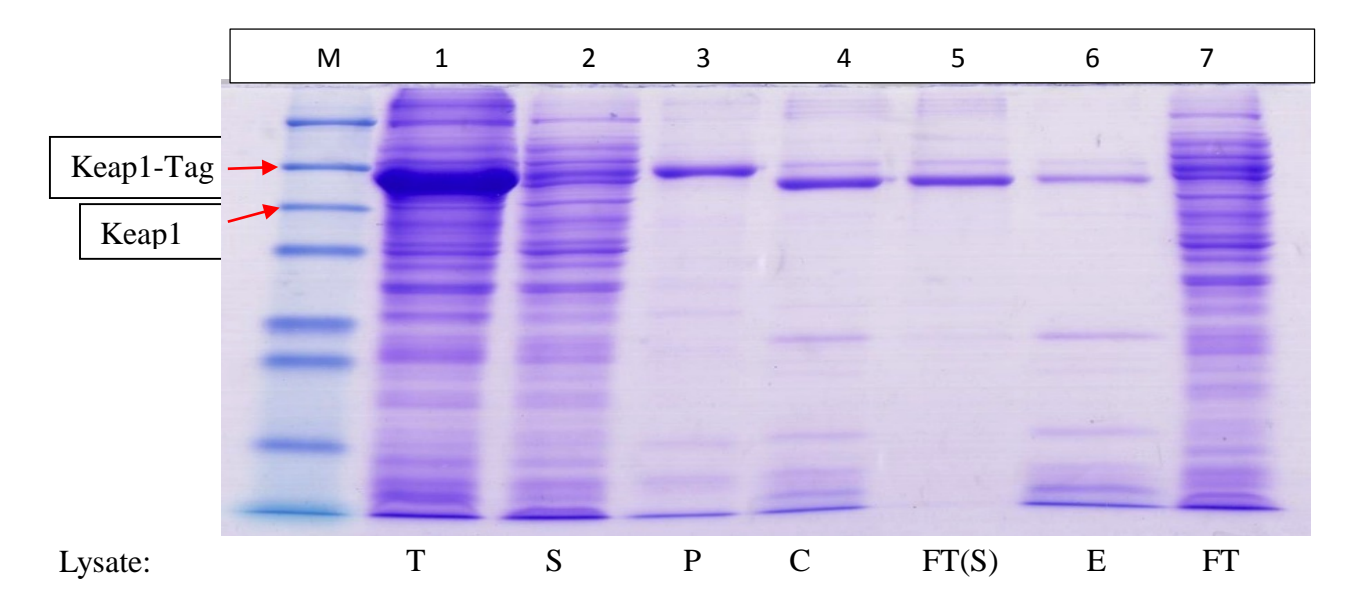


Figure 7.) **Purification of mKeap1 with a Cleaved Sample.** The columns (1-7) were of the mKeap1 protein. The columns contained a total lysate (T), soluble fraction (S), first IMAC pool of elution's (P), cleaved (C), flow through from subtractive IMAC [FT(S)], elution from subtractive IMAC (E), and flow through from first IMAC (FT).

The experiments conducted for the optimization of a protein purification process produced several results. The first of these results can be seen in the SDS-PAGE Gel of the analysis of expression and solubility of the proteins with the use of micro-scale purification in (Figure .1). The results of Figure 1 showed that mTxdcn17 proved to express well with the majority of the protein, being in a soluble form. The 20°C samples proved more successful because of a higher presence of recombinant protein expressed. While, mKeap1 proved to express well at both of the temperatures. The solubility of these proteins was found to be improved slightly with lower temperatures. The second experiment observed the solubility and expression of mTxnip, mTxndc17, and mKeap1 under different buffer conditions. This was done to determine buffer conditions that could positively affect protein extraction. The gel shown in Figure 2-1 and 2-2 showed that mTxnip was insoluble in standard lysis buffer alone or

containing DTT, but became soluble after the addition of urea. Then the addition of both urea and DTT resulted in a diminished yield. Then mTxndc17 was found to be equally soluble under all conditions tested. Then mKeap1 was observed to be only efficiently extracted when a combination of detergent, urea, and DTT were present. The third figure as seen above was an analysis of the purification mTxndc17 and mKeap1 proteins. It was found (Figure. 3) that both of the proteins were mostly pure, although mKeap1 contained some impurities, though a low concentration could be the reason for this result. The next experiment used SDS-PAGE Gel analysis so that the results of test cleavage with TEV protease could be observed. The gel in (Figure. 4) showed this attempt at test cleavage, the results of mTxndc17 cleavage worked well under most all of the conditions with room temperature resulting in almost full cleavage. In the case of mKeap1, cleavage was difficult to observe because of the low concentrations of protein. It can be noted that DTT and room temperature proved to be positive impacts to the cleavage of mKeap1. The next analysis was of the purification, dialysis, and cleavage with TEV protease of mTxnip and mKeap1. The (Figure. 5) shows that the re-thawed lysates appeared to show no improvement and the lysozyme gave way to no band, which it should. The gel also showed that mTxnip only resulted in a faint band at the expected position, then major bands lower down that are most likely contaminants. The next set of results came from the re-analysis of purification for mTxnip and Txndc17 through SDS-PAGE. The gel iuln (Figure. 6) shows that mTxnip purification was not success, while mTxndc17 was found to undergo purification, cleavage, and subtractive Immobilized Metal Affinity Chromatography (IMAC) successfully. The result of the project was the analysis of the purification of mKeap1 protein. The SDS-PAGE gel seen in (Figure.7) showed that purification and cleavage of the His-6 tag were possible for mKeap1 proteins in reasonable quantities.

Discussion

There was a variety of reasons for optimizing a protein purification process centered on the three proteins: Txnip, Txndc17, and Keap1. These proteins had not been purified in the Schmidt Lab before. Therefore, it was necessary to produce a procedure by which these proteins could be expressed and purified so that they could be used in the creation of primary antibodies. The project was successful in producing a purification procedure for both Txndc17 and Keap1 proteins. The protein Txnip proved to be very difficult and it was not possible at the time to develop successful expression and purification procedures for the protein. The issue that complicated the process of developing a method for Txnip protein was the precipitation of the protein out of solution during the dialysis process, perhaps caused by contamination. The other two proteins Txndc17 and Keap1 were both successfully purified. The Txndc17 protein could be successfully purified, cleaved, and undergo subtractive Immobilized Metal Affinity Chromatography; this is illustrated in Figure 7 of the Results section. The procedure specifics that appeared to assist in the expression and purification of the Txndc17 protein was first seen in the micro-scale purification gel Figure 1. This gel evidenced that under the methods used in this process both variants of the experiment provided good expression of the protein with the majority being soluble. The two variants being the growth temperature of either 20°C or 30°C both provided good expression of Txndc17. However, the 20°C condition provided better amounts of the expressed recombinant protein. Keap1 was capable of being expressed at both temperatures. Expression proved to be acceptable, though the solubility's were low with samples at 30°C having no detectable soluble protein, while the 20°C variant produced some soluble protein that could be detected. The Txnip protein samples were lost causing a lack of data for the protein. The next condition test was the usage of urea, DTT, and detergent in an effort to see if

the addition of one or a combination of these reagents would help in the expression and solubility of the proteins. The results of this step of the project can be seen in the gels present in Figures 2.1 and 2.2. These results indicated that Txnip could be extracted efficiently in both conditions with the use of Urea and detergent (Triton X-100), while a lack of DTT appeared to improve the efficiency of extraction. Txndc17 was efficiently extracted in all of the conditions, while Keap1 required a combination of all three additions for efficient extraction. The experiments results observed in Figure 3 provided evidence that Txndc17 protein was easier to manipulate and extract, while Keap1 had lower production and greater impurities in samples. The following test involved both Txndc17 and Keap1, with the variables of normal buffer, buffer with DTT, or buffer with urea either at room temperature or 4°C. The variables tested which had a greater impact in the ability of TEV protease to cleave the His-6 tags of both of the proteins. Txndc17 cleaved well under all conditions, though full cleavage was best at room temperature. In the case of Keap1, it was difficult to visualize the cleavage because of the low protein concentration. However, it is possible though that the protein responded well to room temperature conditions and buffers that contained DTT. Further purification methods for Txnip and Keap1 with the usage of re-thawed lysates showed no improvements for either protein. The gel in Figure 5 showed faint bands because of the low solubility of the target proteins. The final step in the project was to analyze the products of the three target proteins after subtractive Immobilized Metal Affinity Chromatography (IMAC) and total purification. The results of this process can be observed in Figures 6 and 7, where it can be seen that the purification and cleavage of Txnip was not successful with little to no bands produced in the gel. The two successful proteins Txndc17, which could be purified, cleaved, and undergo subtractive immobilized metal affinity chromatography. Then Keap1 protein that could still use improvements in the extraction of the

protein, but currently provides usable quantities of purified protein. In conclusion, an optimized protein purification process was successfully created for two of the three proteins. The future work that will occur from the ability to produce these proteins will be the production of primary antibodies from rabbits. These primary antibodies can be used in a variety of identification methods such as immunostaining, immunohistochemistry, histology, Surface Plasmon Resonance, western blots, and ect. The antibodies produced from this process will also allow for the enhanced study of the function of these redox proteins and their effects on mouse livers, specifically the Redox homeostasis pathway null mice, at the Schmidt Lab. These antibodies will allow for the study of how these proteins are involved in the redox homeostasis pathways of the liver and perhaps provide insight into why these null mice are still viable. The other future project that was created by this project was the continued need of finding a purification process for the mTxnip protein.

Acknowledgements

I would like to thank Edward Schmidt, Ph.D., Justin Prigge, Ph.D., Tomas Gustafsson, M.D., Ph.D., and Emily Talago for their supervision and knowledge provided in the effort to complete this project. I would also like to thank the McNair Scholars Program for their funding and sponsorship (U.S. Dept. of Education grant #P217A130148). I would also like to thank Blake Wiedenheft, Ph.D., for his gift of TEV Protease to the Schmidt Lab for the project.

References

- 1.) Chiang, Peter K., Richard K. Gordon, Jacov Tal, G. C. Zeng, B. P. Doctor, K. Pardhasaradhi, and Peter P. McCann. "S- Adenosylmethionine and Methylation." *The FASEB Journal* 10 (March 1996): 471-80.
- 2.) Gustafsson, Tomas N. et al. "Bacillus Anthracis Thioredoxin Systems, Characterization and Role as Electron Donors for Ribonucleotide Reductase." The Journal of Biological Chemistry 287.47 (2012): 39686–39697. PMC. Web. 4 Aug. 2015.
- 2.) Lu, Jun, and Arne Holmgren. "Thioredoxin System in Cell Death Progression." *Antioxidants & Redox Signaling* 17.12 (2012): 1738-747. *Mary Ann Liebert, Inc. Publishers*. Web. 24 June 2014. http://online.liebertpub.com/doi/full/10.1089/ars.2012.4650.
- 3.) Lu, Shelly C. "Regulation of Hepatic Glutathione Synthesis: Current Concepts and Controversies." *The FASEB Journal* 13 (July 1999): 1169-183. Web.
- 4.) Masterjohn, Christopher. "Glutathione 101, Part 1: Cysteine Misbehaves, But Glutathione Saves." *Weston A Price*. The Weston A. Price Foundation, 7 Apr. 2012. Web. 26 May 2014. http://www.westonaprice.org/blogs/cmasterjohn/glutathione-101-part-1-cysteine-misbehaves-but-glutathione-saves/.
- 5.) Pader, Irina, Rajib Sengupta, Marcus Cebula, Jianqiang Xu, Jon O. Lundberg, Arne Holmgren, Katarina Johansson, and Elias S.J. Arner. "Thioredoxin-related Protein of 14 KDa Is an Efficient L-cystine Reductase and S-denitrosylase." *Thioredoxin-related Protein of 14 KDa Is an Efficient L-cystine Reductase and S-denitrosylase*. Proceedings of the National Academy of Sciences, 8 Apr. 2014. Web. 27 May 2014. http://www.pnas.org/content/early/2014/04/25/1317320111.abstract>.

INTRODUCTION

According to US Census Data there are more than 2.2 million grandparents who identify as the main caregiver for grandchildren (US Census, 2000). Of those grandparents approximately 6,000 reside in Montana. As a rural state, Montana is faced with many challenges regarding the availability and sustainability of services including nutritious food options. In most cases of grandparent's raising grandchildren (GRG) the development of the grandparent's new role is brought about by crisis. The crisis stems from the parents, which may be the result of: death, incarceration, drugs or even teenage pregnancy and other factors. This leaves the grandparents in a position to begin parenting a second time around and further develops levels of exhaustion, stigmas within their community and further inequality amongst the age gap of the grandparent who may have been at the age of retirement (Baldock, 2007). Grandparents also reported a level of satisfaction and rewarding experience when they noted the importance of their new caretaking position and knowing that their grandchildren were safe (Hayslip, Herrington, Glover, & Pollard, 2013). While there was an abundance of information pertaining to a lack of support from services and their peers, there was very little information associated with access, affordability, knowledge and sustainability of support associated with food and nutrition for GRG. The lack of this information resulted in the exploratory nature of this research. Therefore, the purpose of this research project was to explore the availability, knowledge and access to nutritious foods with regard to the age gap between the grandparent and child.

METHODS

IRB approval for this exploratory research project was approved. Through a partnership with the GRG Montana Project, 392 surveys were sent to Montana grandparents who identify as the main caregiver of the household. The survey consisted of 25 questions. The questions were structured as fill in the blank, Likert-like questions, or open-ended questions. The questions on the survey included basic demographics such as grandparent's gender, how long the grandparent has provided care, to how many children, age of the children, and how many meals they provided for their grandchildren. Further questions included probes regarding the grandparent's confidence of understanding nutritional foods, the accessibility and affordability of fresh vegetables and fruits. Likert-like questions were structured to allow three options: 3 = very easy, 2 = easy, 1 = not at all easy. These questions further measured accessibility, knowledge, affordability and sustainability of nutritious foods. Open-ended questions were associated with sample snack and meals, how challenging and how rewarding it was for grandparents to provide meals to their grandchildren. A final open-ended question provided the opportunity for respondents to provide additional information to the research team. An additional question was posed to determine GRG's inclusion in the SNAP (Supplemental Nutrition Assistance Program) program. For those who answered in the affirmative, the participants were asked how much money they spent beyond their budget. Another question regarding budget asked if the grandparents had a time of month when they were not able to afford food and if yes, how often. These results will be disseminated elsewhere.

The results of valid surveys were coded and entered into a database. For the quantitative data, frequencies were used to understand issues associated with knowledge, accessibility, and affordability. The qualitative data for each open-ended question was transcribed verbatim into a word processing document. Content analysis methodology was utilized to identify reoccurring phrases associated with the answers to four open-ended questions. These phrases represented specific themes reported by grandparents. Each member of the two-person research team reviewed and coded the qualitative separately to identify themes. The researchers jointly worked to solidify the themes of the data for each question.

RESULTS

Of the 392 surveys sent to GRG in Montana, 34 were sent back as 'return to sender', 7 were returned invalid because the recipient did not report caregiving for a grandchild under the age of 18, and 42 were deemed valid. The response rate for the returned surveys was 12%. The results of the research indicated that the average number of grandchildren being raised in each household was 2. With grandparents reporting an average of 7.8 years (range = >6 mo. to 7 yrs) of caring for their grandchildren.

Grandparents reported providing on average of 2 meals per day, 3 on weekends. Moreover, grandparents provide on average, 2 snacks during the week and 3 on weekends. Most grandparents reported that it was "very easy" to understand nutritional information (n =28). With regard to access and affordability of fruits and vegetables, most grandparents reported that is was "very easy" (n=17) or "easy" (n=20) to find fresh vegetables and "very easy" (n=20) or "easy" (n=15) to find fresh fruits. However, when asked about the ease of affording fruit grandparents responded that it was "not easy" to afford fresh vegetables (n=15) and "not easy" to afford fresh fruit (n= 17). Thirty-one grandparents reported changing their diet to accommodate their grandchildren, these specific changes are described below.

DISCUSSION

The exploratory nature of the survey design allowed for further questions to arise and direction for future study. The researchers determined that focus groups with the Montana GRG project would allow for more time and an opportunity for the face to face contact to build a relationship and provided the GRG with a foreground in which they can share more about the challenges they face as the custodial guardian of their grandchildren. It was also determined that the development of a guide for GRGs with regard to healthy and cost effective nutritional options would be valuable to this population and also applying a family cooking component to the support meetings where other GRGs can share recipes, food sale information and possibly allowing for family cooking time.

LIMITATIONS

The response rate was low at 12%. This response rate, while lower than hoped for, is not surprising. GRG have limited time and availability to return written survey questions. The research methodology utilized written surveys, which increases the risk of response bias associated with self-reported data. Additionally, the statistical methods available for analysis were limited due to the low return rate (n=42).

CONCLUSION

In conclusion, this study identified a few new avenues for further exploration. The age gap and crisis surrounding grandparents who raise their grandchildren shows a need for further research with regard to nutrition, access and availability.

FUTURE RESEARCH

The purpose of this research project was to explore the affordability and accessibility to nutritional foods in those families headed by grandparents. Based on information obtained through survey data, it has been concluded by the researchers that the topics of access and affordability of nutritious foods, as well as meal preparation should be further researched. The comments from the grandparents were overall supportive and encouraging of further assistance and research. One area of concern that needs further attention is the availability and access to SNAP to help offset the cost of feeding their grandchildren. Further data is needed to understand the complex relationship between access, availability and policies associated with SNAP and why grandparents may be receiving aid. Potential factors include: lack of awareness, complication of the application process, concern for the custody arrangement of the grandchildren or the stigma associated with using public assistance. Several grandmothers reported their generation does not like to ask for help.

Another avenue for future research is to explore another culture of intergenerational families in Greece who regularly provide care and meals for their grandchildren based on a collective culture. Researching these differences would allow the opportunity to cultivate a comparison between cultures specifically associated with two findings presented in the current research project, the challenges and rewards of caring for and feeding grandchildren. As many Montana grandparents comment that sharing a meal with their grandchildren was high on their list of personal satisfaction.

ACKNOWLEDGEMENTS

This work was supported by the McNair Scholars program (U.S. Dept. of Education grant #P217A130148).

REFERENCES

Backhouse, J., & Graham, A. (2010, May). Grandparents raising grandchildren: negotiating the complexities of role – identity conflict. *Child and Family Social Work,* 17, 306 – 315.

Baker, L. A., & Silverstein, M., (2008, October 12). Depressive symptoms among grandparents raising grandchildren: The impact of participation in multiple roles. *Journal of Intergenerational Relationships*, 6:3, 285 – 304.

Baldock, E. (2007). Grandparents raising grandchildren because of alcohol and other drug issues. *Family Matters*, 76, 70 – 74.

Brintnall – Peterson, M., Poehlmann, J., Morgan, K., & Shlafer, R. (2009, April 3). A web – based fact sheet series for grandparents raising grandchildren and the professionals who serve them. *The Gerontologist*, 49:2, 276 – 282.

Hayslip, B., Herrington, R. S., Glover, R. J., & Pollard, S. E. (2013, November 22). Assessing attitudes toward grandparents raising their grandchildren. *Journal of Intergenerational Relationships*, 11:4, 356 – 379.

Kelley, J., Whitley, D. M., & Campos, P. E. (2010, August 5). Grandmother raising grandchildren: Results of intervention to improve health outcomes. *Journal of Nursing Scholarship*, 42:4, 379 – 386.

Robinson, M. M., & Wilks, S. E. (2006). "Older but not wiser": What custodial grandparents want to tell social workers about raising grandchildren. *Journal of the North American Association of Christians in Social Work*, 33:2, 164 – 177.

Strom, P. S., & Stom, R. D. (2011). Grandparent education: Raising grandchildren. Educational Gerontology, 37, 910 – 923.

United States Census Bureau. (200). *Grandparents living with grandchildren: 2000* [Data file]. Retrieved from http://www.census.gov/prod/2003pubs/c2kbr-31.pdf

Numerical Prediction of Microbubble Attachment in Biological Flows

Joshua Gosney and Jeffrey J. Heys Chemical and Biological Engineering Montana State University-Bozeman Bozeman, MT 59717 joshgosney@gmail.com jeffrey.heys@coe.montana.edu

ABSTRACT

Biofilm infections pose a major threat to human health and are difficult to detect. Microbubbles provide an effective and inexpensive method of detection for biofilm-based infections and other diseases such as cancer. The approach studied here examines the potential of targeted microbubbles, with specific antibodies covalently linked to their surfaces for use as ultrasound contrast agents and drug delivery vehicle. This work presents a novel numerical model for estimating the forces on microbubble conjugates in the vascular system. A full computational fluid dynamics simulation of biological fluid flow and the resulting forces on attached microbubbles is presented as well as comparisons with simplified analytical models. Both the computational and analytical predictions are compared with experimental measurements from Takalkar et al., and Schmidt et al., and these comparisons indicate stable microbubble attachment can be anticipated when the total hydrodynamic force on the microbubble is less than 100 pN. Through the examination of typical biological flows, microbubble attachment can be expected up to an average fluid velocity of $0.025 \frac{cm}{s}$ near the microbubble (i.e., a particle Reynolds number on the order of .001). The Stokes drag law was shown to predict the drag force (the dominant force) on the microbubble within an order of magnitude of the force predicted by the numerical model. Finally, it was found that the lift force on a microbubble was small relative to the drag force, and that the Saffman equation prediction differed from the numerical model by more than an order of magnitude for the biological flows examined.

Keywords: microbubble attachment, ultrasound contrast agent, hydrodynamic force, computational fluid dynamics

INTRODUCTION

The NIH estimates that 80% of all microbial infections are biofilms¹, which pose a significant threat to human health. The additional expenditures caused by biofilm infections are estimated to be \$0.3-\$2.3 billion a year^{2, 3}. The current method for determining the presence of a biofilm-based infection on a medical device or tissue is via microscopy through the use of a scanning electron or optical microscope. While highly accurate, this method of detection is very invasive, usually requiring the removal and destruction of an implanted device or tissue. In a study done by Passerini⁴, 81% of indwelling catheters showed evidence of a biofilm on the surface of the device, but a site swab taken at the dermal entry point only detected bacteria 6% of the time. A potential alternative approach, recently demonstrated through an *in vitro* experiment⁵, utilizes targeted microbubbles as a contrast agent for detecting and imaging biofilm infections. This method of detection would be limited to the outside surface of the catheter as a large acoustic impedance mismatch would disrupt detection of biofilms on the inner catheter surface. The microbubbles bind to the biofilm due to antibodies that are bound to their surface, and the microbubbles are imaged using ultrasound due to the density difference between biological fluids and the gas filled microbubbles. The potential advantages of this system for the detection of biofilm infections include lower costs, avoiding invasive medical device removal, and the potential for earlier biofilm detection.

These same microbubbles targeted at the biofilm could also potentially be used as a treatment delivery platform. Experiments conducted *in vivo* have shown that microbubble destruction via sonication is both an effective delivery method for the delivery of therapy agents and microbubble rupture during sonication could be enough to break up the biofilm. Targeted drug delivery to a location adjacent to the targeted tissue is often sufficient because the therapeutic drugs are often capable of diffusing to the target cells and tissues^{6, 7}. Even without microbubbles, focused ultrasound energy can disrupt and fracture tissue or biofilms, a technique known as histotripsy^{8, 9}. For any of these treatments to be utilized, the biofilm must first be detected.

Conjugated microbubbles were first developed in the 1990's and have provided a new avenue for medical imaging that has not been available in the past $^{10-13}$. The combination of ultrasound imaging techniques and targeted microbubbles is becoming more effective than ever before at detecting diseases that express a target that the microbubbles can bind^{10, 11}. Persistent microbial infections, carcinomas, autoimmune disorders and amyloid plaques have proven to be difficult to detect and treat due to the toxicity and limited effectiveness of most current allopathic treatments¹⁴. A wide range of antibodies are commercially available that can be covalently linked to microbubbles and injected into the bloodstream to detect relevant disease targets and deliver therapeutic agents. For example, it has previously been shown that amyloid plaques could be targeted using biotinylated microbubbles¹¹, squamous cell carcinomas can be targeted with Bleomycin microbubbles⁷, and microbubbles can be targeted to the regulatory receptors that cause Crohn's disease 15. Targeted microbubbles have also been experimentally tested in a flow chamber with results indicating that microbubbles have a predictable, target specific attachment frequency that is a function of the flow rate¹⁵⁻¹⁷. The experiments conducted by Takalkar et al. involved flowing microbubbles targeted to P-selectin through a flow chamber with varying surface densities of Pselectin. The principle result of this paper was that attachment and microbubble accumulation depended strongly on the fluid shear stress and the density of target receptors. Schmidt et al. conducted a very similar experiment, using a NeutrAvidin-coated polystyrene substrate. The observations of this paper indicated that shear from the flow was a major factor in microbubble binding and reversible binding caused by low intensity ultrasound could disrupt binding events. Further, they showed high acoustic pressure could cause microbubble destruction and therapeutic agent delivery.

Contrast agent implementations have been researched for the detection and treatment of carcinomas and atherosclerotic plaque, but little research has been conducted on the detection of biofilm infections using microbubbles^{12, 18-22}. Experiments have shown that microbubbles will bind specifically to *S. aureus* in a closed system, but no estimates have been made about the behavior and attachment potential for microbubbles under common biological flow conditions.

There are two primary objectives for this work. The first objective is to develop a FEM model that estimates the hydrodynamic forces that a microbubble is exposed and validate the model by comparing its

prediction of microbubble attachment to targets with experimental measurements of microbubble adhesion under specific, controlled flow conditions. The second objective is to extend the validated FEM model to examine the potential for microbubble attachment under various biological flow conditions. Finally, the force obtained from the FEM-based numerical model are compared to simple analytical approximations of the force for isolated spheres in idealized fluid flow conditions. The environment of a microbubble in the body is somewhat different from where the analytical expressions are expect to be valid, but the FEM model is used to assess the potential accuracy of the simple, analytical approximation of the force for typical biological flows.

METHODS

For Bovine Serum Albumin (BSA) shelled microbubbles, which are a commonly used type of microbubbles, the average shear modulus for the shell has been estimated to be in the range of 6.6 MPa to 16.9 MPa, depending on the microbubble diameter²³. Based on this estimate and stress-strain calculations for a spherical shell, the microbubbles were assumed to be spherical and rigid for the flow conditions and forces of interest within this paper. The fluids were assumed to be incompressible, Newtonian fluids.

For the geometries and flows of interest here, the microbubbles are assumed to be attached to a surface, and the primary direction of flow is parallel to that surface. Under these conditions, only two components of the three-dimensional force vector were non-negligible: one component is parallel to the direction of flow (the drag force, **Figure 1**) and the other is perpendicular to the direction of flow and normal to the attached surface (the lift force). The buoyancy force was neglected as it is at least two orders of magnitude less than the other forces for normal microbubble sizes and under typical biological flow conditions of interest.

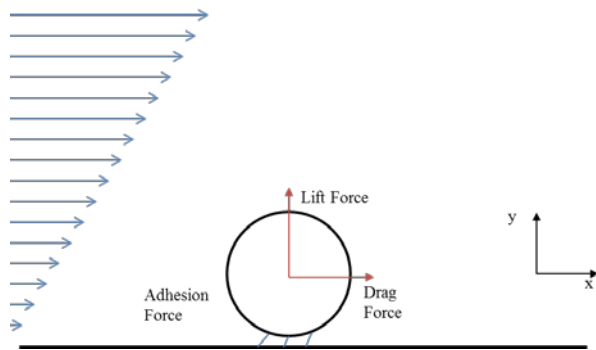


Figure 1:. A microbubble attached to the surface and the forces of interest are shown in a linear flow field (not to scale).

Numerical Model

The main objective of this research is to develop a numerical model that estimates the force on a microbubble under various biological flow conditions and compare these estimates to the analytical model. The numerical studies were conducted using the finite element method to approximately solve the Navier-Stokes equations for incompressible flow²⁴:

(1)
$$-\nabla p + \nabla \cdot \mu [(\nabla u + \nabla u^T)] = \rho (u \cdot \nabla u + \frac{\partial u}{\partial t})$$

(2)
$$\nabla \cdot u = 0$$

where u is the velocity vector, μ is the viscosity, p is the pressure, and ρ is the density of the fluid.

The finite element method was used for the spatial discretization of the Navier-Stokes equations, and the mesh resolutions were varied from 88,762 – 325,000 mixed finite elements (Taylor-Hood tetrahedral elements). Grid continuation studies indicated that the forces on a sphere attached to the wall could be considered relatively (less than 2% change in the drag force with refinement) grid independent for these mesh resolutions as long as the microbubble had at least 3300 elements on its surface (i.e., the mesh had to be sufficiently refined near the microbubble). As the number of elements increased, the microbubble geometry was captured more accurately, and the grid continuation studies showed that the number of elements on the boundary of the microbubble was the most important factor in determining the numerical model accuracy.

Blood was assumed to be a Newtonian fluid with a density of 1040 kg/m^3 and a constant viscosity of $3.5 \times 10^{-3} \text{kg/m/s}$. Blood is a suspension of cells and exhibits the behavior of a shear thinning fluid, but

testing with a non-Newtonian blood flow model showed negligible deviation from the simpler Newtonian model for the flow rates and geometries described here so a Newtonian model was used. Flows with higher shear rates often require a non-Newtonian viscosity model for blood. Consistent with previous experimental results, the fluid in the model had the physical properties of PBS (Phosphate Buffered Saline) with a constant viscosity of $1.05x10^{-3}$ kg/m/s. The forces on the microbubble were calculated by taking an approximate integral over the surface of the microbubble.

Two computational geometries were used in this study. A parallel plate flow channel geometry is used for comparison to previously published experimental results of Schmidt et al. and Takalkar et al., and the dimensions of the model domain match as closely as possible the flow channel used in those experiments (**Table 1**)^{16, 17}. In addition, representative blood vessels including capillaries, veins and arteries were modeled using a straight, cylindrical geometry (**Table 1**). The length of the blood vessel sections used in the model ranged from 10 microns (capillaries) to 3 cm (vein) with internal diameters ranging from 10 microns (capillaries) to 1 mm (vein)²⁵. Thus, even the smallest diameter cylinders were larger than the typical microbubble diameter, which vary from 3.5 to 6 microns.

Table 1: Description of numerically assessed geometries and their flow rates.

Geometry	Dimensions	Average inflow velocity	Domain/
		Particle Reynolds number	microbubble
			size ratio
Parallel Plate ¹⁶	0.6 mm x 8mm	$V_{avg} = 0.2 \frac{cm}{s}$ to 1.5 $\frac{cm}{s}$	215
(Schmidt et al.)			
		$Re_p = 0.00017 \ to \ 0.0013$	
Parallel Plate ¹⁷	0.25mm x 3.5mm	$V_{avg} = 0.0806 \frac{cm}{s} \text{ to } 0.4 \frac{cm}{s}$	145
(Takalkar et al.)			
		$Re_p = 0.0001 \ to \ 0.0008$	
Capillary ²⁵	Diameter = $10 \mu m$	$V_{peak} = 0.0001 \frac{cm}{s} \text{ to } 0.03 \frac{cm}{s}$	3
		$Re_p = 1 \cdot 10^{-6} \text{ to } 1.8 \cdot 10^{-4}$	
Venule ²⁵	Diameter = $100 \mu m$	$V_{peak} = 0.1 \frac{cm}{s} \text{ to } 0.3 \frac{cm}{s}$	36
		$Re_p = 2.7 \cdot 10^{-4} \text{ to } 8.4 \cdot 10^{-4}$	
Vein ²⁵	Diameter = 1 mm	$V_{peak} = 1 \frac{cm}{s} \text{ to } 5 \frac{cm}{s}$	360
		$Re_p = 1.5 \cdot 10^{-4} \text{ to } 7.3 \cdot 10^{-4}$	

Large ranges of length scales were present in some problems where the ratio of the fluid domain size to microbubble diameter exceed 100. In these cases, it was impossible to generate a finite element mesh that was both computational feasible (i.e., did not require billions of elements) and did not contain invalid elements with negative Jacobians or extremely high aspect ratios. For these problems with a large range of length scales (i.e., for all problems where the total domain size to microbubble diameter ratio is greater than 100), a multi-scale modeling technique is employed to separate the larger length scales from the smaller length scales near the microbubble. When this technique is used, the larger fluid domain is modeled first without the microbubble explicitly included in the large length scale problem because it is significantly smaller than the individual elements. Then, after the larger length scale flow problem has been solved, the solution from the large scale problem is used to obtaining boundary conditions for the microbubble scale model, which only includes the fluid near the microbubble (i.e., the fluid within approximately 20 microbubble diameters of the center of the microbubble).

The boundary conditions for the parallel plate geometries are given in the experimental comparison section below. The capillary and venule simulations employed a range of flow rates (see

Table 1), and boundary conditions were set based on a Pouiseulle flow profile. Early simulations of flow in the larger blood vessels (vein) included the effects of wall elasticity and displacement on both the velocity gradients near the wall and the forces on the microbubble. These early results showed that the largest forces would be generated with a rigid wall, consistent the observations of others²⁶, so all results shown below are based on the most difficult conditions for microbubble attachment: the rigid wall vessel.

Experimental Comparisons

The experimental measurements by others that are used here for numerical model validation were assumed to be at steady state with a fully developed flow profile. The fluid shear stress near the wall in the experimental channel can be calculated through the equation ¹⁶:

$$Q = \frac{\tau h^2 w}{6\mu}$$

where τ is the wall shear stress, h is the channel height, and w is the channel width. The velocity in the mathematical model was set so that the wall shear stress matched the experimental wall shear stress values of 0.02, 0.05, 0.1 and 0.15 Pa 16 . The shear stresses for the second set of experiments by Takalkar et al. were 0.02, 0.03, 0.06, 0.1 and 0.17 Pa 17 . The channel height, h, was 0.6 and 0.254 mm for the Schmidt et al. and Takalkar et al. experiments, respectively, and since the channel width in both experiments was at least an order of magnitude greater than the height, a 2-dimensional model was used for the macroscale fluid model. (A full 3-dimensional model was used for the micro-scale model of flow around the microbubble.) The boundary conditions used to simulate the experiments (i.e., the boundary conditions for the macro-scale model) include:

- no-slip (u = 0) at the upper and lower walls,
- the normal stress in the normal direction is zero at the outlet, and
- tangential velocity of zero at the inlet and outlet.

For the micro-scale model, the solution from the macro-scale model was used to specify the velocity boundary conditions. The adhesion forces between the microbubbles and surfaces containing the targets were estimated based on previous Atomic Force Microscope (AFM) measurements and are used as a basis for comparisons between experiments and model predictions²⁷.

Analytical Models

The drag force on a sphere in an infinite, uniform, creeping flow can be approximated by the well-known Stokes drag law equation:

$$(4) F_D = 6\pi a\mu V$$

where a is the radius of the microbubble, V is the characteristic velocity around the outer perimeter of the microbubble's surface, and μ is the viscosity. The Stokes drag law assumptions include low Reynolds number flow (Re < 10), no particle-particle interactions, and an infinite body of fluid around the spherical particle. The Reynolds number for this problem is defined as: $Re = \frac{V \cdot L \cdot \rho}{\mu}$, where V is characteristic velocity (defined as the mean fluid velocity), L is the characteristic length (the microbubble diameter unless otherwise specified), and ρ is the fluid density⁷.

The Saffman equation²⁸ can be used to estimate the lift force (i.e., the force perpendicular to the primarily flow direction) on a spherical particle due to a velocity gradient:

(5)
$$F_L = KVa^2 \frac{k^{1/2}}{v^{1/2}}$$

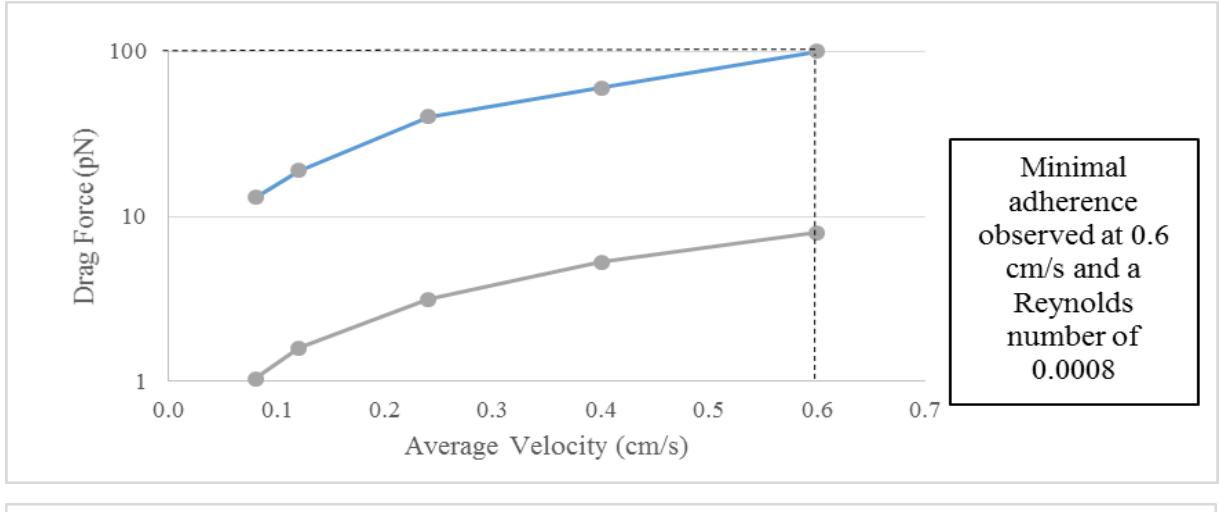
where ν is the fluid's kinematic viscosity and k is the velocity gradient. Assumptions for the lift force estimate include symmetrical flow around the center of the sphere, and a semi-infinite body of fluid around the sphere, meaning that the microbubble should be surrounded by ample fluid on all sides.

Results and Discussion

The numerical simulation results are divided into two sections: first the results of the parallel plate simulations are described and compared to previous experimental measurements, and then in the second section, the results of simulations in cylindrical blood vessel geometries are presented.

Parallel Plate Simulations

The first set of simulations was focused on the square channel geometry used in previous experimental observations to estimate the microbubble binding strength. **Figure 2** shows the drag force predicted by the numerical simulation for a range of Reynolds number in a geometry consistent with Schmidt et al. and Takalkar et al. ^{16, 24}. The range of drag force values predicted by the model was from 14 to 100 pN for



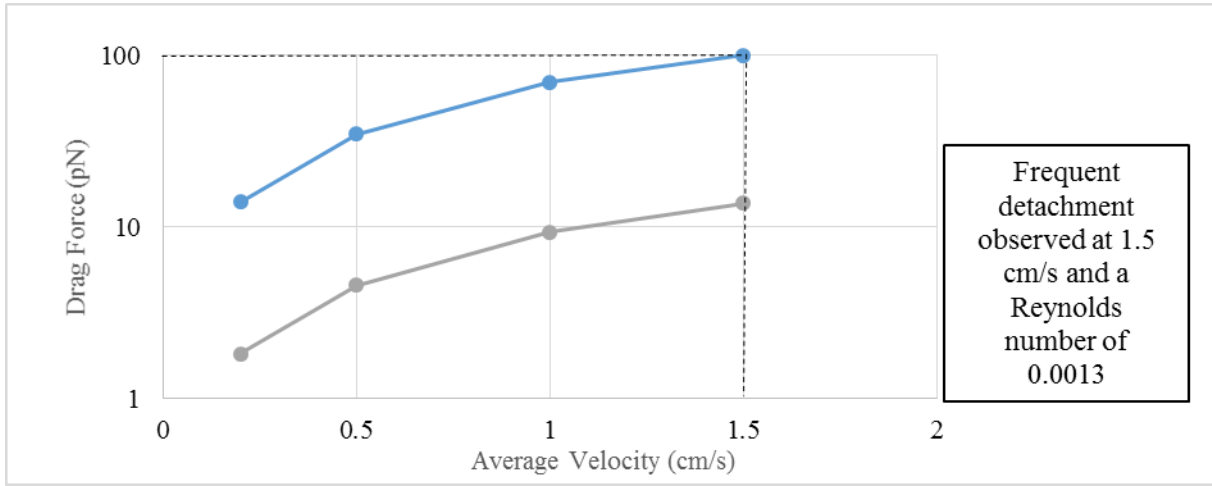


Figure 2: The numerical model predictions of drag force (blue) at different average velocities. The attachment/detachment of microbubbles based on experimental measurements by the Takalkar et al. (top) and Schmidt et al. (bottom) are indicated by the vertical dashed line. The Stokes drag law predictions of drag force are shown in gray. The model prediction of drag force combined with the experimental measurements of detachment suggest a drag force of 100 pN results in detachment.

superficial velocities between $0.2 \frac{cm}{s}$ and $1.5 \frac{cm}{s}$. Schmidt et al. observed microbubble detachment at a velocity of approximately $1.5 \frac{cm}{s}$ for their flow cell, and the model predicts a drag force of 100 pN under these conditions. Takalkar et al. showed a similar result, observing detachment at a superficial velocity of $0.6 \frac{cm}{s}$, corresponding to a drag force of 100 pN according to the model. Thus, based on the experiments of Takalkar et al. and Schmidt et al., the model predicts microbubble attachment when the drag force is 100 pN or less, and no attachment when the drag force is greater than 100 pN.

Recent experiments have attempted to measure the total microbubble adhesion forces through the use of an atomic force microscope (AFM). These experiments showed a median adhesion force of 93 pN²⁷. This result is consistent with the drag force estimate from the numerical simulation combined with flow cell measurements. Since the AFM measurements are believed to have measured the adhesion force of individual bonds, the implication is that each microbubble is primarily held in place by one or a few antibody bonds. This is intriguing since the surface density of the microbubbles has been estimated to be approximately 2500 antibodies per m^{2-17} , so there is the potential for multiple bonds between the microbubble and the target. However, the formation of many bonds would require a high density of receptors on the target and, if there were multiple bonds, their binding strengths are unlikely to be additive because just a few bonds would be expected to be under tension as described by Ward et al. ²⁹. The drag force on the upper part of the microbubble furthest from the surface attachment bonds is likely to result in a 'peeling' or 'unzipping' of individual antibody bonds from each attachment sites.

Blood Flow Simulations

The second set of results is focused on predicting whether or not microbubble attachment is likely or unlikely for a range of blood vessel sizes and a range of blood flow velocities. The goal was to evaluate a sufficient range of vessel sizes and blood flow velocities to represent most of the conditions found in the cardiovascular system. The results are focused on predicting microbubble attachment in a "worst case" scenario and thus the model predictions of attachment may be conservative. The prediction of microbubble attachment is based on three regions of the vascular system: capillaries, venules, and veins. Additionally, these blood vessel results are compared with the predictions of the Stokes drag law. If the

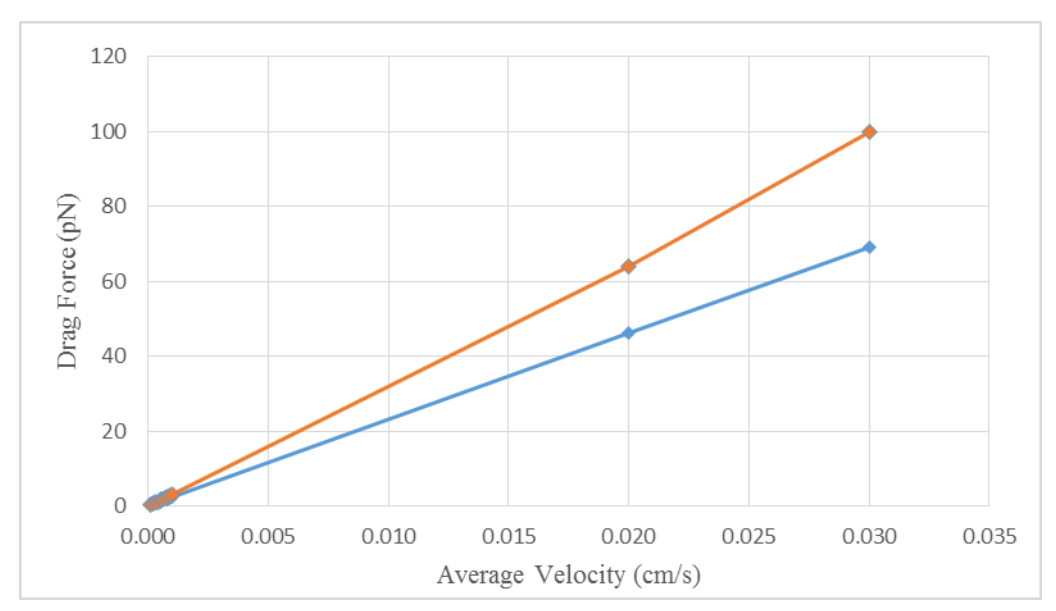


Figure 3: Numerical results (orange) from the capillary indicate that microbubbles should stay attached at all velocity. Stokes drag results (blue) are similar but diverge from the numerical results. This is most likely due the small capillary diameter to microbubble diameter ratio around .001

Stokes drag law results are consistent with the numerical model, it would allow for the use of simplified equations to predict microbubble behavior in a wide range of flow conditions throughout the body without the use of computational modeling software. For all simulations, the microbubble is attached to the vessel wall and the hydrodynamic forces on the bubble are estimated.

The first vessel examined is the capillary geometry, and the force increases nearly linearly with the Reynolds number over the range of flow rates examined (**Figure 3**). Although the total hydrodynamic forces from fluid flow are unlikely to prevent attachment based for the typical range of velocities in the capillaries (i.e., the forces are less than 100 pN), the additional force from the impact of red blood cells, or other small particles could be significant and potentially lead to detachment. The force predictions from the Stokes drag law differed from the more accurate numerical simulation calculation of drag by no more than 50% at low Reynolds numbers ($Re_c \ll 1$) found within capillaries. The agreement between the numerical simulation and Stokes drag law is somewhat unexpected because the Stokes drag law was derived using an infinite, unbounded body of fluid. As the flow rate increases in the capillary, however, a separation between the Stokes drag and numerical results is observed and is due to the acceleration of additional fluid through the space between the microbubble and opposing wall.

The second set of numerical results address forces on the microbubble in flow regimes similar to those found in venules. It can be seen once again that the forces increase approximately linearly with velocity. In flow regimes where the velocity is less than $0.15 \frac{cm}{s}$, microbubble adherence should be

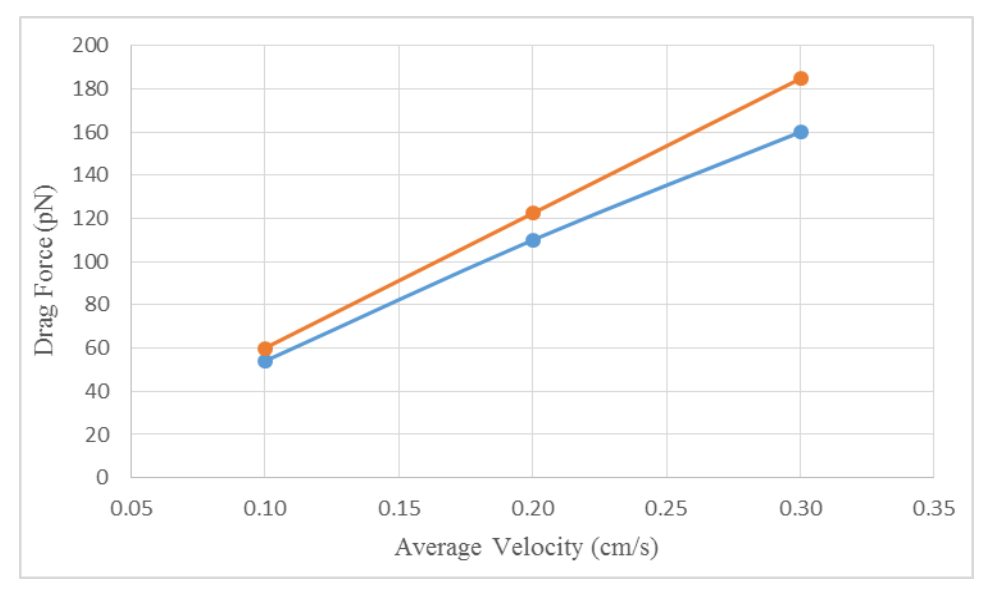


Figure 4: Numerical results in the Venuole flow regimes (orange) indicate that microbubble adherence is observed at velocities less than approximately 0.20 cm/s. The results also indicate that the Stokes drag (blue) is a relatively accurate approximation of the force within these regimes.

observed for this vessel, which has a much larger diameter than the capillary. Velocities above $0.15 \frac{cm}{s}$ are predicted to result in frequent detachment and infrequent adherence of microbubbles. The microbubble is very small relative to the vessel size, so the microbubble is not directly in the flow path, but it does extend far enough into the main flow channel to be detached by the larger hydrodynamic forces away from the wall of the vessel. Unlike capillary flows, these vessels are much larger, so effects from red blood cells and other particles should be less pronounced. The Stokes drag law prediction of the

drag force is similar to the numerical results in this regime, showing a variation of less than 10% between the two approximations (**Figure 4**).

The third and final set of numerical studies were conducted on the flow regimes typical for a vein. Because the microbubble is much smaller than the vein, these results were collected using the multi-scale modeling techniques described in the Methods section. The results indicate that the microbubble was likely to stay attached in areas where the average velocity in the vein was less than $1.5 \frac{cm}{s}$ (**Figure 5**). By contrast, detachment is predicted in the much smaller venule at velocities above $0.15 \frac{cm}{s}$. This difference is not a surprising result because the microbubble is over 1000 times smaller than a vein, but only about 50 times smaller than a venule. In other words, the microbubble is a tiny fraction of the diameter of the

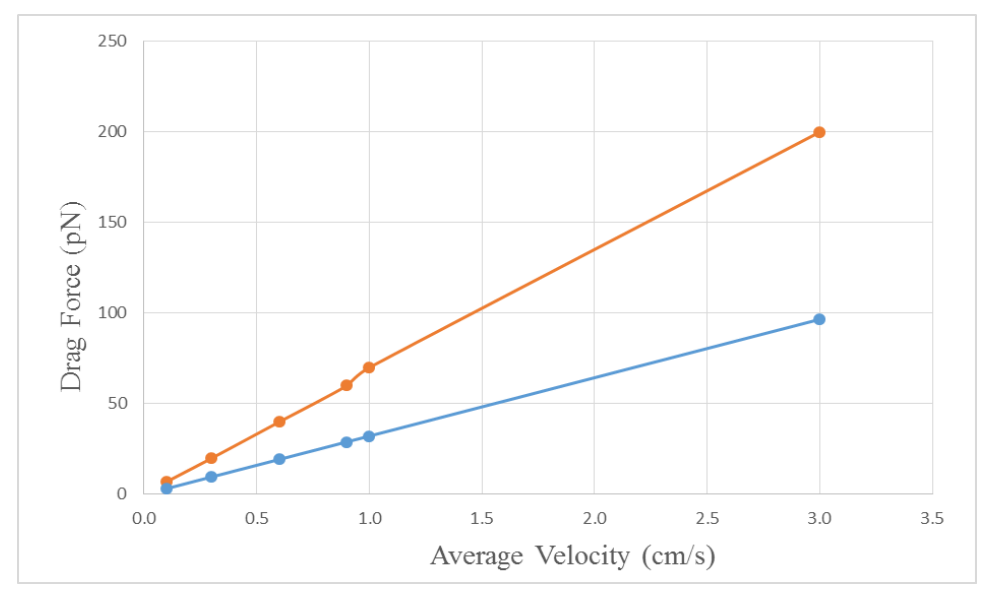


Figure 5: Numerical results from the vein flow regime (orange) indicate that microbubble attachment is observed at velocities less than 1.5 cm/s. Additionally a divergence from the Stokes drag law is observed, but the Stokes drag law was accurate within an order of magnitude for the flow regimes of interest.

vein and completely out of the main fluid flow. Additionally, increasing differences between the Stokes drag law force prediction and the numerical model were observed. This is partially because the Stokes drag law can only be considered accurate at Reynolds numbers much less than one. However, the Stokes drag law is still within a factor of 2 for the flow regimes of interest, making it a potentially useful tool for predicting the overall force on a microbubble.

The final goal of this work was to analyze the potential effectiveness of the Saffman equation (**Equation 5**) for predicting hydrodynamic lift forces on the microbubble. The Stokes drag law prediction of the drag force has already been discussed and is consistently less than the numerical model results. The Saffman equation for estimating the lift force was also compared to numerical results for all of the cases outlined. The Saffman equation predicted that the lift force was consistently the same order of magnitude as the drag force, but the numerical results indicated that this was not the case (**Figure 6**). For all of the problem geometries and flow rates of interest, it was found that the results from the Saffman equation for predicting the lift force were at least two orders of magnitude greater than the numerical results. The Saffman equation was derived based on the assumption that the particle was in an unbounded shear flow (far from the wall), and the violation of this assumption in the problems of interest probably

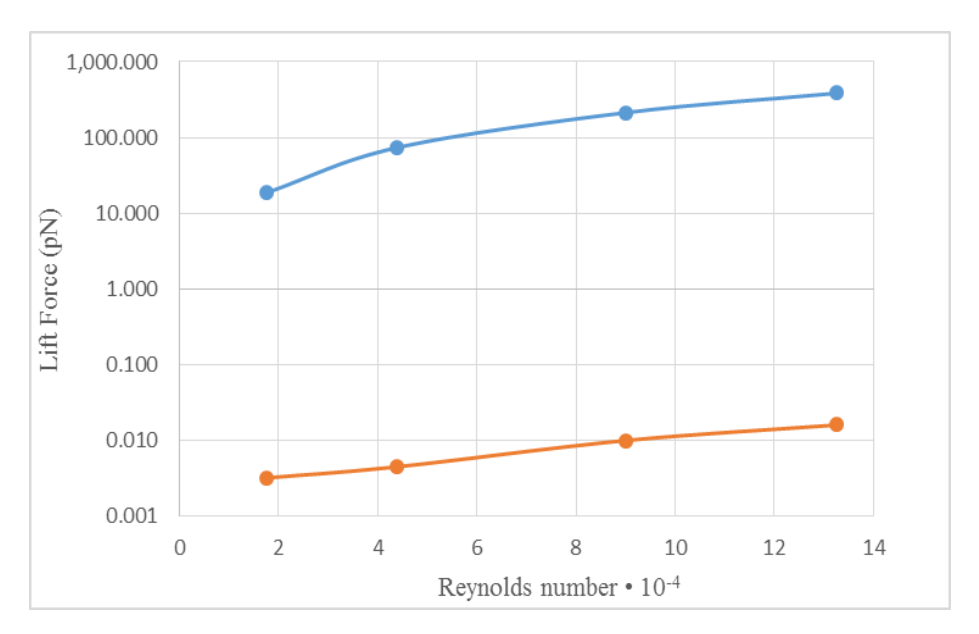


Figure 6: The numerical lift force (orange), is much smaller than the lift force predicted by the Saffman equation. This is not a surprising result, as Saffman's equation of lift is only valid when the particle is very far from the wall.

leads to this difference. The numerical results indicated that the lift force on the microbubble could be considered negligible for all cases of interest, displaying a lift force that was at least one order of magnitude less than the drag forces.

CONCLUSION

There were two primary objectives for this work. The first objective was to develop a numerical model of the forces on a microbubble in order to predict microbubble attachment/detachment, and then to validate the model based on previously published experimental measurements. The mathematical model predicted that the microbubble would adhere to its target unless it was exposed to forces greater than 100 pN. This result was consistent with AFM experiments with microbubbles that showed the median force of microbubble attachment is about 100 pN. The result suggests an unzipping effect, seen in other experiments²⁹, may be important when there are multiple bonds between the microbubble and the target surface, and this effect would allow multiple antibody bonds to rupture in a sequential manner. The second objective was to develop a numerical model to predict the potential for attachment of microbubbles in various flow conditions throughout the body. The principle result from this objective is that microbubble adhesion is predicted to occur in most capillaries, some venules and some veins, depending on the velocity (or Reynolds number) of the flow.

The numerical modeling results were compared to analytical equations that predict hydrodynamic forces on spherical particles. The results indicated that the lift force predicted by the Saffman equation did not agree with the numerical model predictions, primarily because the derivation of the equation was based on the assumption that the spherical particle was in an unbounded flow (far from the wall). The results also indicated that the Stokes drag law is typically within one order of magnitude of the drag force prediction of the numerical model. Limitations of the numerical model include the assumption of a Newtonian fluid, the assumption that both the vessels and the microbubbles where rigid, and the absence of erythrocytes in the model.

Future work on this project is focused on two objectives. First, the numerical model will be extended to model therapeutic drug delivery via the target microbubbles. Using targeted drug delivery would allow not only the detection of a biofilm based infection, but would also enable the immediate delivery of either therapeutic drugs. The second future objective is additional experimental measurements to validate the microbubble attachment model, assess the effects of nearby medical device materials on the feasibility of ultrasound imaging of microbubbles, and evaluate treatment options including therapeutic drug delivery and the disruption of the physical structure of the biofilm using either ultrasound energy directly or the rupturing of microbubbles.

ACKNOWLEDGEMENTS

This work was supported by the McNair Scholars program (U.S. Dept. of Education grant #P217A130148) and NSF grant CBET 1249950.

REFERENCES

- 1. Harro, J. M., Peters, B. M., O'May, G. A., Archer, N., Kerns, P., Prabhakara, R., and Shirtliff, M. E. (2010) Vaccine development in Staphylococcus aureus: taking the biofilm phenotype into consideration, Fems Immunol Med Mic *59*, 306-323.
- 2. Frasca, D., Dahyot-Fizelier, C., and Mimoz, O. (2010) Prevention of Central Venous Catheter-related Infection in the Intensive Care Unit, Intensive Care Medicine: Annual Update 2010, 223-234
- 3. Mermel, L. A., Farr, B. M., Sherertz, R. J., Raad, I. I., O'Grady, N., Harris, J. S., and Craven, D. E. (2001) Guidelines for the management of intravascular catheter-related infections, Clin Infect Dis *32*, 1249-1272.
- 4. Passerini, L., Lam, K., Costerton, J. W., and King, E. G. (1992) Biofilms on Indwelling Vascular Catheters. Crit Care Med 20, 665-673.
- 5. Anastasiadis, P., Mojica, K. D. A., Allen, J. S., and Matter, M. L. (2014) Detection and quantification of bacterial biofilms combining high-frequency acoustic microscopy and targeted lipid microparticles, J Nanobiotechnol *12*.
- 6. Shohet, R., Chen, S., Zhou, Y. T., Wang, Z. W., Meidell, R. S., Unger, R., and Grayburn, P. A. (2000) Targeted gene delivery to the left ventricular myocardium using ultrasound-triggered microbubble destruction, J Am Coll Cardiol *35*, 444a-444a.
- 7. Wilkes, J. O. (2006) *Fluid mechanics for chemical engineers with Microfluidics and CFD*, 2nd ed., Prentice Hall Professional Technical Reference, Upper Saddle River, NJ.
- 8. Bigelow, T. A., Northagen, T., Hill, T. M., and Sailer, F. C. (2008) Ultrasound Histotripsy and the Destruction of Escherichia Coli Biofilms, Ieee Eng Med Bio, 4467-4470.
- 9. Schade, G. R., Keller, J., Ives, K., Cheng, X., Rosol, T. J., Keller, E., and Roberts, W. W. (2012) Histotripsy Focal Ablation of Implanted Prostate Tumor in an ACE-1 Canine Cancer Model, J Urology *188*, 1957-1964.
- 10. Chapuis, J. C., Schmaltz, R. M., Tsosie, K. S., Belohlavek, M., and Hecht, S. M. (2009) Carbohydrate Dependent Targeting of Cancer Cells by Bleomycin-Microbubble Conjugates, J Am Chem Soc *131*, 2438-+.
- 11. Rand, A., Gilman, G., Kane, D., and Belohlavek, M. (2008) Biotinylated Microbubbles Targeted to Amyloid., The Open Clinical Chemistry Journal *1*, 75-78.
- 12. Ferrara, K., Pollard, R., and Borden, M. (2007) Ultrasound microbubble contrast agents: Fundamentals and application to gene and drug delivery, Annual Review of Biomedical Engineering *9*, 415-447.
- 13. Bloch, S. H., Dayton, P. A., and Ferrara, K. W. (2004) Targeted imaging using ultrasound contrast agents, Ieee Eng Med Biol *23*, 18-29.
- 14. Brady, R. A., Leid, J. G., Kofonow, J., Costerton, J. W., and Shirtliff, M. E. (2007) Immunoglobulins to surface-associated Biofilm Immunogens provide a novel means of visualization of methicillin-resistant Staphylococcus aureus Biofilms, Applied and Environmental Microbiology *73*, 6612-6619.
- 15. Brobst, T., Rombola, C., Ungerleider, S., Voncannon, S., and Ward, B. (2013) Targeted Microbubble Drug Delivery in an Experimental Treatment Model of Crohn's Disease, The Spectra, 27-35.
- 16. Schmidt, B. J., Sousa, I., van Beek, A. A., and Bohmer, M. R. (2008) Adhesion and ultrasound-induced delivery from monodisperse microbubbles in a parallel plate flow cell, J Control Release *131*, 19-26.
- 17. Takalkar, A. M., Klibanov, A. L., Rychak, J. J., Lindner, J. R., and Ley, K. (2004) Binding and detachment dynamics of microbubbles targeted to P-selectin under controlled shear flow, J Control Release *96*, 473-482.
- 18. Stride, E. P., and Coussios, C. C. (2010) Cavitation and contrast: the use of bubbles in ultrasound imaging and therapy, P I Mech Eng H 224, 171-191.

- 19. Tinkov, S., Bekeredjian, R., Winter, G., and Coester, C. (2009) Microbubbles as Ultrasound Triggered Drug Carriers, Journal of Pharmaceutical Sciences *98*, 1935-1961.
- 20. Dayton, P. A., and Rychak, J. J. (2007) Molecular ultrasound imaging using microbubble contrast agents, Front Biosci *12*, 5124-5142.
- 21. Klibanov, A. L., Rychak, J. J., Yang, W. C., Alikhani, S., Li, B., Acton, S., Lindner, J. R., Ley, K., and Kaul, S. (2006) Targeted ultrasound contrast agent for molecular imaging of inflammation in high-shear flow, Contrast Media Mol I *1*, 259-266.
- 22. Unger, E. C., Porter, T., Culp, W., Labell, R., Matsunaga, T., and Zutshi, R. (2004) Therapeutic applications of lipid-coated microbubbles, Advanced Drug Delivery Reviews *56*, 1291-1314.
- 23. Finnoy, A. (2013) Acoustic and Mechanical Properties of Microbubbles Stabilized by Polymeric Nanoparticles, In *Department of Physics*, Norwegian University of Science and Technology, Trondheim.
- 24. Gresho, P. M., Sani, R. L., and Engelman, M. S. (1998) *Incompressible flow and the finite element method:* advection-diffusion and isothermal laminar flow, Wiley, Chichester.
- 25. Fung, Y. C. (1984) *Biodynamics : circulation*, Springer-Verlag, New York.
- 26. Box, F. M. A., van der Geest, R. J., Rutten, M. C. M., and Reiber, J. H. C. (2005) The influence of flow, vessel diameter, and non-Newtonian blood viscosity on the wall shear stress in a carotid bifurcation model for unsteady flow, Invest Radiol 40, 277-294.
- 27. Sboros, V., Glynos, E., Ross, J. A., Moran, C. M., Pye, S. D., Butler, M., McDicken, W. N., Brown, S. B., and Koutsos, V. (2010) Probing microbubble targeting with atomic force microscopy, Colloid Surface B 80, 12-17.
- 28. Saffman, P. G. (1965) Lift on a Small Sphere in a Slow Shear Flow, Journal of Fluid Mechanics 22, 385-&.
- 29. Ward, M. D., Dembo, M., and Hammer, D. A. (1994) Kinetics of Cell Detachment Peeling of Discrete Receptor Clusters, Biophys J *67*, 2522-2534.

Student Authors

Joshua Gosney received his A.S. degree in economics from Flathead Valley Community College in 2010. In 2012, Mr. Gosney began his academic pursuits at Montana State University, where he is currently seeking his B.S. degree in Chemical Engineering. Mr. Gosney is conducting research in the computational bio-fluids laboratory under the advisement of Dr. Jeffrey Heys, and their work is focused around developing a targeted drug delivery system with use of Microbubble conjugates. Mr. Gosney is a proud Native American and an active member of the American Institute of Chemical Engineers student group, U.S. Green Building Council, Sustainability committee, Leadership Institute and the Undergraduate Scholars Program. Joshua's ultimate goal is to obtain his Ph. D in chemical engineering, with a focus in biomedical research.

Summary

The inability to noninvasively detect some diseases such as biofilm-based infections and cancer is a significant challenge. The combination of targeted microbubbles and ultrasound has been shown to potentially be an effective and inexpensive method of detection for diseases such as biofilm-based infections, cancer, and the formation of atherosclerotic plaque, among others. This study focuses on determining the biological flow conditions where microbubbles are likely to be an effective targeting agent in the human body versus flow conditions where microbubble attachment is unlikely due to large hydrodynamic forces on the microbubble. The goals of this project were to develop a numerical model predicting the forces on a microbubble, validate the model using published experimental measurements, assess the potential for using a simplified analytical model for predicting the hydrodynamic forces, and, finally, assess the potential for microbubble attachment under various biological flow conditions within the human body.

A Sustainable Model for Health Programs: A Case Study in Zambia Heidi Hanson, McNair Research Project

McNair Research Mentor: Wendy Bianchini-Morrsion

Montana State University, McNair Scholars Department

Abstract

Akros is an international non-government organization founded in Lusaka, Zambia (Winters &Winters, 2015). One of their goals is to use a community based model to implement their water, sanitation and hygiene (WASH) program through Community Led Total Sanitation (CLTS). Building and using latrines can make a large impact on the health habits developed in the community and surrounding areas. By involving the community, Akros can encourage and bridge communication with its staff, local government, tribal government, and resources that are already implemented (Kjell, 2011). Akros invited a group of 14 MSU students to survey and observe Akros protocol and operations. Interviews were conducted with government officials and members of Zambian tribes/towns. Technology use between tribes/towns that may not have power has been a noted difficulty for Akros to receive data, but overall the current system of involving community members to participate in taking charge of their own health has been successful in spreading awareness and implementing adequate latrines and sanitation protocol into many districts (Unite for Sight, 2015).

Introduction

A non-government organization (NGO) is an organization which takes on human rights, animal rights, environmental, educational, health or governmental issues to improve awareness and implement plans to further progress their mission (Ngo.org, 2015). International non-government organizations (INGOs) may be set up in different countries and expanded into other regions of the world where they may be experiencing a similar difficulty the origin country may have. Anyone may set up an NGO, but an integral part of starting up an NGO includes a primary focus on a specific problem, acquiring funding, participation through volunteers which it affects,

and volunteers with some knowledge in the topic and country it is being created for. Working with other governments, organizations and individuals who can help with funding and resources includes having networking abilities to gain funding and recognition for their organization and the organization's focus.

Models for NGOs and Continued Sustainability

Sustainable community development is "development that meets the needs of the present without compromising the ability of future generations to meet their own needs." (International Institute for Sustainable Development [IISD], 2013). The IISD (2013) explains the two main concepts of the community's needs and the limitations have to be in the forefront of formation when creating sustainable ideas and productions. The term "going green" typically fulfills the idea of "making something environmentally friendly." Sustainability often reaches beyond "going green." Sustainability encompasses using systems that most impact our human behaviors (Ganguly, 2012).

Creating a sustainable balance between communities and their environment may further help how companies and organizations need to function to continue productive work within their system and their goals. Without creating a sustainable plan, organizations such as NGOs may run out of funding, lose employees, or lose trust with locals. Creating a system intertwined with community members ensures that knowledgeable employees are in charge and in tune with the community's true wants and needs.

There are two very common models which non-profits, NGOs and other organizations may choose to use when approaching a problem with a solution in mind. Both the "top-down" and "bottom-up" models have success and failure stories, but one may have a more successful

approach when working with other communities, organizations, and even government when trying to solve an issue (Unite for Sight, 2015).

The "top-down" model begins with a general idea and supporters who may have a lot of data and a solution in mind. Their goal is to implement a plan that has facts, data, and expertise of research on the problem they would like to solve. Community members who are interested in changing the community are the most common expertise called on to help the organization get a foot-hold in the community. Members of the community who are vocal and well respected are also often asked to be a part of the organization's mission. Using a community member who is well-respected and well-known may help an organization get recognition and spread their mission throughout the community quicker (Dessai & Hulme, 2004).

A bottom-up model uses a more community based approach when tackling community or international development. Here, the organization begins with the community, where their ideas are gathered and chosen as a group effort. What the community sees as an issue may be very different from what a community *wants* to happen in their community. Unite for Sight (2015) discusses how top-down solutions may fail to take into account both the needs and wishes of the community members.

Akros is a health specialized INGO currently operating in Zambia, its headquarters in the capital city, Lusaka. Akros' main goal is to provide a sustainable model for Zambians to take control of their own needs and wants in relation to malaria control and sanitation practices. Their first approach to promoting healthier lives in Zambia was to research data on malaria rates in Zambia and finds a way to target malaria cases and find a statistical way to track and eliminate transmission of malaria through their technological advances with the program "mSpray" (Winters & Winters, 2015).

Recently, Akros has expanded their program to target water, sanitation and hygiene (WASH) issues that would also exponentially increase health in Zambia. The Community Led Total Sanitation (CLTS) program focuses on helping individual districts in increasing the local government's awareness, access, and action in collecting and monitoring data on the community's water sanitation methods compared to other districts. Using cell phones, tablets, and the community members keeps them updated and "inside," which helps them understand how community members feel about CLTS and mSpray (Winters & Winters, 2015).

The ultimate goal for Akros is to create programs that will continue to be funded and managed by the local and national government. Akros uses an approach similar to the bottom-up processing model used for creating an engaged and active program within a community (Dessai & Hulme, 2004). By including every system of sustainability and every level of human participation, a community can succeed on its own by giving it the road map to the community's resources. Helping transition the programs to the government will increase community and government ownership. When a government has the responsibility to take care of its citizen's health, it involves everyone in the nation to get involved and get invested in their own health (Kjell, 2011).

Possible Challenges

Geis and Kutzmark (2003) make the bold prediction that "communities of the future will be very different from the ones we live in today." (pg. 43). Their prediction encompasses a large assumption that our growing technological advances will dramatically alter how we approach sustainability and our ability to globalize those efforts. They predicted this technological advancement 12 years ago, but how far into the "future" did they necessarily predict? Our

technology has advanced and is being implemented in many programs, but is the technology helping to eliminate poverty, hunger, disease and other problems NGOs are looking to eliminate?

Although there appears to be a great advancement towards collecting data and identifying sources to improve the problem, there is little evidence to prove that technology is expediting or alleviating difficulties when it comes down to the human aspect of implementing a program. Especially in Zambia, Akros is using computer tablets to collect and send information to their headquarters. But receiving electricity to charge tablets and a person's skill or ability to use a tablet is a huge problem. Many villages do not have clean water or electricity, and at the very least, do not know how to use or run tablets which are able to collect useful data. Once these issues are addressed, it is hard to tell if these will be the only issues along the way. Persevering to help the community and the organization find a solution together is an excellent way to integrate trust and the relationship between a community and an organization trying to solve an issue (Dessai & Hulme, 2004).

Community Champions are the members in the community who volunteer their time to help Akros collect and report data to Akros (Winters & Winters, 2015). Cell phones are given to Community Champions through Akros as reimbursement for time spent collecting data from individual members of the community. Many members travel various miles a day to collect from several tribes and villages. Common complaints heard from Community Champions during interviews were the lack of compensation and availability of cell service to report data.

Receiving compensation is very important to most of the Community Champions, who need to support their families but cannot when they spend all day travelling many miles (most by foot or bicycle) taking time off of work that could compensate them.

Methods

Fourteen MSU students interning at Akros were sent to different districts to perform a new qualitative assessment to gauge progress of CLTS in districts across Zambia. The students were split into small groups of 2-3 students and sent with an Akros Surveillance Officer to survey their assigned districts by conducting interviews with Community Champions and district level employees. All students were instructed to interview government officials with a standard Akros questionnaire, aimed at answering questions about involvement in CLTS programs, activities, and technology.

One group that was selected traveled to three different districts in western Zambia:

Kazungula, Namwala, and Sinazongwe, with Kaluba Lombe, the Akros Surveillance Officer for those districts. Every district has different officers that overtake duties involved in CLTS activities and program needs. Several members on different levels of government authority were surveyed on facts, opinions, commitment, and involvement in CLTS activity in their district.

Officials were attempted to be surveyed alone to get individualized and more accurate gauge on the level of communication between and amongst the government staff, Community Champions, and Akros.

Once the data was collected it was compiled to rank the districts on their successful knowledge and participation in the CLTS program. Rankings ranged from a score of bronze (0-70), silver (71-85), and gold (86-100). After collecting the data on the three districts, the students reported the findings on the three districts. Surveillance Officers which represented all of the districts heard a presentation of the program's strengths and challenges identified by the officials and the questionnaire. Akros plans to acknowledge their role in helping districts gain independence and work to overcome these identified issues that may slow progress with CLTS, with the ultimate goal of the districts achieving "open defecation free" status, or ODF.

Results

The district Kazungula received the lowest rating, a "bronze" rating. The government officials did not appear to be fully committed to implementing CLTS in their district, and did not communicate within the district effectively to receive the correct information. The Secretary of the district, who would be equivalent to an American mayor, did not know what CLTS's goals were or any water and sanitation facts about his district. His communication and patience when meeting us was cut short after being asked several questions he did not know the answer to.

Reporting government officials below the Secretary answered various questions on the questionnaire differently, and one of the employees had only been filling in for another employee for about a week. He reported that he did not have any files or means of communication from the official he took over for, which may account for his lack of accuracy or interest in answering the questionnaire.

Sinazongwe received a "bronze" rating as well, but for different reasons than the Kazungula district. Sinazongwe is on the Southern border of Zambian where the terrain is very rocky, sandy and by Lake Sinazongwe. The combination of poor terrain and lack of funds availability has decreased the interest in attending or creating events for CLTS centered education/implementation. With additional funding the government officials would like to provide educational training and incentives to communities who participate in CLTS activities and trainings. Akros may not be able to fully fund each district, but communication on what Akros is able to provide and where to find resources indicates there is a lack of communication between the NGO and the Zambian districts. Lastly, Namwala received a gold rating for their extensive knowledge on CLTS procedures, interest in the CLTS program, their districts capabilities and knowledge of their districts available resources. Although Namwala has not

become ODF, they appear to be well on the way, and a great model for how other districts may be able to succeed in their own.

Although there appears to be a great advancement towards collecting data and identifying sources to improve the problem, there is little evidence to prove that technology is expediting or alleviating difficulties when it comes down to the human aspect of implementing a program.

The main difficulties we found when talking with government officials are the communication between departments and the Community Champions.

Having access to utilize technology was also another concern expressed with Community Champions and government officials. In Zambia, Akros is using cell phones to collect and send information to their headquarters. But have access to consistent electricity to charge the phones and having enough phone card minutes to send in the data were challenges identified. Once these issues are addressed, it is difficult to estimate if these will be the only issues with technology or communication along the way.

Persevering to find solutions together is an excellent way to integrate trust and the relationship between a community and an organization trying to solve an issue. Akros can work with government officials from separate districts to ensure that individualized problems are addressed with individualized solutions to best fit the district's needs. Fine tuning the qualitative questionnaire to overtake many of the quantitative questions will help Akros and Surveillance Officers understand where districts are struggling and excelling. Issues need to be addressed quicker, and have a more uniform way to report with the district's chain of command and with their designated Surveillance Officer. Each district has very different terrain, leadership, and individual variances that need to be addressed to ensure that the bottom-up processing model stays focused the district's wants/needs. There has been improvement with each district that has

been triggered; the CLTS terminology for initiating awareness of the sanitation problems in a community, and it appears that there can only be positive growth and improvement on Akros' CLTS program.

Conclusion

NGOs may succeed using a top-down process model, but there are large advantages to using the bottom-up process model when looking for long-term sustainable development and community ownership. Akros has used the bottom-up method by involving and encouraging a community to find its own system of sustainability and ability to access its own resources on local and national levels. The model Akros has been using is flexible for change in the community, government and the wants/needs of community members. Surveying the community members, Akros team members and the government branches, they are able to monitor the progress towards making Zambia open-defectation free and adjust what they can do to help districts that are struggling to become open-defectation free.

The bottom-up development method gives the community and government a chance to see what works for their specific district that may not work when a top-down process model is implemented without input from the community members. Akros still has some kinks and issues to work out with technology and communication between communities, officials, and officers. But overall, there is positive improvement in various districts on becoming open-defectation free and creating awareness about open defectation across Zambia. Akros is still expanding its mission throughout Zambia, and hopes to expand to other countries after successfully implementing CLTS in all districts.

Acknowledgements

This work was supported by the McNair Scholars Program (U.S. Dept. of Education grant #P217A130148).

References

- Dessai S., & Hulme M., (2004). Top-down bottom-up model. Does climate adaptation policy need probabilities? *Climate Policy*, *Vol.* 4(2), 107-128.
- Ganguly, A. (2012). Philosophy of sustainable development. Sustainable Sphere. Retrieved from: http://www.sustainable-sphere.com/2011/07/philosophy-of-sustainable-development.html
- Geis D. & Kutzmark K. (2003). Developing sustainable communities: The future is now.

 Urban Planning Overseas, 2, 43-46.
- International Institute for Sustainable Development (2013). What is sustainable development?

 Environmental, economic and social well-being for today and tomorrow. Retrieved from https://www.iisd.org/sd/.
- Kjell, O. (2011). Sustainable well-being: A potential synergy between sustainability and well-being research. *Review of General Psychology*, *Vol.* 15(3), 255–266.
- Ngo.org (2015). Definition of ngos. Retrieved from http://www.ngo.org/ngoinfo/define.html
- Unite for Sight (2015). Module 2: Why bottom up instead of top down? Retrieved from http://www.uniteforsight.org/community-development/course1/module2
- Winters B. & Winters A. (2015). Personal communication. Lusaka, Zambia.

Research Paper for Summer McNair Research

The Effects of Anthocyanin Antioxidant Supplementation on Reactive Oxidative Stress Markers and Metabolic Flexibility After a Low-Intensity,

Treadmill Exercise

Erica Latorre B.S., Dr. Mary Miles PhD. Montana State University Nutrition Research Laboratory

> Submitted to McNair Scholars Program Montana State University

Abstract

The increased concentrations of reactive oxidative species found in the blood from the increase in metabolism during exercise can cause damage to lipids, protein, and even DNA nucleotides. Antioxidants are known to neutralize many of the ROS; however, the addition of an exogenous antioxidant source on neutralization of these increased ROS concentration is under debate. Rationale: Antioxidants are a family of compounds in the body and in food that have the ability to neutralize free radicals and reactive oxidative species (ROS). They may have potential health benefits for a consumer and positive effects on exercise responses; however, to what extent these benefits may be is unclear and of great debate. Purpose: To determine if an exogenous antioxidant supplement will positively effect a subjects metabolic flexibility and concentration of ROS in blood during a low intensity hour long treadmill exercise. Methods: 12 subjects between the ages of 18 and 24, with BMI's between 18 and 30 kg/m² participated in the study. Six males and six females made up the subject group and all were split up into two supplemental groups randomly. The two supplements were an antioxidant supplement which was of main concern in the study and another control fiber supplement. Three males and three females ended up being assigned to each supplement making for an even distribution of supplements between the sexes. Results: The statistical analysis of the collected data showed that there were no significant changes in delta RER, kcal Fat, or kcal CHO that occurred other than by chance (p<0.05) Conclusions: The antioxidant supplement did not significantly affect the participants metabolic flexibility. Further analysis of the ROS data is still underway.

Introduction

Antioxidants are substances that are found in many food products from fruits, vegetables, wines, teas, and even cocoa. They are especially present in large quantities in berry fruits such as raspberries, blueberries, wolf berries, agai berries, etc. (3). They encompass a group of phytonutrients named flavonoids, carotenoids, phenolic acids, and polyphenols that have many helpful abilities in the human body (in vivo) (2, 3). Their roles in vivo range from the reduction of inflammation to removing potentially damaging oxidizing agents by inhibiting oxidation (1). Many studies on antioxidants have found that they also may be helpful in reducing the risk of some cancers and agerelated macular degeneration (4, 6).

By reducing oxidizing agents, antioxidants fulfill their main purpose in the physiological setting by keeping these damaging species at low levels such that cell damage doesn't transpire (7). The human body can employ its own internal, endogenous antioxidants or it can utilize exogenous antioxidants that are collected from ingested food sources. In a normal nonexercising state the human body is capable of using it's own endogenous antioxidants to combat what are called reactive oxidative species (ROS). These ROS accrue from the normal metabolic processes occurring daily to keep our bodies functioning (9). The fallout with only using endogenous antioxidants is that there isn't a large enough quantity to accomplish the same demand in a more active, exercising state. These ROS that are left in the body begin causing damage.

Whilst there is a vast amount of knowledge that details how increases in metabolism resulting from exercise produces

increased ROS (8), there is still debate on whether and at what level exogenous antioxidants should be put into the body to help bridge this increase. This is a main goal of the study, to observe the impact of a food based exogenous antioxidant supplement on the body's production of ROS and also to observe its affect on metabolic flexibility. Usually the main goal of exercising is to increase healthy adaptations in the individual undergoing the activity; however, the increase in activity means that same increase in damaging oxidative species. This is a main concern when the focus of training is to accrue optimal exercise performance and adaptations.

During bouts of exercise, especially exercises comprised of eccentric muscle lengthening, which damages the muscle more than concentric shortening (8), mitochondria release free radicals and peroxides that cause unwanted redox reactions. These metabolic reactions that produce ROS are damaging to lipids, proteins, and even DNA nucleotides (9). As stated above, the body does reduce some of these free radicals and unwanted redox reactions through the use of endogenous antioxidant enzymes; however, not all of the ROS can be neutralized and their build up induces what is known as muscle fatigue. The main debate over antioxidants can be simplified down to whether an increase in ROS decreases beneficial exercise-induced adaptations by increasing muscle fatigue and lengthening recovery time or if the ROS are needed to produced signals in the body resulting in an increase in protein synthesis. These proteins can then help to accrue beneficial exerciseinduced adaptations.

A variety of different studies examining the effects of antioxidants on

combating ROS have produced conflicting results. The contradictory outcomes of these studies leaves room to question how antioxidants specifically effect the body after a bout of exercise. More testing is needed in order to determine which side of the spectrum exogenous antioxidants are actually on in relation to combating ROS from exercise and determining how one's metabolic flexibility is altered. The goal of this study is to further examine the effects antioxidants have on the body after a bout of exercise. An exogenous antioxidant food-based supplement, Maqui berry, in the form of a powder will be evaluated to determine it's antioxidant effects on participants who have completed a low intensity treadmill exercise. The main values being examined will be the ROS quantity in the blood and the metabolic flexibility of participants pre- and post-supplementation. The study will be a short 4 to 5 weeks study from start to finish and consist of 20 participants undergoing one of two conditions. The first condition will be an antioxidant food-based supplement and the second condition will actually be the control consisting of a insoluble, cellulose, fiber supplement. The participants will be blinded so that they are unaware of which condition they are receiving and to eliminate any placebo effects that would occur from knowledge of the condition. The study will not be double blind due to the need for the researcher to prepare the supplements for participants. The markers, ROS and metabolic flexibility, used to analyze the results of the study will be seen by running the blood samples taken through an ROS assay and seen on a metabolic chart during the exercise protocol.

The hope for this study is to obtain useful information that will cement antioxidants as an effect dietary treatment

measure for reducing ROS that are related to both exercise adaptations and to prevention of other important diseases. The main disease groups being cancer, obesity, and other vascular diseases (5).

Materials and Methods

Subjects.

A total of twelve male and female recreationally active subjects (age = 18-24years, and body mass = 18% - 30%) of the Montana State University student body participated in this study. All but one participant was able to complete the entire study for a total of 11 participants. All participants took the AHA/ACSM Health/ Fitness Facility Pre-participation Screening Questionnaire as well as a Physical Activity questionnaire. They were free of anemia, musculoskeletal limitations, inflammatory conditions, diabetes, heart disease, kidney problems (excluding kidney stones), smoking, chronic use of anti-inflammatory medications (including over-the-counter), and lipid lowering medications. The test procedures were approved by the Montana State University IRB Committee, and written informed consent forms were obtained from all subjects prior to their participation in the study.

Protocol.

All exercise protocols were performed in the Nutrition Research Laboratory in Herrick Hall on Montana State University's campus. Participants were asked to complete three laboratory visits and a supplementation period of three weeks with one of the two supplements. Supplement A was an anthocyanin antioxidant supplement and Supplement B was a fiber-based control supplement. Upon subjects initial visit they

signed all official paperwork including the informed consent and two health related questionnaires. The participants were then run through a few anthropometric body tests. The body testing was completed with the use of a BodPod machine and a Bioelectrical Impedance Analysis (BIA) machine that measured participants BMI as well as muscle mass and bodily water retention. The participants were then asked to complete a submaximal VO2 treadmill exercise in order collect data to determine their 50% heart rate for the exercise protocol on visits two and three.

On the next visit (the presupplementation visit) the participants blood was drawn prior to exercise through the use of lancets. Around 400 micro-liters of blood was obtained. After blood collection the participants were fitted with a mouthpiece and heart rate monitor and an hour long exercise protocol was started. The speed and grade of the treadmill was increased until the participants reached their 50% heart rate. calculated from the visit one submaximal VO2 testing. Throughout the exercise protocol, metabolic flexibility measurements were taken for three minutes every ten minutes. (measurements began on the seven minute mark of every ten minute interval). At the end of the exercise the participants walked at 2.0 mph speed with no incline for three minutes to cool down. Blood was then drawn again from the participants in the same manner as before the exercise. At the end of Visit 2 the participants were given their three week supply of the supplement that they were randomly selected to take and sent home until three weeks later for their last visit (postsupplementation visit). The participants took 5 grams a day of their supplement in order to mimic a normal amount of the anthocyanin antioxidant that would be found in a food.

After completion of 21 days of supplementing the participants were asked to return for their last visit within one to three days after cessation of supplementation (day 22 ± 2). The exact same protocol from visit 2 pre-supplementation was followed so as to eliminate any factors except for the only independent variable, the supplement. After the visit the participants were paid and thanked for their participation.

Metabolic flexibility data was assessed immediately following the end of visits 2 and 3. Blood samples being stored in a sub-climate freezer (-78°C) were run using a TBARS lipid peroxidation assay all together in two batch runs.

Data and Analysis

The factors of metabolic flexibility and substrate utilization pre- and postsupplementation were compared using an Anova analysis. This measurement determined if the supplement had indeed effected the participants ability to switch between fats and carbohydrates as energy substrates. The graph in Figure 1 shows this analysis. The analysis of substrate utilization during the exercise pre- and postsupplementation was accomplished by averaging the last two minutes of ratio quotient (RQ) data for each ten minute interval and comparing the two trials side by side. The RQ is a measure of the fats to carbohydrates being utilized for energy during an exercise. The pre- and postsupplementation blood samples were centrifuged for fifteen minutes at 1500 rpm immediately after collection. The serum was then removed (200 micrometers + 50 microliters) and a few micrometers of THB was added to stall any changes in the serum. The samples were then vortexes and then stored in a sublimate freezer until further analysis.

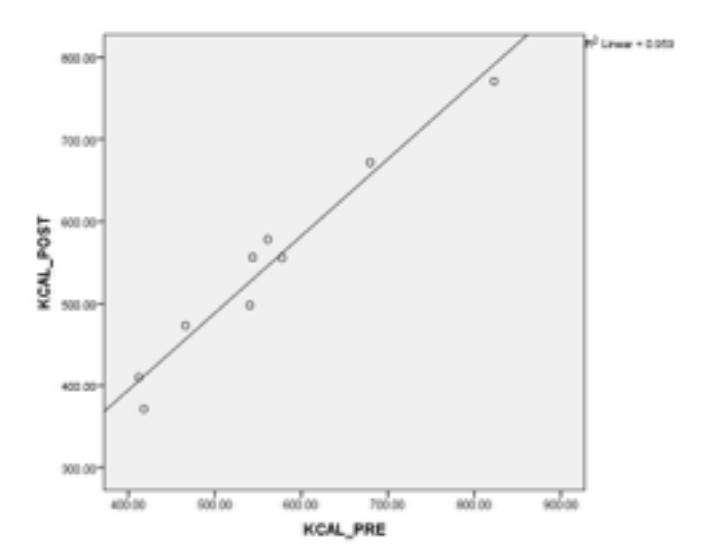


Figure 1: Pre-supplementation Kcal usage vs postsupplementation Kcal usage. p<0.05 for delta RER, kcal FAT, and kcal CHO. Total Kcal between the 2 exercise bouts was identical (r=0.979)

Weeks later the samples were thawed and run through a TBARS lipid peroxidation assay in order to determine if the concentration of ROS was effected by the supplement. Two assay batches were run. Participants 1-5,7,9, &12 were run in batch one, while participants 8,10, and 11 in batch two. The reason for two batches was performed only due to a time restraint to analyze data. Not all the participants had completed all the visits by the time data was required. Participant 6 was unable to finish all the required visits and thus the results were not usable.

Results

Of the 12 participants that began the study, 11 of them fully completed all the protocol visits and thus only their data (91.67%) was encompassed in the results. Metabolic flexibility changes, energy substrate utilization changes (amount and type) as well as the change in ROS concentrations in the blood were factors studied and reported. Though the use of ANOVA statistical analysis (p < 0.05) it was found that there was no significant changes in the participants metabolic flexibility that

wasn't due to chance. The amount of kilocalories used pre-supplementation was almost equivalent to the amount used in the post-supplement exercise. The substrate utilization was as expected for a low intensity exercise as fats was the major utilized energy source. It was found however, that in the post supplementation exercise the ratio of fats to

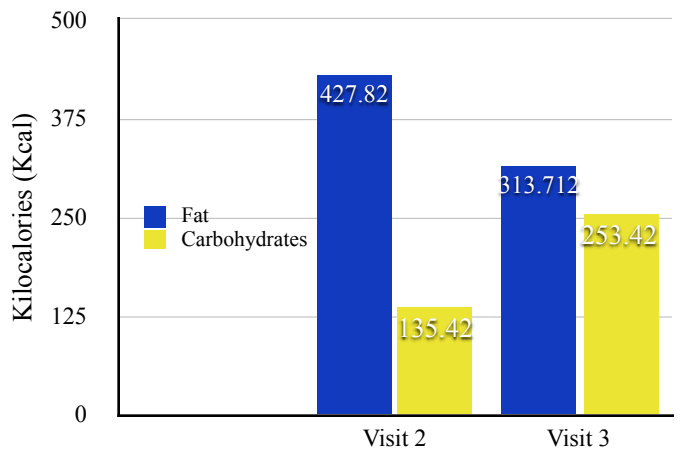


Figure 2: The average substrate utilization of 9 of the 12 participants. Substrates utilized includes fats and carbohydrates. Energy substrate utilization in both pre-supplementation (**visit 2**) and Post-Supplementation (**Visit 3**) saw fats as the main source, but an increase in carbohydrates utilized in visit 3.

carbohydrates used decrease. More carbohydrates were utilized in the post supplementation exercise than in the pre supplementation exercise, but with fats still predominating as the main energy substrate in both instances. Figure 2 shows this data below.

The TBARS assay data was not viable due to some error in the process of blood collection or analysis. More testing is needed to determine if the concentration of ROS in the participates blood was effected by the supplementation.

Discussion

The main purpose of this study was to examine the effects of a food based antioxidant supplement on the factors of metabolic flexibility, substrate utilization, and the concentrations of reactive oxidative species in the blood. After four months of running participants through a three visit study protocol, it was found that the antioxidant supplement (A) had similar effects on these factors as did the control supplement (B). These statistical results lead us to conclude that the supplement did not effect the participants in any manner that could not be attributed to random chance. The data relevant to the concentration of ROS in the subjects bodies was unable to be obtained due to a main source of error throughout the collection and analysis process.

Previous studies examining the effects of antioxidants on the human body have found mixed results. Some found no effect or positive effects in relation to decreasing the damage that occurred due to ROS created through exercise. Not as numerous of an amount of studies found negative effects of antioxidants; however, due to a few that did the question still stands as to the true effects that antioxidant substances have on the body.

Limitations

The main limitations within this study was the lack of control that was able to be maintained with the supplementing and schedule of the participants. Many confounding variables could have arose within the time between pre- and post-supplementation visits including but not limited to: type of diet, exercise amount and type, stress level of the participant, accountability of participants to adhere to supplementing correctly everyday, etc. Time

restraints of this study also created a rigor that may have induced unwanted and unforeseen error in the protocol. This time restraint also had a significant impact on the subject pool size

The last limitation that effected the study was the fiscal ability to pay participants. A larger participation payment would allow for a study with more structured parameters of the participants lives. This more structured study would help to eliminate confounding variables. In the future, a more structured study should be designed when studying the effects of a supplement on only a few bodily factors such as those focused on in this experiment.

Conclusion

The study showed that the anthocyanin antioxidant supplement had a similar effect as the fiber control supplement and thus was concluded to have a minimal if any effect on the metabolic flexibility of the study participants. Any noticeable effects seen were due to normal fluctuations in the participants bodies. The blood analysis to determine concentration of ROS before and after supplementation was inconclusive due to error that occurred during the process of running the assays. Further analysis of blood samples is needed to determine if this factor was indeed affected by the supplement.

References

- 1. Antioxidant. (2012, March 19). Retrieved July 4, 2015.
- Heim, K., Tagliaferro, A., & Bobilya, D. (2002). Flavonoid antioxidants: Chemistry, metabolism and structureactivity relationships. The Journal of

- Nutrtional Biochemistry, 13(10), 572-584. doi:10.1016/S0955-2863(02)00208-5
- 3. Hogan, S., Chung, H., Zhang, L., Li, J., Lee, Y., Dai, Y., & Zhou, K. (2009). Antiproliferative and antioxidant properties of anthocyanin-rich extract from açai. Food Chemistry, 118(1), 208-214. doi:10.1016/j.foodchem. 2009.04.099
- 4. Jakemanl, P., & Maxwell, S. (1993). Effect of antioxidant vitamin supplementation on muscle function after eccentric exercise. European Journal of Applied Physiology and Occupational Physiology, 67(5), 426-430. Retrieved April 12, 2015, from http://link.springer.com/article/10.1007/BF00376459
- Neto, C. C. (2007), Cranberry and blueberry: Evidence for protective effects against cancer and vascular diseases. Mol. Nutr. Food Res., 51: 652–664. doi: 10.1002/mnfr.200600279
- 6. Seeram, N. P. (2008). Berry Fruits for cancer prevention: Current status and future prospects. Journal of Agricultural and Food Chemistry, 56(3), 630–635.
- 7. Seifried, H. E., Anderson, D. E., Fisher, E. I., & Milner, J. A. (2007). A review of the interaction among dietary antioxidants and reactive oxygen species. The Journal of Nutritional Biochemistry, 18(9), 567–579.
- 8. Silva, L., & Born, K. (2013). Effect of eccentric training on mitochondrial function and oxidative stress in the skeletal muscle of rats. Brazilian Journal of Medical and Biological Research, 46(1), 14-20. doi: 10.1590/1414-431X20121956
- 9. Wei, Y.-H., & Lee, H.-C. (2002). Oxidative Stress, mitochondrial DNA

mutation, and impairment of antioxidant enzymes in aging.
Experimental Biology and Medicine, 227(9), 671–682.

Running Header: STRENGTHS BASED EXERCISE PRESCRIPTION IN THE CANCER COMMUNITY

Strengths Based Exercise Prescription in the Cancer Community

Jaycie Loney (McNair Scholar)

Dr. Lynn Owens (McNair Mentor)

Montana State University Bozeman

INTRODUCTION AND BACKGROUND

Many research studies have found that people who engage in regular and moderate exercise experience physical benefits including increased bone density, decreased risk for heart disease, weight control, and decreased high blood pressure (Mayo, 2014). In addition to these physical benefits, there are other ways that health is affected by exercising. Multiple researchers have published studies that have shown improvements in mood, energy, increased sex drive and improved quality of sleep all stemming from regular exercise (Mayo, 2014; Rendi, Szabo, Szabo, Velenzi, & Kovacs, 2008). These findings are often motivational factors that compel people to want to exercise. Additionally, these advantages also encourage cancer patients to want to improve their lives even though ill.

According to the American Cancer Society's Facts and Figures 2015, there will be approximately 1,658,370 people diagnosed with cancer in 2015 (American, 2015). Out of these diagnosed an estimated 589,430 people will die from the disease. This represents an increase from an estimated 585,720 people in 2014 (American, 2015). Doctors, researchers and other health care professionals have been looking for ways to improve the lifestyles of cancer patients during and after treatment. Physical activity is an extra precaution to take when trying to manage the symptoms caused by cancer and treatment (Spellman, Craike, & Livingston, 2014). Therefore, the purpose of this research is to find the connection between patient's strengths of personality and their motivation to stay physically active during and after treatment. Specific research questions include 1.) Who and what makes this population want to become or remain physically active? 2.) Can health care professionals better prescribe exercise in a way that

increases motivate to adhere to the program? 3.) Can health care professionals use strengths of personality to better motivate patients?

LITERATURE REVIEW

Exercise prescription is a way of suggesting a certain exercise program in order to encourage a person to improve their physical functioning. Strengths of personality are aspects of one's personality that are defined as traits. Using Professional DynaMetrics Programs (PDP) tools allows for identification of strengths and the amplitude of those strengths for each individual person. Combining exercise prescription with an understanding of strengths of personality can lead to effectively prescribe exercise to a patient in a way that that they are most naturally "wired" to adhere based on their unique individual strengths.

EXERCISE PRESCRIPTION

It is important to understand previous research relating successful cancer rehabilitation to physical activity. The research on this topic is extensive. Several different studies have been conducted to see if there is a positive correlation between physical activity and cancer rehabilitation. Additionally, experimental studies to determine if there is a cause and effect relationship between the variables of exercise and mortality and relapse rates have been conducted. Four main areas of benefits have been identified. These include physical, psychological, social and cancer specific benefits.

Researchers have conducted studies that suggest that increasing physical activity, both during and after treatment, has physical benefits (Bulmer, 2012; Courneya, 2007; Korstjens, 2011). These benefits include regaining range of motion, increased strength and flexibility, improved sleep cycles, increased aerobic fitness, decreased body mass, increased lean body

mass, and less joint pain. Another important, and immediate, benefit of moderate to high intensity exercise is the reduction in side effects due to cancer treatment, such as nausea, joint pain, fatigue, and muscle tension (Mcgrath, Joske, & Bouman, 2010; Denmark-Wahnefried, 2006). Many people with cancer are not aware of how to properly and safely exercise, especially if they are in the middle of treatments (McGrath et al., 2010).

Psychological benefits of physical activity have been reported as well. Participants viewed exercise as a way to regain control of their lives, as well as, an attempt to gain a small amount of control over their disease. Exercise acts as a positive counterbalance to the toxic chemotherapy that is trying to attack the cancer, but in turn, harms their bodies (Bulmer, Howell, Ackerman & Fedric, 2012). Exercise is viewed as a way to move forward in life. Research findings suggest that patients in the post-treatment stages of cancer reported wanting to push cancer into their past. Exercise allowed them to start a new program in life with new goals, rather than goals that only have to do with beating cancer (Clough-Gorr, Rawowski, Clark, & Silliman, 2009). Additionally, exercise is an effective stress outlet for participants. For cancer patients particularly, exercise is an escape from the ominous stress of dying, steep financial responsibility and trying to act happy around family and friends (Bulmer, et al., 2012). In one study, a physical activity group, called the "Chemo Club," reported benefits of exercise such as increased personal meaning, increased morale, decreased anxiety, decreased depression, a more comfortable exercising environment compared to a gym, and a regained sense of control (McGrath et al, 2010). Researchers with the "Chemo Club" stated that the expected time to feel improvement in physiological state, due to physical activity, takes roughly 20 minutes (Rendi et al., 2008). The purpose of many of these studies was to show that, in addition to physiological benefits, psychological benefits have also been reported which help cancer patients mentally push through

the emotional and physical deterioration that cancer causes (Bulmer et al., 2012; Clough-Gorr et al., 2009; Rendi et al., 2008).

Further studies examined the benefits of physical activity on the social lives of people with cancer. People reported having a more normalized experience when they were surrounded by other people going through the same or similar situations (McGrath, et al., 2010). Participants reported that being around others with cancer, in an environment other than the hospital, was relieving. Patients reported feeling exhausted after having to act like they were feeling fine in front of family members. This stemmed from family who did not completely understand that cancer makes you feel awful and scared of the unknown (Bulmer et al, 2012). There are days that people do not feel motivated to beat cancer and it can be difficult constantly pretending like they are. Because patients socialized with other people while in their workout classes and formed lasting relationships while sharing this common life event, in the "Chemo Club" study participants did not feel bad or embarrassed about not exerting themselves on days when they were feeling ill. They knew others sympathized (McGrath et al, 2010).

Benefits of exercise that relate directly to cancer include decreased chance of relapse and longer life expectancy. Weight gain and increase in total body fat percentage have been linked to relapse, shortened survival rates and increased risk of comorbid conditions (Denmark-Wahnefried, 2006). Comorbid conditions are additional health conditions that develop because of a previous condition or disease. Being overweight and sedentary prior to diagnosis has been linked to an increased risk of being diagnosed with cancer (Holmes, Chen, Feskanich, Kroeke & Coldits, 2005). Previous studies suggest that, for patients with cancer, a larger reduction in mortality occurs in individuals that are of normal weight compared to individuals that are overweight. (Zhong, Jiang, Ma, Zhang, Tang, Chen & Zhao, 2014). It has also been speculated

that weight gain is negatively correlated with self esteem and quality of life. This decrease in self esteem due to weight gain can be detrimental to cancer patients that feel as if they are fighting for life (Courneya et al, 2007).

When someone transitions to being a survivor of cancer, rather than a current cancer patient, they are often motivated to make major lifestyle and behavioral changes (Spellman et al, 2014). It is at this point that physical activity should be encouraged as a behavioral change. If medical professionals inform patients about all the benefits that physical activity can provide, patients are more likely to hear it and incorporate it into their lives (Spellman et al, 2014). Spellman, Craike and Livingston (2014) conducted a study in which they found that while doctors may provide verbal advice to encourage patients to undertake an exercise regimen, they rarely provided written benefits. Many doctors reported that prescribing physical activity was not part of their duty to the patients during the time they spend together in the appointments. Doctors who were described as prescribing some type of exercise to their patients were described as older, confident in providing advice, knowledgeable about risks and convinced that exercise helps (Spellman et al, 2014).

A study conducted by Holmes, Chen, Feskanich, Kroeke and Coldits (2005) was the first to provide guidelines regarding the amount and type of exercise, which might be adequate for obtaining a reduced risk of dying from breast cancer. These guidelines suggested women who walked an hour or more in a week had a better survival rate, with maximal benefits for women who walked 3 to 5 hours a week. A similar study was conducted in men and women with colorectal cancer, and a similar reduction in mortality rates was found (Meyerhardt, Giovannucci, Holmes, Chan, Chan, Colditz, et al, 2006).

Ideally, doctors would like to tell patients that proper exercise and nutrition will absolutely slow progression of cancer and risk of relapse, but research has not yet proven it as absolute fact (Holmes et al, 2005). Instead doctors, nurses, physical therapists and personal trainers need to be able to effectively motivate their patients to exercise even though it is not a statistically proven way to stop the cancer. If medical professionals can gain better insight into what people perceive about their well-being and fitness levels, they can better communicate how important exercise is in a way that holds meaning to each individual (Clough-Gorr, et al, 2009).

Results from research suggest that all parts of a healthy body and mind are aided with the addition of physical activity to daily lives of patients with cancer. Physiological benefits include increased range of motion, strength and aerobic fitness (Bulmer et al., 2012, McGrath et al., 2010). Psychological benefits include a stress outlet, a sense of gaining control of their lives, and increased personal meaning (Bulmer et al., 2012, Clough-Gorr et al., 2009, Rendi et al., 2008). Social benefits include surrounding themselves with people who can empathize with what they are going through and making life long friends who share a common experience (McGrath et al, 2010). Benefits of exercising in the cancer community include a decreased risk of relapse and mortality in physically active people and a decreased chance of weight gain which can lead to comorbid conditions (Holmes, et al., 2005, Zhong, et al., 2014). Spellman, Craike and Livingston (2014) found that the older, more confident, and knowledgeable about the risks involved, the more likely physicians were to prescribe exercise to patients. By understanding ways to best prescribe exercise to those with cancer based on their unique strengths of personality, doctors may be more effective in decreasing the effects of cancer and cancer treatment and in increasing patient overall wellbeing.

METHODS

The purpose of this research was to understand the connection between patient's strengths of personality and their motivation to stay physically active during and after treatment. Data collection consisted of a series of two structured surveys. One survey was created to collect demographic information as well as to understand participant's experiences with exercise and exercise prescription. This survey was administered through Survey Monkey to a convenience sample of participants. For participants providing a name and email address, a second survey was administered. The Professional DynaMetrics ProScan survey was used to gather data on each participant's strengths of personality. The participants for this research were people between the ages of 18 and 65 who have, or have had, any type of cancer in the past five years.

Data analysis consisted of both quantitative and qualitative methods. Survey Monkey will analyze the data to reveal descriptive statistics. Qualitative methods of constant comparison, triangulation and text analysis were used to reveal themes. PDP ProScan results will be analyzed by Professional DynaMetrics Programs.

INSTRUMENTS

Every person who is prescribed exercise has a unique set of traits that encompasses their strengths of personality. While previous research has focused on understanding exercise patterns relating to personality, this study will attempt to understand the connection between strengths of personality and the experience of exercise.

The fact that every person has a completely unique personality is extremely intriguing. Knowing that each person is different suggests that each person is motivated differently. If basic personality traits can be better understood maybe that will lead to key ways those type of people can be motivated to exercise. Professional Dynametric Programs (PDP) ProScan® Survey is a

survey developed in 1977 to provide a statistically validated quantitative measurement of personality. The PDP was administered to an original sample of 1,024 persons that represented a cross section of adults. The survey consists of a list of 60 descriptors that allow subjects to rate themselves on a 1 to 5 Likert scale.

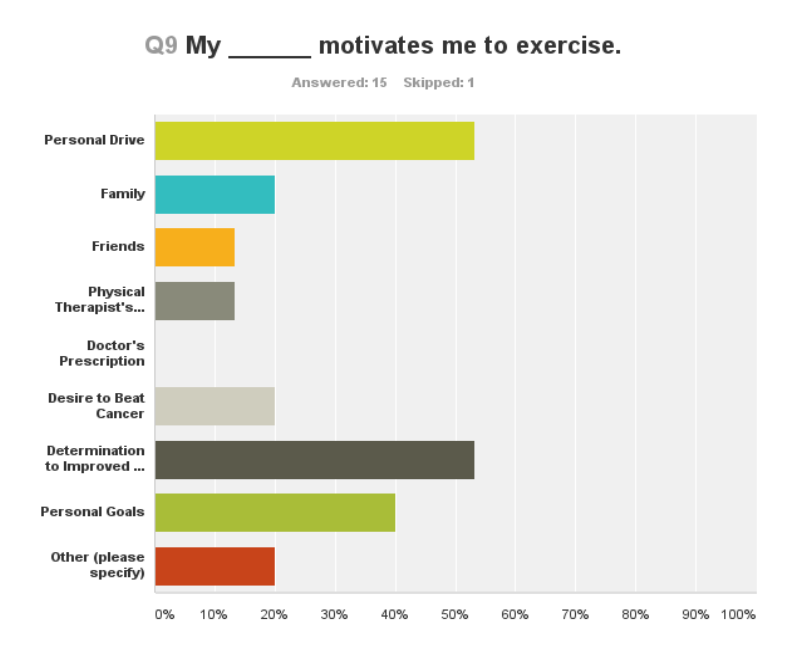
The ProScan has been administered to over 4.5 million people. Data from each survey in is statistically analyzed against this database. PDP's survey instruments have intrinsic and extrinsic validity, with coefficients of reliability above .94. Results of the ProScan survey reveal three perspectives of a person's strengths. The Basic/Natural Self is the most instinctive way that a person thinks, feels, and makes decisions. The Basic/Natural self measures seven metrics; dominance, extroversion, pace/patience, conformity, logic, energy styles, and kinetic energy. The Priority environment is how that person changes their basic natural self to fit a situation. This changes in a job, position of authority, position of lower authority and around groups of people. This environment is quantified in terms of energy drain. In order to adjust your personality you will need to supply energy to change it. This is measured and shows the amount of energy you are spending to adjust that characteristic and how satisfied you are with how you are with your adjusted personality. The Predictor/Outward Self is the third category the survey quantifies how others view that person's outward personality.

According to PDP, high scores in dominance suggest a type of person who is task oriented, competitive and enjoys risk-taking behaviors. A person low in dominance would be careful, evade confrontation and risky situations. A person high in extroversion would be persuasive, welcoming, and people oriented. A person low in extroversion would be shy, quiet and introverted. A person with a high trait of pace would show dependability and stability while also being relaxed and likeable. A person low in pace would show intensity and a sense of

urgency in tasks. A high score of conformity would suggest the person is very structured and accurate in projects; while a person low in conformity would signify independence, open-minded and does not fit a routine oriented lifestyle (Hubby, et al., 2003).

Because each high trait is important in predicting behavior of the person, health care professionals can appeal to that strong trait in order to help with their delivery mechanism in exercise prescription. The basic/natural self and priority environment categories are the most important for the purpose of this study. It will showcase how the person is at their core as well as how the person's personality has changed due to the stress of cancer on their lives.

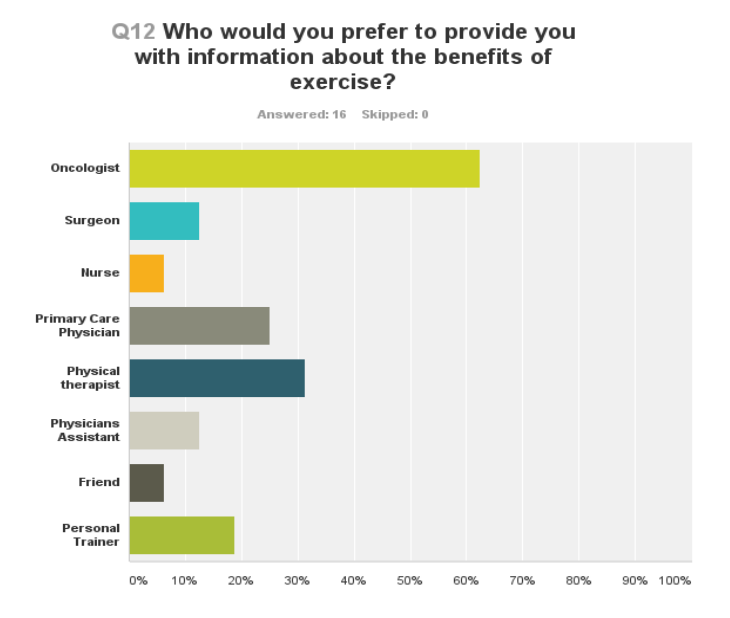
RESULTS



<u>Figure 1: Motivational Factors:</u> Figure depicts where the motivation to exercise comes from within the original population of 16. Determination to improve quality of life, personal drive and

obtaining personal goals ranks highest. None were motivated by a doctor's prescription. Other category was selected with the explanations below.

- "watching others deteriorate"
- "Desire to lose weight"
- "Mental clarity/balance"



<u>Figure 2: Motivational Person:</u> Bar graph exemplifies the person who each participant is more likely to listen to when being prescribed exercise. Oncologist was at the top of the list. Physical therapist and Primary care physicians were second. Friends and nurses were chosen the least, most likely due to the fact that they are not experts in the field in question.

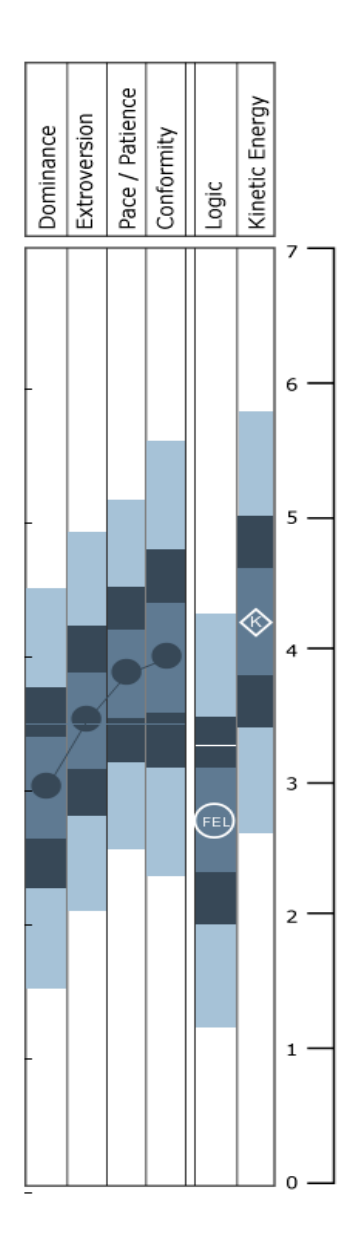


Figure 3: Composite Model of Participants based on PDP ProScan® Results.

Explanation of behavior if there were no outside pressures for adjustment. Functioning at the most natural and efficient level. This graph is an example of each person composed together.

This population has a high trait of Conformity and a low trait of Dominance.

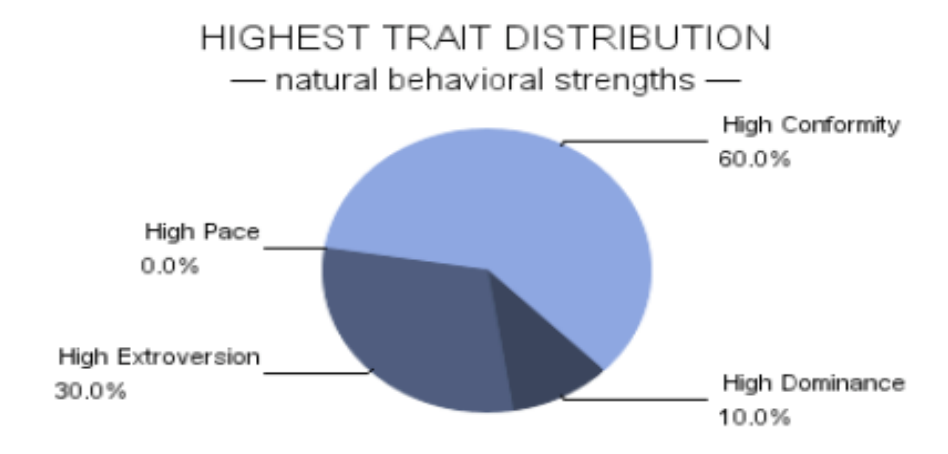


Figure 4: High Trait Distribution:

Figure depicts that 6 out of the 11 participants showed a high trait of conformity. High trait of conformity characterizes a person as procedural, precise, conscientious, careful, prudent, loyal, meticulous and dedicated.

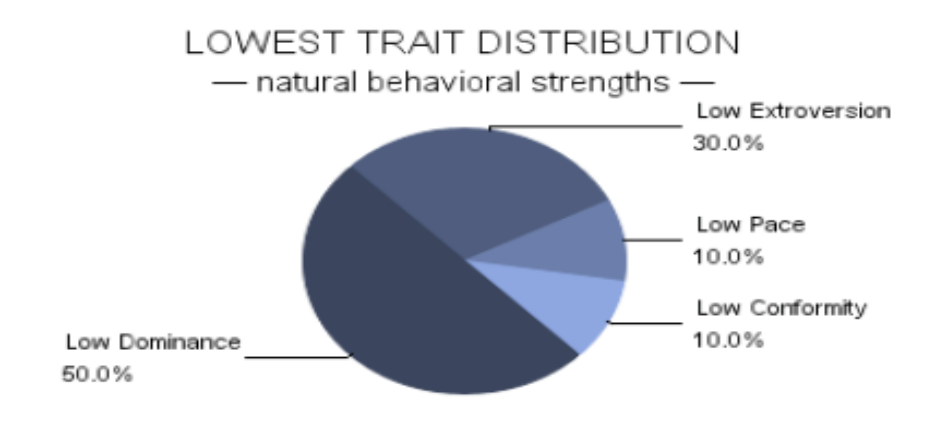


Figure 5: Low Trait Distribution:

Figure represents the populations low trait distribution.5 out of 11 participants had a low trait of dominance. Low trait of dominance characterizes a person as supportive, collaborative, moderate, accepting, helpful and non-controlling.

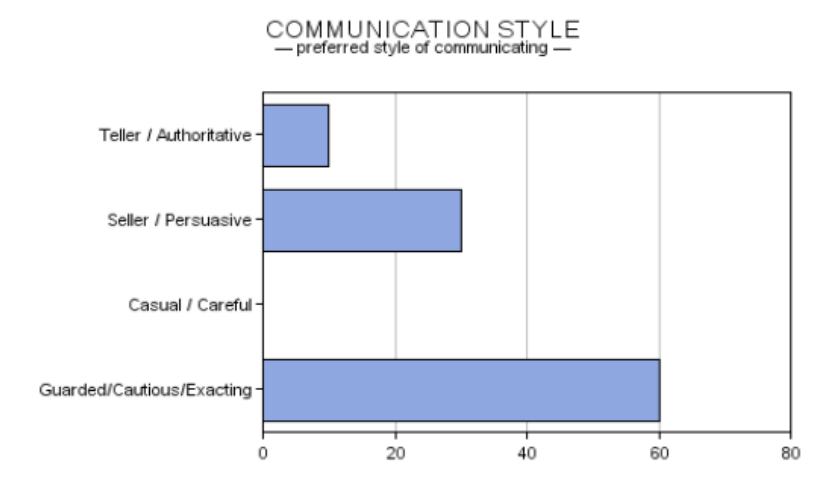
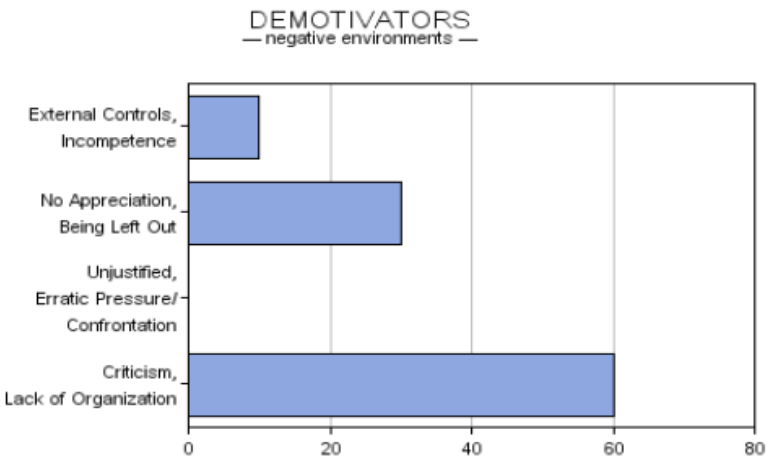


Figure 6: Preferred Communication Style:

Chart exhibits distribution of participants communication styles. Most participants use a mildly persuasive style of communicating when speaking with others. Are often concerned and conscientious. They prefer to be communicated with is a way that provides procedures and systems, with respectful language and tone of voice with written guidelines. 27.3% of participants showed a communication style of seller/persuasive. These people are convincing and influential. They enjoy talking, speak positively, motivationally and are encouraging when they communicate. They prefer to be communicated with in a way that is friendly, gives recognition and being included in team discussions.



<u>Figure</u> <u>7:</u>

Demotivators:

Figure is an example of the kinds of situations that demotivate a person. 60% of participants had demotivators in the criticism category. These people do not respond well to criticism, lack of organization or incompetent leadership. The list of demotivators are very useful when prescribing exercise to patients.

CONCLUSION

From the data shown in the results section themes were gathered and analyzed. Below are the four themes collected that allude to the relationship between strengths of personality and motivation to exercise.

Theme 1- Listen to concise information

Referencing figure 4 it can be seen that 6 out of the 11 participants from the study were high traits of pace and conformity. Conformity characterizes a person as concerned, thoughtful, structures, prudent and system-oriented, detailed and accurate. These people expressed on the questionnaire that they would prefer to be "provided with a system of exercise that is specific and detailed." This answer speaks to the fact that they are a high trait in conformity type of person.

Theme 2- Motivators vs Demotivators

Many of the participants had an array of situations they consider demotivating, reference figure 7. Many do not respond well to criticism, lack of organization, feeling left out, not being appreciated. 2 of the 11 participants were demotivated by things such as external controls and incompetence of people they are working with. Within the scope of clinical practice medical professionals need to understand what types of things demotivate their patient because everyone is drastically different. By taking a quick questionnaire about what motivates each patient, figure 1, medical professionals can make a care plan that appeals to the patient's wants and needs, while simultaneously making a conscious effort to avoid demotivating factors.

Theme 3- Preference for Experts

This study's population consisted of a majority of people with Pace and Conformity above the midline, reference figure 3. A person high in pace is characterized by a persistent, cooperative and harmonious persona. They are patient, steady, unhurried and good listeners. They put their trust in a person who is an expert in the field in question. People in this study who had high Pace traits responded to the question of who they would prefer to be prescribed exercise by with answers such as: Oncologist, Physical Therapist and Personal Trainer. Due to the fact that the survey was about exercise and cancer these people would put their trust in those particular experts. Within a clinical setting this theme can be used by proving to the patient that as a person giving them medical and exercise advise that you are in fact an expert in the field. This allows patients to trust more in what is being said and adhere to the exercise program suggested.

Theme 4- Communication Styles

Figure 6 shows the preferred communication styles of each participant. 54.5 % of the population has a style of guarded/cautious and exacting, 27.3% were seller/Persuasive. This particular finding helps explain why it is not only important to know and understand your patients communication style but also to know your own. Medical professionals should know how they prefer to communicate and adjust that delivery of communication to how their patient prefers to communicate.

Combining Themes into a comprehensive message

Results of this research suggest that understanding patient strengths of personality would be beneficial when working in the cancer community particularly in prescribing a comprehensive care plan. Combining knowledge in all areas found from this research can assist medical professionals to effectively motivate their patients to exercise. By analyzing personality carefully in order to make a care plan based on strengths, preferred communication, and demotivators, medical professionals can better customize their care plans to specific strengths of their patients. Additionally, by understanding who the patient finds most influential concerning the topic of cancer and exercise would potentially increase the amount of time their patients spend exercising. Since recent research has suggested that risk of mortality in patients diagnosed with cancer is less within normal weight limits then in overweight patients (Zhong, 2014), by understanding what makes each patient "tick" the risk of relapse and mortality rates will potentially decline.

Future research on this subject should include a study that is statistically significant with random assignment of participants to two groups. The first group would have individualized programs that appeal to each person's strengths of personality. The second group would all be on the same exercise program delivered in one specific communication style. This type of project will show if the delivery of the program is what is important when getting people to adhere to an exercise program.

The trend seen within the population studied was a high trait in Conformity. Further research should be done to investigate if there is a trend in personalities among people diagnosed with cancer. If there is a relationship between cancer and personality, what specifically is the connection?

ACKNOWLEDGEMENTS

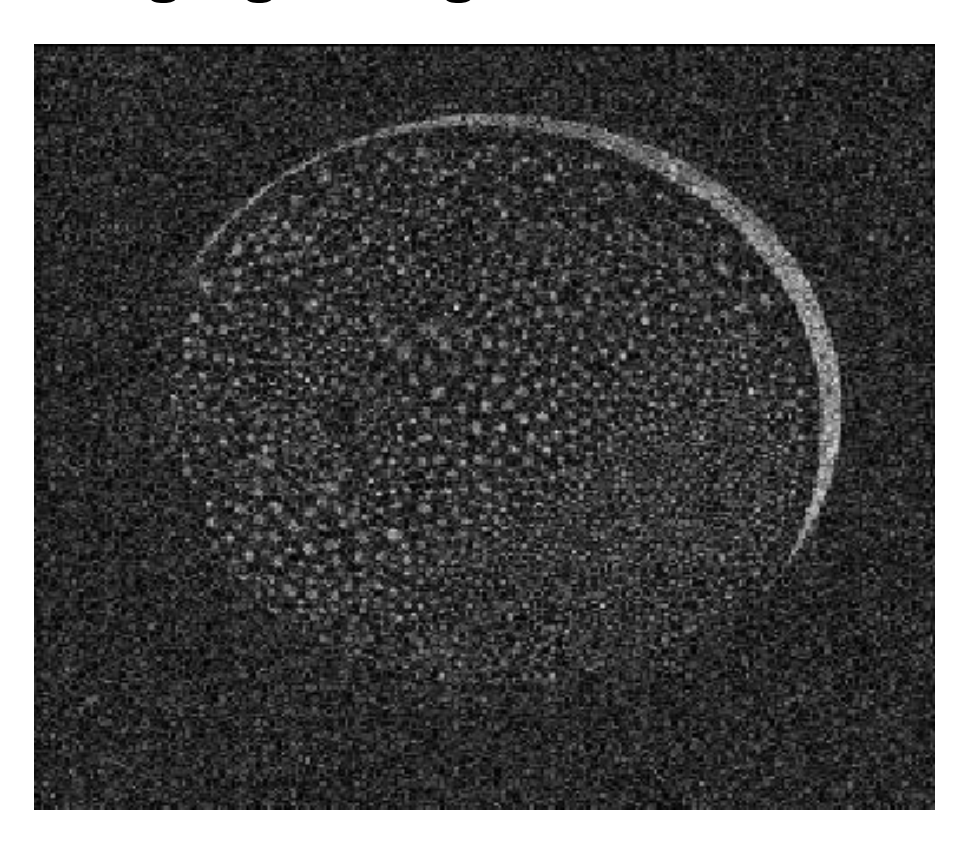
This work was supported by the McNair Scholars program (U.S. Dept. of Education grant #P217A130148).

REFERENCES

- American Cancer Society, (2014) Cancer Facts and Figures 2014. Retrieved from: http://www.cancer.org/acs/groups/content/@research/documents/webcontent/acspc-042151.pdf
- American Cancer Society. (2015) Cancer Facts and Figures 2015. Retrieved from: http://www.cancer.org/acs/groups/content/@editorial/documents/document/acspc-044552.pdf
- Bulmer, S.M., Howell, J., Ackerman, L., Fedric. R. (2012) Women's Perceived Benefits of Exercise During and After Breast Cancer Treatment, *Women & Health*, 52:8, 771-787
- Clough-Gorr, K. M., Rakowski. W., Clark. M., Silliman, R.A., (2009) The Getting-Out-Of-Bed (GoB) Scale: A Measure of Motivation and Life Outlook in Older Adults with Cancer, *Journal of Psychosocial Oncology, 27:4, 454-468.*
- Courneya, K.S., Segal, R.J., Gelmon, K., Reid, R.D., Friedenreich, C.M., Ladha, A. B., P. C., V. J., L. K., Y. Y., McKenzie, D.C., (2007) Effects of Aerobic and Resistance Exercise in Breast Cancer Patients Receiving Adjuvant Chemotherapy: A Multicenter Randomized Controlled Trial. *Journal Of Clinical Oncology* 25:8 4396-4404
- Denmark-Wahnefried, W., (2006) Cancer Survival: Time to Get Moving? Data Accumulate Suggesting a Link Between Physical Activity and Cancer Survival. *Journal Of Clinical Oncology* 24:22 3517-3518
- Gordon, N. F., Gulnick, M., Costa, F., Fletcher, G., Franklin, B. A., Roth, E., Shephard, T., (2004) Physcial Activity and Exercise Recommendations for Stoke Survivors. Retrieved from http://circ.ahajournals.org/content/109/16/2031.full
- Holmes, M. D., Chen, W, Y,. Feskanich, D., Kroeke, C.H., Coldits, G.A., (2005) Physical Activity and survival after breast cancer diagnosis *The Journal of American Medical Association*. 293:20 2479-2486
- Kordtjens, I., Mesters, I., May, A.M., Van Weert, E., Van Der Hout. J., Ros. W., Hoekstra-Weebers, J., Van Der Schans. C., Van Der Borne, B., (2011) Effects of Cancer Rehabilitation on Problem-Solving, anxiety and depression: A RCT comparing physical

- and cognitive-behavioral training versus physical training. *Psychology and Health 26, 63-83.*
- Mayo Clinic Staff, (2014) Exercise: 7 Physical Benefits of Regular Physical Activity. Retrieved from http://www.mayoclinic.org/healthy-living/fitness/in-depth/exercise/art-20048389?pg=1
- McGrath, P., Joske, D., Bouman, M., (2010) Benefits from Participation in the Chemo Club: Psychosocial; Insights on an Exercise Program for Cancer Patients, *Journal of Psychosocial Oncology*, 29:1, 103-119
- Meyerhardt, J.A., Giovannucci, E. L., Holmes, M. D, Chan, A.T., Chan, J.A., Colditz, G. A., Fuchs, C.S., (2006) Physical Activity and Survival after Colorectal Cancer Diagnosis. *Journal of Clinical Oncology* 24 3527-3534
- Paramanandam, V. S., Roberts, D., (2014) Weight Training is not harmful for women with breast cancer-related lymphoedema: a systematic review. *Journal of Physiotherapy 60:3 136-143*
- Rendi, M., Szabo, A., Szabo, T., Velenzei. A., Kovacs, A., (2008) Acute Psycological Benefits of aerobic exerciseL A field study into the effects of exercise characteristics. *Psychology, Health and Medicine 13: 2 180-184*
- Spellman, C., Craike, M., Livingston, P., (2014) Knowledge, attitudes and practices of clinicians in promoting physical activity to prostate cancer survivors. *Health Education Journal*, 73:5 566-575
- Zhong, S., Jiang, T., Ma, T., Zhang, X., Tang, J., Chen, W., Zhao, J., (2014) Association between physical activity and motality in breast cancer: meta-analysis of cohort studies. *European Journal of Epidemiology 29 391-404*

Formation and Magnetic Resonance Imaging of Alginate Gels



McNair Scholar: Amanda Parsons^{a,b}
McNair co-mentors: Elmira Nybo^a, Sarah L. Codd, Ph.D.^{b,c}, and Joseph D. Seymour, Ph.D.^{a,b}

College of Engineering Montana State University Summer 2015

^a Chemical and Biological Engineering, Montana State University, Bozeman MT 59715

^b Center for Biofilm Engineering, Montana State University, Bozeman MT 59715

^c Mechanical and Industrial Engineering, Montana State University, Bozeman MT 59715

Formation and Magnetic Resonance Imaging of Alginate Gels

Amanda Parsons^{a,b}, Elmira Nybo^a, Sarah L. Codd^{b,c}, and Joseph D. Seymour^{a,b}

College of Engineering Montana State University Summer 2015

Abstract

Alginates are biopolymers extracted from the cell walls of brown algae and some strains of bacteria. In the presence of a divalent cation such as copper or calcium, the alginate forms a gel structure. These gels are useful for many applications such as waste water treatment and tissue engineering [1-3]. Using nuclear magnetic resonance (NMR) imaging however, it is possible to view the structure of the gels in a non-invasive way. With these images the structural differences between the copper and calcium heterogeneous gels as well as clearly see no real structure in the homogeneous gel. NMR uses radio frequency energy to excite the nuclei of atoms such as hydrogen ¹H in order to record the amount of signal obtained from these excited nuclei. The purpose of this research is to learn the process behind creating these gels as well as the technique of imaging them in order to see the structure of the gel formed, and to look at the velocity profiles formed from flow through gel plugs.

^a Chemical and Biological Engineering, Montana State University, Bozeman MT 59715

^b Center for Biofilm Engineering, Montana State University, Bozeman MT 59715

^c Mechanical and Industrial Engineering, Montana State University, Bozeman MT 59715

Table of Contents

Abstract	ii
Introduction	1
Background	
Alginate Structure	1
Nuclear Magnetic Resonance	2
Materials and Methods	
Heterogeneous Gels	3
Homogeneous Gels	3
Gel Plug and Flow System	4
Imaging and Velocity Imaging Procedure	4
Results	
Gel Formation	5
Imaging and Troubleshooting Procedure	5
Velocity Imaging	7
Discussion	8
Conclusion	9
Acknowledgements	10
References	11

Introduction

Algal alginate is a biopolymer extracted from the cell walls of brown algae. It is used in a variety of applications including but not limited to: pharmaceuticals such as wound dressing, encapsulation for drug delivery, as well as tissue engineering [4-7]; waste water treatment to absorb heavy metals present in industrial waste [8-10]; and in the food industry as a thickening agent, for texture modification, and recently to potentially reduce obesity [11]. Brown algae isn't the only source for alginate, there are also certain strains of bacteria, including Pseudomonas aeruginosa, which secrete bacterial alginates. One such secretion is found in the lungs of cystic fibrosis patients [12].

The alginate solution will form a gel in the presence of a divalent cation. The method the cation is introduced, slowly or quickly, determines which type of gel is formed, heterogeneous or homogeneous, respectively [13]. While little is known about the uses of homogeneous gels, heterogeneous gels have been studied quite a bit since it has been found that if the cation is introduced slowly enough capillaries form [13]. These capillaries are of such interest because they are similar to those that naturally occur in nature.

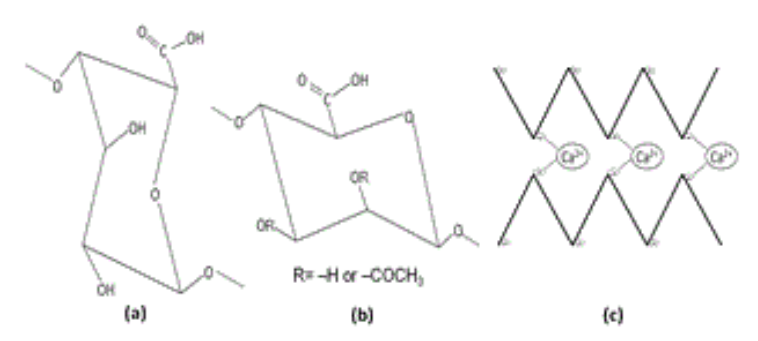


Figure 1: The structures of the polymers the alginate is comprised of and the structure of the gel. (a) The G units. (b) The M units. (c) The egg box structure that is formed in the presence of the cation [2, 3].

The purpose of this research is to provide a basic overview of the known chemistry and methods of this gel formation. As well as provide a background in these gels so as to better assist the current PhD student in the lab with her project on these gels where pressure driven flow is involved.

Background

Alginate Structure

The alginate is composed of two types of polymers α-L-guluronate (G units) (Figure 1a) and β-D-mannuronate (M units) (Figure 1b) joined by a β -1-4-glycosidic linkage; the order of which these polymers are organized depends on where the alginate came from [3]. As can be seen from Figure 1 the main differences between the α-L-guluronate and the **β-D-mannuronate** is the β-Dmannuronate may have different functional group attached to the oxygen atoms bonded to the 2 and 3 carbons than that of the α-Lguluronate.

When a divalent cation such as calcium is introduced into the alginate, the G units will bond with one another forming GG blocks. Multiple GG blocks will bind together into egg box structures (Figure 1c) as demonstrated by Grant et al. [14] trapping a cation in each individual box formed. Though

more recent research has shown that MG blocks, a G unit binding with an M unit, are also important in the formation and structure of the gels [14]. While all of this is known about the polymer structure, the mechanism of formation is still not well known. There have been proposed theories such as a Rayleigh-Bénard-like instability [15] and more recently spinodal decomposition [13] to model the gel formation.

Nuclear Magnetic Resonance

Nuclear magnetic resonance (NMR) spectroscopy is a non-invasive imaging technique that uses radio frequency energy (rf) to excite atomic nuclei and measure the signal during the relaxation of the these nuclei. A common nuclei used is hydrogen [16].

In the spectrometer there are three coils, these coils are important as each coil creates its own magnetic field using basic physics principles electromagnetism. of outermost of the three coils creates the main magnetic field referred to as Bo. This field aligns all of the nuclei in the same direction so that all of the signal measurements are taken from the same point of reference. The rf coil is attached to a probe that is inserted in to the magnet. It is removable in order to be able to center the sample in the middle of the coil before attaching the coil to the probe and then placing sample and probe in the spectrometer. The rf coil both creates an oscillating magnetic field and receives the voltage generated by the precession of the nuclei. The oscillating field generated is referred to as B₁ and in order to ensure the maximum signal is obtained from the precessing nuclei, the B₁ field is usually applied as either a 90° pulse, where the nuclei are rotated 90° from their initial position in B_o or they are rotated a full 180° with an 180° pulse. The last coil, the middle one, is different than the other two, whereas the coil is wrapped uniformly on the other two it is not the case for the middle coil also known as the gradient coil. The gradient coil is wrapped around the bore hole of the magnet in such a way that the magnetic field can be manipulated in three direction, x, y, and z by changing the current sent to the coil [17].

Applying rf energy to the sample and exciting the spins from thermodynamic equilibrium, it is possible to track the movement of the hydrogen nuclei and determine their location at any given time. The data received from the spectrometer has

to be Fourier Transformed at every data point in order to create images [18, 19]. Depending on how the data is collected, two different types of images can be created, static and dynamic.

In static imaging, data is collected in k space and then Fourier Transformed to create an image. Dynamic NMR uses q space to record data. The difference between k and q space is where k space collects the information about the nuclei position and records it in both real and imaginary. q space only records the data that is in real space. In a dynamic NMR experiment a sample is exposed to a magnetic field gradient which then gives off a phase shift. Signal collected can then be Fourier Transformed to produce parts of real and imaginary images. Each

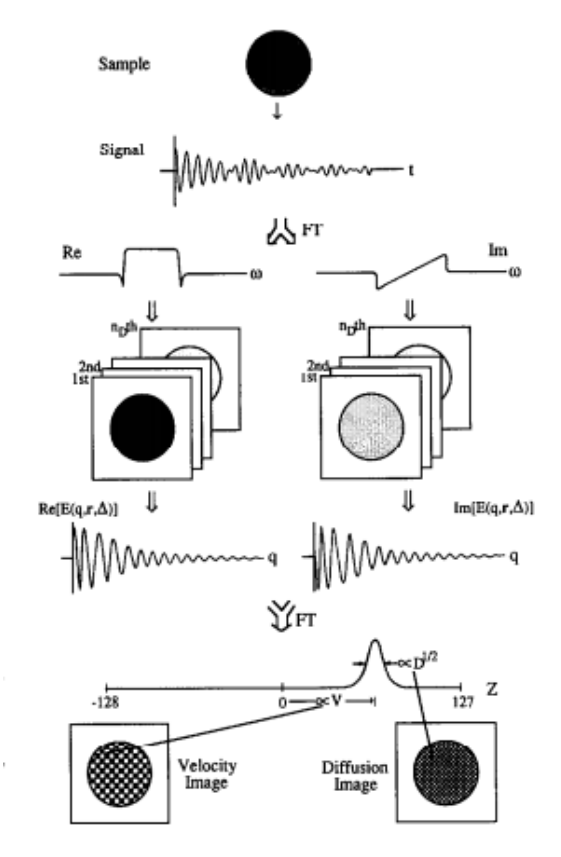


Figure 2: The progression of steps in the NMR experiment for a dynamic image. This image was taken from "Velocity and Diffusion Imaging in Dynamic NMR Microscopy" by Callaghan and Xia [1, 2].

image represents a step in q space. Using these multiple slices, it becomes possible to create lines of signal by tracking the change of signal strength at each pixel. In Figure 2, above these lines are shown to be continuous, but actually they are discreet. These lines of signal are referred to as q space FIDs, and they undergo another Fourier Transform creating another line of signal with only one peak. Computations are then performed on the signal allowing for both diffusion and velocity images to be created [2].

Materials and Methods

Heterogeneous Gels

To prepare the sample gels first alginate solution and ion solutions had to be created. For the heterogeneous gels a 1.5 wt% alginate solution in a 0.1 M NaCl was used. This was created by stirring alginic acid, sodium chloride and deionized water for 24 hrs. at room temperature to ensure all of the alginate had been mixed in. Afterwards it was immediately placed in the fridge to prevent bacterial growth. The calcium (II) chloride or copper (II) chloride solutions were made to a 0.5 M solution by stirring the compound with deionized water until dissolved.

Before the gel could be created, 11.4 mm inner diameter test tubes had to be coated with the alginate solution. To do this, alginate solution is painted on the inside of the test tube, and left to dry in a furnace for an hour at 110°C. This is repeated two more times to ensure there's alginate on the walls, necessary to prevent the gel from pulling away from the walls later. Approximately 2 mL of alginate was then placed in the test tubes and left over night in a refrigerator to debubble. This step is important when imagining the samples with the NMR spectrometer, since air bubbles disrupt the

homogeneity of the sample and magnetic field. Once the alginate was degased, a membrane was formed on the top of the using the spray mist technique [1] with the metal cation (Ca²⁺ or Cu²⁺) solution. After allowing the membrane to set up, at least 2 mL of the cation solution was placed in the test tube. The test tubes were left sitting out at room temperature as the cation solution diffused through and the capillaries were formed.

Homogeneous Gels

To prepare homogeneous gels however the procedure is quite different since with homogeneous gels, capillaries aren't trying to be formed. A 1 wt% alginate solution was created by mixing deionized water and alginic acid, 2.1 g of alginate was then measured out into an 13 mm test tube (for this type of gel no test tube coating is required), exact measurements are crucial for this type of gel formation. The alginate was left to sit in the test tube to degas overnight, as air bubbles in the gel are undesirable. Then 0.77 mL of 27.5 mM CaCO₃ was added to the test tube and mixed on a vortex mixer until it was evenly dispersed throughout the alginate, if it's not the gel won't form properly. With the CaCO₃ dispersed, 0.77 mL of 55 mM gluconic acid δ-lactone (GDL) was added and also mixed into the solution using the vortex mixer. It was mixed until the entire solution had visible been gelled. Once the gel had formed it was placed in an ice bath under a vacuum for an hour to allow the gel to setup. Afterwards it was removed, and air bubbles were visible in gel. The gel was then placed in the refrigerator overnight and bubbles were gone the next day. The gel was left in refrigerator until it was imaged as homogeneous gels keep better there.

Gel Plug and Flow System

Using the heterogeneous gel formation method with a few slight modification previously established by Elmira Nybo, whereby 10 mm OD NMR test tubes are cut to a length of 11 cm creating two open ends. The NMR tubes were then coated in alginate similarly to the heterogeneous procedure. From the bottom, the end that was cut, of the coated NMR tube a polymer plug wrapped in Teflon tape is inserted to create the gel plug

in the middle of the test tube. Two 1.5 mm OD glass capillary tubes are placed in the center held in place by poster tack to form capillaries which penetrate the entire sample as the spontaneously formed capillaries are never that long. Approximately 1.5 mL of alginate is then added to the NMR tube without bumping capillaries; it is then allowed to degas in the refrigerator overnight. Calcium chloride solution (0.5 M) is slowly added to the alginate till the NMR tube is full, then left to sit on the counter as the alginate gels. Once the gel had completely formed, it was then connected to the

flow system where 0.05 M CaCl₂ was flowed through it.

The flow system was a compilation of a pharmaceutical pump. Pharmacia, P-500.

pharmaceutical pump Pharmacia P-500, various sizes of small tubing, and connectors allowing the small tubing from the pump to flow into the NMR tube. All fittings and connectors were wrapped in Teflon tape to prevent any leaks. A glass wool pack and two glass bead packs were later added to the system to reduce the vibrations caused by the pump, as these vibrations were transferring to the sample in the magnet, thereby creating artifacts in the images obtained. To create the glass wool pack a piece of silicon tubing was

packed with glass wool and a filter on each end to prevent the glass wool from clogging up the pump. The glass bead packs were created in a similar manner with filters both before and after the bead packs in order to prevent the beads from moving throughout the system. The system was assembled and tested on the lab bench with any modification before testing it was placed in the magnet.

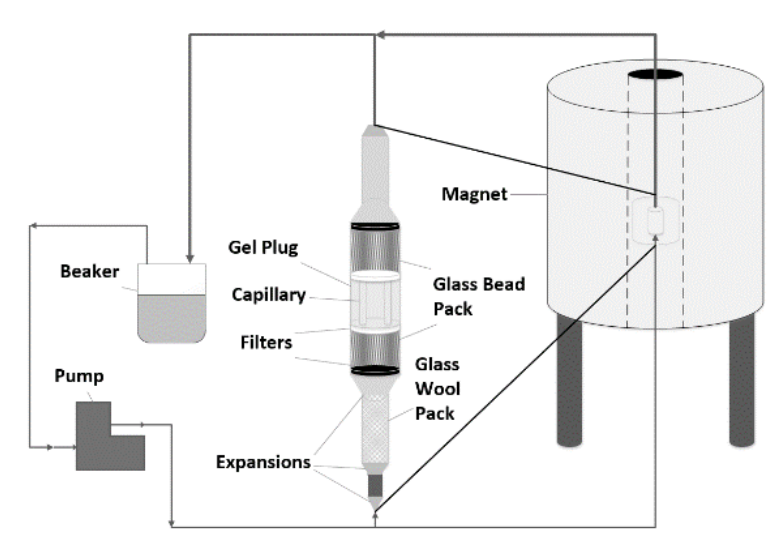


Figure 3: Schematic of the final flow system used when taking the velocity images.

Imaging and Velocity Imaging Procedure

The gels made using the spray mist technique and the homogeneous gels were imaged using a Bruker 300 MHz spectrometer, a micro 2.5 probe, and a 15 mm rf coil. While the gel plugs were imaged using a Bruker 250 MHz spectrometer, with a micro 2.5 probe, and a 10 mm rf coil. To take an image the sample was placed in the rf coil, attached to the probe and loaded into the magnet.

Once all of this has been done, the imaging sequence is ran on both the calcium and copper samples with echo times of 200 ms and 10.567 ms and relaxation times of 1000 ms and 500 ms respectively.

Along with cross sectional and coronal images of the gel plugs, velocity maps were also taken when fluid was flowing through the gel. Initially CaCl₂ was used to troubleshoot the flow system as well as create a baseline for comparison for the CuCl₂ tests. Velocity maps were obtained using the basic slice selective spin echo imaging pulse sequence with magnetic field gradient for displacement measurement.

All images were analyzed in Prospa v3.13, as the data received from the magnet is just either data points in k-space or q-space that need to be Fourier Transformed in order to see the images obtained from the samples.

Results

Gel Formation

Using the three different techniques, two different gel types were successfully made (Figure 4). The possible ways a gel can go wrong during the formation procedures was also observed. Copper gels form faster than the calcium gels do using the spray mist technique, but the homogeneous gels form

the lab bench, but were better seen in the spectrometer.

Imaging and Troubleshooting Procedure

The homogeneous gel was easily able to be imaged and the resulting image (TE = 100ms, TR = 1000 ms, $FoV = 20 \times 15 \text{ mm}$, spatial resolution = $0.78 \times 0.059 \text{ mm/pixel}$, slice thickness = 1.0 mm, matrix size = 256×256) was as homogeneous as the gel appeared to be sitting on the counter. The images of heterogeneous gels weren't as successful as they could have been as when the gel is formed the salt from the cation solution starts to precipitate on the surface of the gel, which reduced the maximum signal that was able to be acquired. The images obtained show that the capillaries in the calcium gel (TE = 50 ms, TR = 1000 ms, FOV = 20 x 15 mm, spatial resolution = $0.78 \times 0.059 \text{ mm/pixel}$, slice thickness = 1.0 mm, matrix size = 256×256) are wider in diameter, shorter in length, and less are formed than the copper gel (TE = 10.67 ms, TR = 500 ms, FOV = 20 x 15 mm, spatial resolution = 0.78 x 0.059 mm/pixel, slice thickness = 1.0 mm, matrix size = 256 x









Figure 4: The different types of alginate gels made using the different procedures from left to right: calcium based gel plug, calcium based spray mist technique gel, copper based spray mist technique gel, and the calcium based homogeneous gel.

even faster than copper as there are no capillaries to form, it gels almost instantaneously. The heterogeneous gel capillaries that were formed were visible on

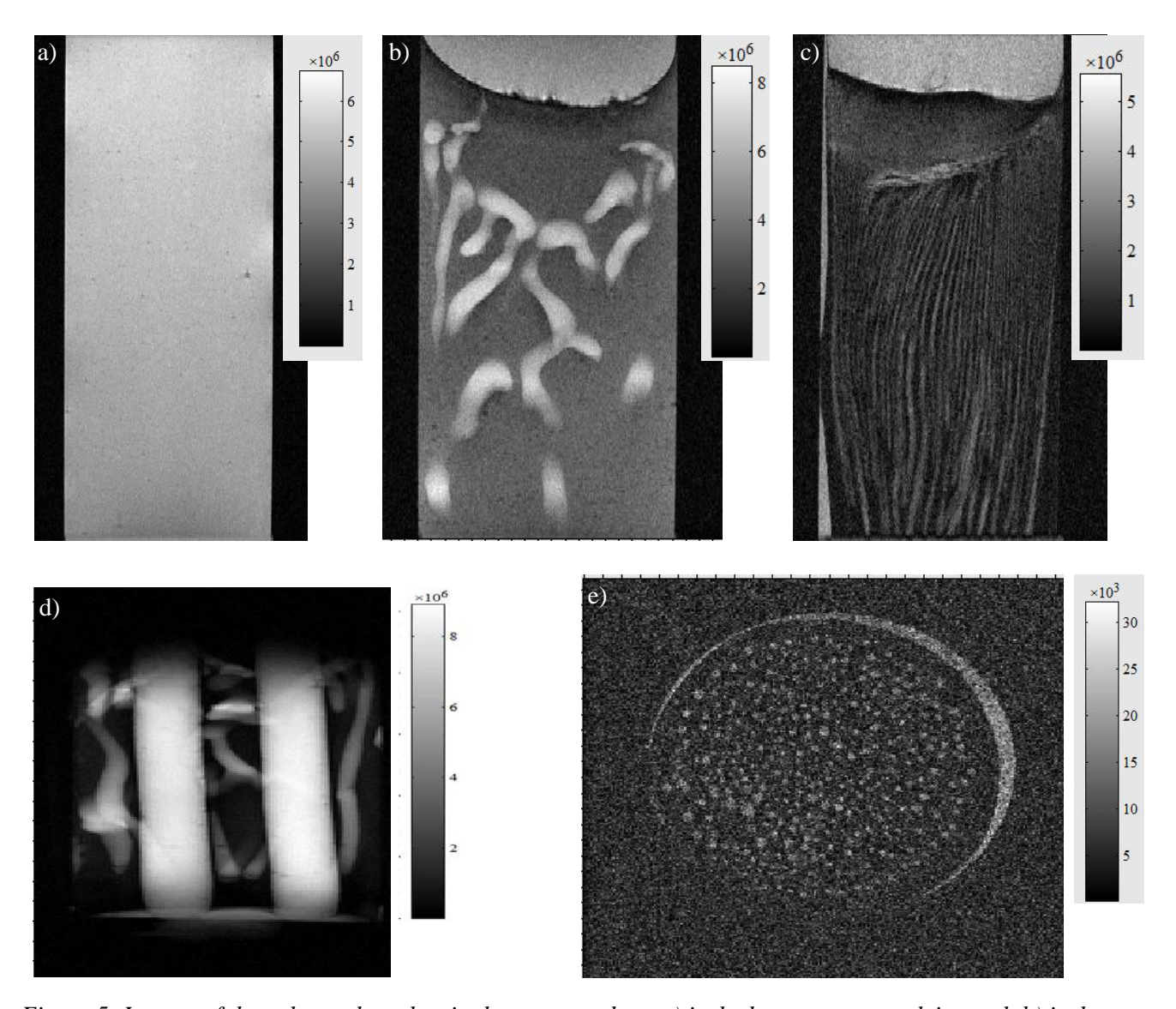


Figure 5: Images of the gel samples taken in the magnet where a) is the homogeneous calcium gel, b) is the heterogeneous calcium gel, c) is the heterogeneous copper gel, d) is a coronal slice of the gel plug, and e) is an axial image of the copper heterogeneous gel.

256) alternative, as can be seen in Figure 5. The cross sectional area of the copper gel (TE = 8.007 ms, TR = 500 ms, # of averages = 4, FOV = 15×15 mm, spatial resolution = 0.78×0.059 mm/pixel, slice thickness = 0.5 mm, matrix size = 256×256) is also shown in Figure 5 to demonstrate that the capillaries are present throughout the sample

While images of the gel plugs were taken without difficulty and both the artificial and spontaneous capillaries could easily be seen, taking the velocity map images proved to be more difficult. At low flow rates, 20 mL/hr or less, a ghosting artifact occurred creating two lines of capillaries going up and down across the axial image where there should have only been two. At higher flow rates, 50 mL/hr or more, the ghosting effects were less however a second artifact developed going sideways across the sample. When a glass wool pack

was added it reduced the amount of ghosting that occurred, but it was still evident. Adding the glass bead packs helped to eliminate the unwanted vibration and applying a filter removed the second artifact proved successful, as can be seen in Figure 7, and experiments of both CaCl₂ and CuCl₂ were able to be conducted.

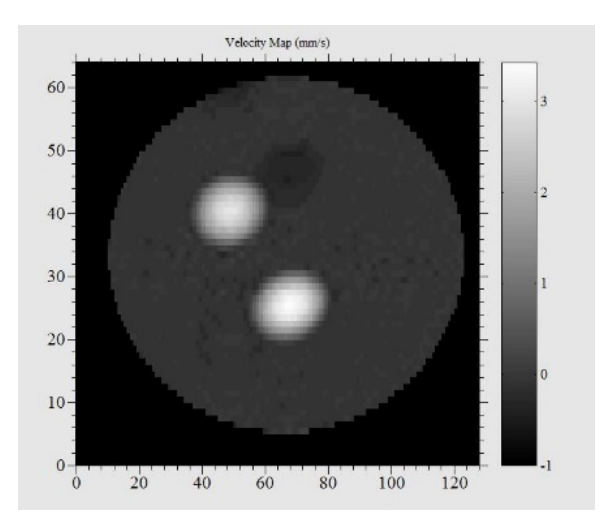
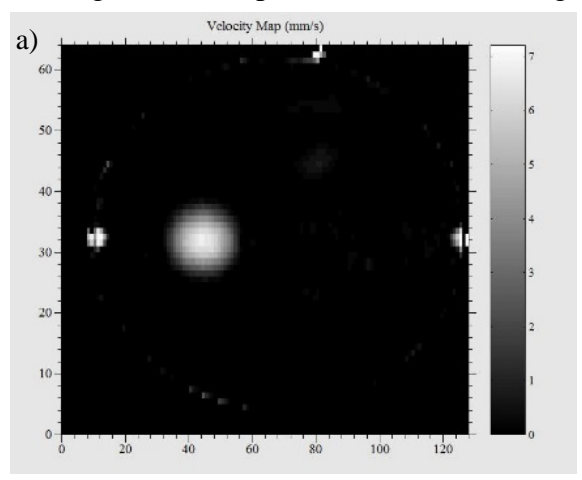
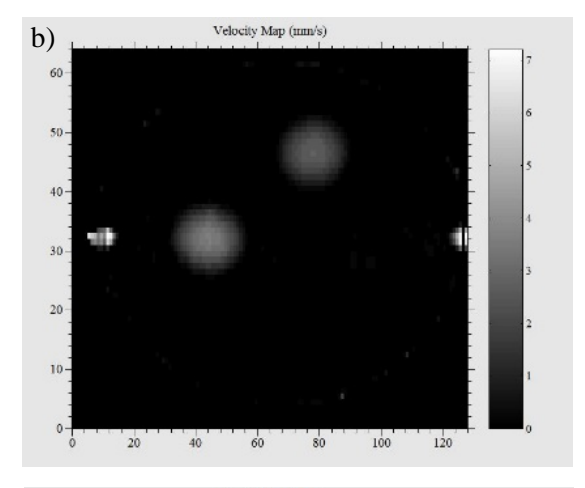


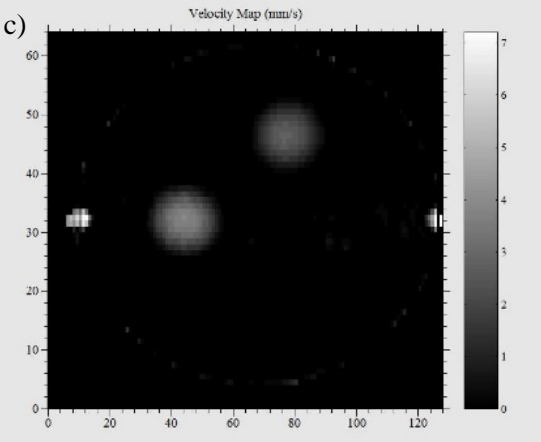
Figure 7: Velocity map of CaCl₂ flowing at 20 mL/hr.

Velocity Imaging

The flow experiment results differed between the two solutions being flowed. With the 0.1 M CaCl₂ solution, the flow was initially only in one capillary with an average velocity of 6.5 mm/s but over time began flowing in both capillaries and the average







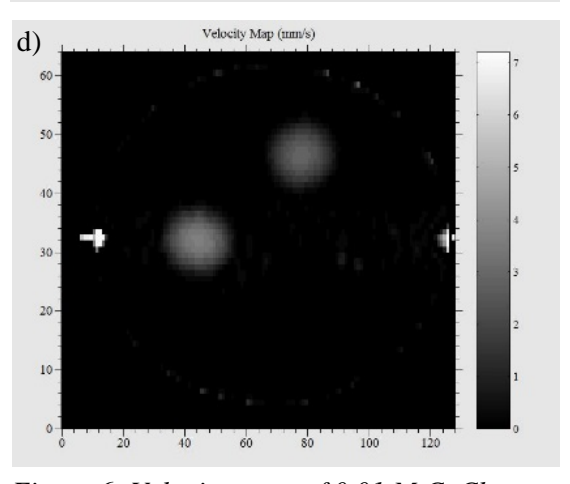


Figure 6: Velocity maps of 0.01 M CaCl₂ at different times throughout the experiment: a) 1.1 hr, b) 2.3 hr, c) 3.4 hr, and d) 15.9 hr.

velocity was then 3.5 mm/s in both capillaries. Once solution began to flow in both capillaries the average velocity was constant throughout the experiment. The

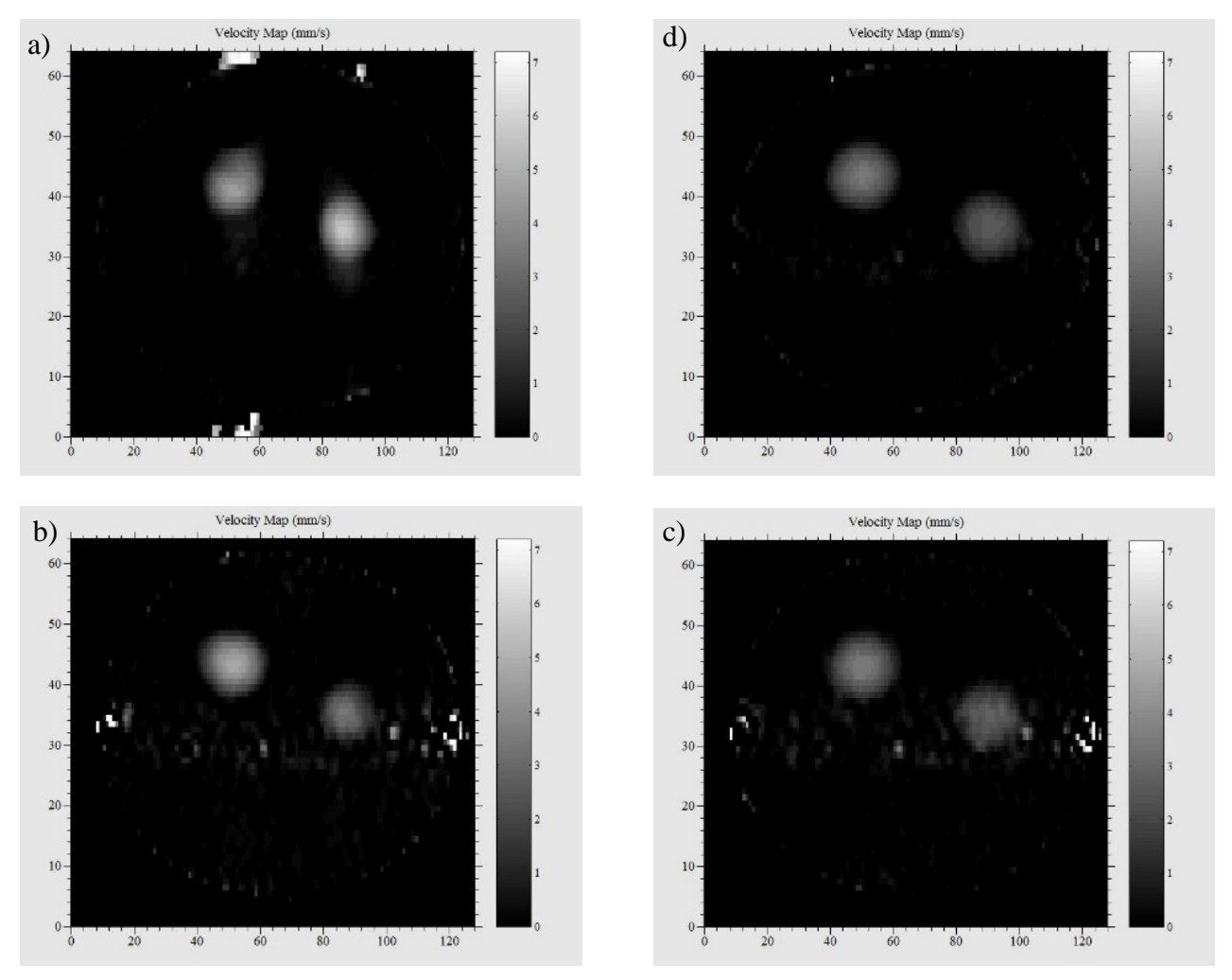


Figure 8: Velocity maps of CuCl₂ flowing at 20 mL/hr for different lengths of time: a) 0.9 hr, b) 1.8 hr, c) 2.7 hr, and d) 15.3 hr.

0.001 M CuCl₂ solution on the other hand had solution flowing through both capillaries for the entire experiment the initial average velocity in both capillaries was 5 mm/s. Over the course of 15 hrs., the average velocity dropped to only 3 mm/s in each capillary.

Discussion

Making the gels, especially the heterogeneous gels, is a fairly straight forward process. However the mechanism for the capillary formation is still not well understood and there are more details that should be considered. When making the

homogeneous gels both the stoichiometry has to be exact and the gel has to be entirely mixed in order to actually gel the sample entirely. The heterogeneous gels on the other hand have their own challenges of creating a perfect gel sample. The test tubes have to be coated evenly with alginate or else the final gel will pull away from the wall. Figure 5 shows the copper gel pulling away from the wall by the light crescent on the top right side of the image. It's lighter because instead of a rigid gel being there, there is solution. If the alginate isn't entirely degassed before gelling, the gel matrix will have air bubbles trapped within the matrix. Air bubbles disturb

the homogeneity of the magnetic field and kill the signal as there are no hydrogen atoms to excite in an air bubble. Using the spray mist technique, it was important to prevent drops of the CuCl₂ or CaCl₂ from running down the inside of the test tube as the drops instantly gel the sample and prevent the formation of capillaries. The gel plug samples had similar issues as the spray mist technique gels, but instead of dealing with drops it was trying not to bump the glass capillaries. It was important to avoid dislocating the glass capillaries in the samples, in order to fix them in the same position.

Working with the pumps on the lab bench was useful; it allowed an opportunity for trouble shooting to occur before setting the experimental setup up in the magnet. When leaks happened in the fittings or another piece of tubing was needed to optimize the flow system, it was much easier planning that out ahead of time. The lab bench also allowed for the flow rate to be easily timed. These flow rates become more important with the velocity imaging.

It is better to image the heterogeneous gels when they are fresh in order to obtain maximum signal and have minimal salt precipitation. Age doesn't appear to be a factor in the quality of the image of the gel plugs though as any salt accumulation is drained when setting up the flow system.

The artifacts that appeared in the initial velocity maps, given a large enough pressure drop and a filter in Prospa, were able to be eliminated. It took several different setups with the glass wool and then glass beads to create enough of a pressure drop to prevent the artifacts from occurring. Continuing to try different pressure drops and flow rates led to the eventual decision to go with a flow rate of 20 mL/hr.

The different velocities from the velocity maps of both solutions still needs to be examined more to determine the cause. At this point in time it is still unknown why there is only flow in one capillary to begin with instead of both with the CaCl2, it could potentially be caused by the calcium being washed out slowly over time since the solution being flowed is a 0.1 concentration where the gel was created with a 0.5 M concentration, though further testing is needed to support or disprove this conclusion. It could also explain why the phenomenon isn't observed with the copper since as soon as the copper makes contact with the gel it begins replacing the calcium, this reaction could drive the excess calcium out faster to where there is no noticeable flow in only one capillary. This doesn't explain why there is a lower velocity in the copper solution after time though. More experiments will have to be conducted along with taking before and after pictures of the gels in order to compare and obtain better results.

Conclusion

In conclusion, it is possible to create different types of algal alginate gels using different techniques to form them. Upon imaging the gels, the structural differences between the homogeneous gel, calcium based heterogeneous gel, and copper based heterogeneous gel can be easily seen. It is also possible to image flow through a gel using velocity imaging techniques. Further testing will need to be done in order to better explain the results of the initial velocity experiments.

Acknowledgements

Thank you to my faculty sponsor Dr. Joseph Seymour and the graduate student that

I worked under on this project Elmira Nybo. Thank you to the Magnetic Resonance Microscopy lab staff and students. Thank you to TRiO, the Department of Education grant #P217A130148, the McNair Scholars Hogan, Shelly Dr. Program, the Undergraduate Scholars Program, and the University Montana State Alumni Foundation, along with David O. Kem and Judith L. Raines for providing this opportunity.

References

- 1. Schuster, E., et al., Microstructural, mechanical and mass transport properties of isotropic and capillary alginate gels. Soft Matter, 2014. **10**(2): p. 357-366.
- Callaghan, P.T. and Y. Xia, VELOCITY AND DIFFUSION IMAGING IN DYNAMIC NMR MICROSCOPY. Journal of Magnetic Resonance, 1991. 91(2): p. 326-352.
- 3. Fabich, H.T., et al., *Microbial and algal alginate gelation characterized by magnetic resonance*. Journal of Biotechnology, 2012. **161**(3): p. 320-327.
- 4. Venkatesan, J., et al., Alginate composites for bone tissue engineering: A review. International Journal of Biological Macromolecules, 2015. **72**: p. 269-281.
- 5. Venkatesan, J., et al., Seaweed polysaccharides and their potential biomedical applications. Starch-Starke, 2015. **67**(5-6): p. 381-390.
- 6. Schmitt, A., et al., Calcium Alginate Gels as Stem Cell Matrix Making Paracrine Stem Cell Activity Available for Enhanced Healing after Surgery. Plos One, 2015. **10**(3).
- 7. Deng, S., et al., Self-adhesive alginate wound dressing, has wound dressing main body comprising PU film, alginate dressing core and cover paper, and adhesive coated on surface of PU film, where alginate dressing core is covered with paper. JIANGXI 3L MEDICAL PROD GROUP CO LTD (JIAN-Non-standard).
- 8. Jang, L.K., D. Nguyen, and G.G. Geesey, EFFECT OF PH ON THE ABSORPTION OF CU(II) BY ALGINATE GEL. Water Research, 1995. 29(1): p. 315-321.
- 9. Jang, L., D. Nguyen, and G.G. Geesey, An equilibrium model for absorption of multiple divalent metals by alginate gel under acidic conditions. Water Research, 1999. **33**(12): p. 2826-2832.

- 10. Lagoa, R. and J.R. Rodrigues, Evaluation of dry protonated calcium alginate beads for biosorption applications and studies of lead uptake. Applied Biochemistry and Biotechnology, 2007. 143(2): p. 115-128.
- 11. El Khoury, D., H.D. Goff, and G.H. Anderson, *The Role of Alginates in Regulation of Food Intake and Glycemia:*A Gastroenterological Perspective. Critical Reviews in Food Science and Nutrition, 2015. **55**(10): p. 1406-1424.
- 12. McCaslin, C.A., et al., Impact of alginate-producing Pseudomonas aeruginosa on alveolar macrophage apoptotic cell clearance. Journal of Cystic Fibrosis, 2015. **14**(1): p. 70-77.
- 13. Maneval, J.E., et al., Magnetic resonance analysis of capillary formation reaction front dynamics in alginate gels.

 Magnetic Resonance in Chemistry, 2011.

 49(10): p. 627-640.
- 14. Grant, G.T., et al., Biological Interactions
 Between Polysaccharides and Divalent
 Cations: The Egg-Box Model. FEBS
 Letters, 1973: p. 195-198.
- 15. Thumbs, J. and H.H. Kohler, *Capillaries in alginate gel as an example of dissipative structure formation*. Chemical Physics, 1996. **208**(1): p. 9-24.
- 16. Callaghan, P. and M. Halse, Introductory NMR and MRI with Paul Callaghan: Video 2: Introduction to Nuclear Magnetic Resonance. 2009.
- 17. Callaghan, P. and M. Halse, *Introduction* to NMR and MRI with Paul Callaghan: Video 3: How the Terranova-MRI works. 2009.
- 18. Callaghan, P. and M. Halse, *Introduction* to NMR and MRI with Paul Callaghan: Video 8: Magnetic Resonance Imaging. 2009.
- 19. Callaghan, P. and M. Halse, Introduction to NMR and MRI with Paul Callaghan: Video 9.2: k-Space in Multiple Dimensions. 2009.

The Kinematics of Slope Style Skiing: Dominant vs. Non-Dominant Rotations in Professional, INTERMEDIATE & BEGINNER Level Athletes

Arielle Richard, McNair Scholar

Dr. John Seifert, McNair Faculty Research Mentor Montana State University 2013-2014

ABSTRACT

Skiing is a sport that encompasses a broad range of disciplines. Slope-style skiing consists of "terrain-park" and "urban" features in which athletes perform spins and flips off of jumps and grind rails on their skis. Most resorts have professionally built "freestyle terrain-parks" designated for these free ski athletes. These features range in difficulty levels from "beginner to advanced," and complications arise when athletes attempt tricks that are too advanced for the skill levels. In terms of going off of jumps, riders perform tricks such as 180°, 360°, 540°, 720°, 900° rotations. Athletes often go inverted and "off-axis" in many of these tricks, performing backflips, flat-spins, double spins, and even triple spins. This sport is growing rapidly with children as young as 11 years old entering the competition scene at a professional level, and it has recently been accepted into the Winter 2014 Olympics. Because of this, it is crucial that researchers begin investigating and exploring the kinematics, kinetics, and other factors that are required to successfully execute and safely land these tricks. An exploration of some of the most basic factors involved in executing a 360o rotation in an athlete's dominant and non-dominant directions of rotation will yield useful data for freestyle coaches, teams, and athletes because it will provide a foundation for identifying each athlete's strengths and weaknesses, and will allow coaches and/or athletes to begin implementing drills and techniques to build the athlete's skills. These skills are necessary for all slope style skiers to master before further progression can occur.

INTRODUCTION

"With the increasing popularity of freestyle skiing and snowboarding, many ski resorts have constructed their own terrain parks including several jumps, rails, and pipes. In order to prevent risks of high-impact injuries in jumping, an adequate construction of the landing hill is very

important." (Bohm, 2007). These features (i.e. jumps, rails, halfpipes, etc.) range in difficulty levels from beginner to advanced, and complications arise when athletes attempt tricks that are too advanced for the skill levels. In terms of going off of jumps, riders perform tricks such as 180°, 360°, 540°, 720°, 900° rotations. Athletes often go inverted and "off-axis" in many of these tricks, performing backflips, flat-spins, double spins, and even triple spins. As the complexity of these tricks increases, it becomes clear that the rider is at an inherently higher risk for sustaining injuries if the proper skills and techniques are not mastered prior to attempting the trick. Further, proper maintenance and building of these features rely heavily on the expertise of the terrain park staff of the ski resort. Because errors in building are often a likely possibility, signs are placed at the entrance of the parks to inform riders that they perform and attempt tricks/features at their own risk, and also remind them to "start small" and work up to more difficult features. The purpose of this research was to describe the kinematic factors involved in executing a very basic trick, a 360° rotation, in both the clockwise and counter-clockwise directions, one being the dominant, or preferred, direction of rotation for the athlete, and the other being the non-dominant, un-natural direction of rotation.

Skiing and snowboarding injuries sustained in terrain parks compared to those sustained on traditional slopes, specifically head and spine injuries, have been found to be higher and more severe (Brooks, 2009). One of the primary reasons for this may be due to the lack of experience and mastery of these basic skills before performing larger tricks, especially off of larger features, which have an inherently higher risk due to greater velocities and higher vertical distances from the landings. Progression that occurs too quickly without a solid foundation of basic skills can cause serious injury and/or death to athletes. As the skill levels of the tricks become more and more technical, a higher level of risk accompanies the sport, and therefore the athlete. As a result, an exploration of some of these basic factors involved in executing a basic 360° rotation will yield useful data for freestyle coaches, teams, and athletes because it will provide a foundation for identifying an athlete's strengths and weaknesses, and will allow coaches and/or athletes to begin implementing drills and techniques to build the athlete's skills. In this way, slope style athletes, especially those working to build on their most fundamental skills, can fully understand the kinematic factors required to perform the most basic tricks. Mastery of these skills is necessary for the athlete before moving on to further progression of tricks. The winner of the 2013 winter X-Games big air competition, Henrick Harlaut, successfully executed and landed the first ever "nose butter triple cork 1620," making history. This trick involves going inverted three times while simultaneously rotating a total four times – it is highly complex and involves a difficult set of skills. As a professional athlete, Harlaut started skiing at two years old, and is now 22 years old. In this way, professional athletes serve as role models to many aspiring skiers because they have spent a great deal of time learning the basics, and from there were able to build their skills to push the sport to the high level it is at today.

This research examines the importance of "starting small" and building a solid skill foundation before progressing on to larger and more difficult rotations and inverted tricks off of ski jumps. It was found useful to test these kinematic factors among three distinct slope style athlete levels – a professional athlete, an intermediate athlete, and a beginner athlete. In this way, comparisons and differences were able to be observed among the data. The data were then able to be analyzed and used as a resource to help coaches and athletes safely progress through learning tricks.

METHODS

Before beginning any research, approval from the International Review Board (IRB) was obtained. A detailed summary regarding the specifics of the procedures used in the experiment was written, including all safety procedures that would be implemented. A letter from the Bridger Bowl Ski Area was also obtained that explained that they knew of the research being conducted in their professionally built terrain park. Each athlete signed a waiver which informed them of the rights and that their participation in the research was voluntary and at their own risk.

On March 8th, 2013, athletes and researchers met at Bridger Bowl Ski Area terrain park near Bozeman, MT to perform the experiment. The athletes were allowed to take two warm up runs in the terrain park to allow them to get used to the overall feel of the jump. A shadow box accelerometer was then programmed and securely attached to each skiers left ski behind the heel binding via duct tape. It was used to measure the velocities and spin rates generated by each athlete at various points in performing the trick. Data was collected at a sampling frequency of 100 Hz.

The temperature at the time of the experiment was 30° Fahrenheit. The terrain park jump was considered a "small to medium" jump at 3 meters (10-15ft) in vertical height. It was built and maintained by the experienced terrain park crew at Bridger Bowl, and at the time of the experiment, the jump had been freshly groomed, and the snow was hard packed and fast. The in-run to the jump was 25 meters long. Both the in-run and the landing of the jump had smooth and hard packed snow.

Both the professional and the intermediate athletes performed two 360° rotations in their dominant direction (counter-clockwise) as well as in their non-dominant direction (clockwise). The beginner athlete performed the rotation only in the dominant direction (clockwise). After the data collection was complete, the data was downloaded to the computer using the Ride-

Tracker software. The data was then analyzed to determine each athlete's take-off velocity, deviation velocity, and initial z-spin rates in the transverse plane of rotation.

Both the professional and the advanced athletes performed three 360° rotations in their dominant direction (counter-clockwise) as well as in their non-dominant direction (clockwise). At the top of the jump, each athlete's skis were removed and dried as thoroughly as possible using paper towels. Next, a hand was placed over the ski to help warm it up, so that the duct tape would stick better to it. Then the accelerometer was carefully and securely attached to the ski just behind the back of the left ski binding. Next, the accelerometer was turned on and the rider's name was selected. Before dropping into the jump, the athlete lifted his leg up and down quickly, so as to mark the start of his descent. Then, the athlete dropped into the in-run of the jump, gained speed, and performed a 360° counter-clockwise rotation in his dominant direction (to the left). Upon landing the trick, the device was turned off, and the rider hiked back up to the top of the in-run for the second jump. The same procedures were followed for the next rotations, however, the spin was performed in the clockwise direction (right), which in this case was the athlete's non-dominant direction of rotation. Next, the intermediate athlete performed his two rotations following the same procedures, followed by the beginner athlete. The beginner athlete performed a 360° clockwise rotation (right), which in this case was her dominant direction of rotation, opposite the other two athletes. However, she did not perform the counterclockwise (non-dominant) rotation because she was uncomfortable executing the trick in this direction. Each athlete performed one more rotation in each direction, providing two trials for each spin to account for possible errors that may have occurred in the first trial.

The data were then uploaded into the computer system via ride tracker software and data was recorded for the Z-Spin Rate, which consisted of the rotational, side-to-side (mediolateral) spin rates. The athletes' initial take off velocity and deviation velocity were record. The deviation velocity marked the point at which the athlete began to set, or wind-up, for the spin at the moment before leaving the jump. The maximum vertical distance, or peak-height, reached during each rotation was also recorded.

Finally, the data was analyzed and comparisons were made between the dominant directions of rotation in each case, between the non-dominant rotations, and between both the dominant and non-dominant rotations for each individual athlete. Then, comparisons of the data were made among the athletes and the differences were noted.

RESULTS

KINEMATICS OF PROFESSIONAL, INTERMEDIATE, AND BEGINNING FREESKI ATHLETES

Athlet	Direction	T.O.	Deviation	Initial Z-	Max
е		Vel	Velocity	Spin	Ht
		(m/s	(m/s)	Rate	(m)
)		(°/sec)	
PRO	CCW	15.1	15.3	279.3	4.0
	cw	11.2	12.1	124.8	4.0
INT.	CCW	14.7	14.6	285.0	3.35
	cw	10.3	8.4	404.9	3.87
BEG	cw	11.2	7.5	462.8	1.76

TABLE 1: Counterclockwise vs. Clockwise Rotations in Professional, Advanced, and Intermediate Level Athletes.

CCW – Counterclockwise Rotation CW – clockwise rotation

PRO - Professional Athlete

INT – Intermediate Athlete

BEG - Beginner Athlete

DISCUSSION

Overall, an inverse relationship was found between a skier's deviation velocity and their initial Z-spin rate. This was easily observed in the beginning athlete, in which data was recorded only for the dominant (clockwise) direction of rotation. It was found that the initial velocities were low and the spin rate was high to compensate for the lack of air time off of the jump. When compared to the velocities and spin rates of the intermediate and professional athletes, the beginner athlete's deviation velocity was much lower and had the highest spin rates. As a result of this slower deviation velocity, the maximum height reached off of the jump by the intermediate athlete was much lower than that of the intermediate and professional athletes.

This was significant because it suggested that the beginning athlete may tend to have lower levels of confidence in executing a basic 360° rotation, even in the dominant direction. Therefore, they may not take as much speed into the jump and will therefore have less air time (less vertical height) off of the jump, and must compensate for this by having a very fast spin

rate so as to land the trick in a shorter amount of time. Athletes and coaches can use this information to practice building confidence off of jumps before athletes even attempt a spin. By "straight airing" the jump several times to *feel* for the right speed, athletes can feel safer and more confident about safely landing their spin because they will have a comfortable amount of air time and won't have to huck their spin as hard to get it around in time. Hucking a spin can be dangerous for the athlete because it means they have more torque with their bodies, and if they land too high up on the landing or do not complete their spin, they have a higher chance of sustaining an injury such as an ACL tear in the knee.

When each individual athlete's dominant and non-dominant rotations were compared, the data showed that both the intermediate and professional athletes' take-off and deviation velocities tended to be faster when they approached the jump and prepared to spin in the *counterclockwise* direction, which in both cases was the athletes' dominant direction of rotation. Similarly, the initial Z-spin rates tended to be lower for these rotations, indicating that there was a higher level of confidence for these athletes as they performed the rotation in their dominant direction.

Conversely, when the intermediate athlete approached the jump and prepared to execute the rotation the clockwise (non-dominant) rotation, the initial and deviation velocities were found to be slower than those of the counter-clockwise (dominant) direction. This indicated that there was likely more stress in performing the rotation in the non-dominant direction. However, the professional athlete's initial z-spin rate was actually slower than his spin rate for his dominant rotation. This difference suggested that the professional athlete was perhaps more confident or equally as skilled in executing the rotation in both directions.

APPLICATION

This data suggests that even athletes at the highest levels of slope style skiing understand that there is an inherently higher risk in performing tricks in the non-dominant directions. This is why at competitions, un-natural tricks score higher points — although they are the same trick, they are more difficult in the opposite direction. It is crucial that coaches and athletes of all levels, especially beginning/intermediate athletes, understand this concept so that they can identify their athletes' dominant sides, master those, and then work them through the appropriate progressions to learning the trick in the opposite direction; in this way, they work to ensure their safety and reduce their risks for injuries as they progress and learn new tricks. Techniques and drills to develop skills are up to the discretion of the athletes and/or the coach(es), but some common examples may be having the athlete(s) straight the jump and practice "popping" higher off the lip, practicing grabs in the air to work on body control and

awareness in the air, and having them perform the trick with different grabs or in simpler steps (i.e. a 180 first, then a 360). It was clear that the beginner athlete in this research had not perfectly mastered a 360 in her dominant direction – she had to huck the spin and did feel extremely comfortable going fast off of the jump. Thus, she should continue to work on these skills, perfect them, and then move on to trying the trick in the un-natural direction.

By exploring the kinematics of slope-style skiing, coaches and athletes can begin to have a better understanding of safe progression and of the importance of taking all of the proper steps to learn a basic trick before moving on to more advanced tricks. The data yielded in this experiment may prove especially beneficial to those coaches who are active in training younger skiers who are just beginning to build a foundation of their skills. It can be difficult for athletes who desire to compete at intermediate or higher levels and who just want to move on to the harder, more "fun" tricks; this can be very dangerous if the athletes have not had the proper training and taken the right steps to build their skills and perhaps more importantly, their confidence. Building this foundation of performing basic tricks is important for athletes who wish to further their skills and who hope to compete in competitions, and also to ensure their safety. If athletes try to progress too quickly through skills, they have a higher risk of making errors and of getting injured.

FURTHER RESEARCH

Further research in this field may consist of exploring more advanced tricks, such as inverted flips or off-axis (corked) spins. As these athletes continue to reach higher skill levels, their risk of injury increases because not only are the tricks more difficult and complex, but higher velocities and much bigger jumps become involved. The importance of understanding these basic kinematic factors is clear.

In addition to exploring the more basic kinematic factors involved in performing these tricks, a more in depth exploration of the kinetics and forces involved in successfully executing these tricks, both basic and complex, can prove especially useful because athletes and coaches can have a better understanding of the specific actions and reactions that must occur and in what ways to ensure proper execution and landings; this would further work to promote and enhance their safety.

Aside from exploring the specific kinematic and kinetic factors that the athlete must generate and work with, research examining the specific builds and conditions of the jumps and features may prove especially beneficial. Making sure these jumps are at the right angles and that their in-runs and landings are long enough for the athletes to generate enough speed to clear the flat

zones and land safely on the landing and at the right angles is also a very important safety factor for all slope style athletes.

Overall, the sport of slope style is becoming increasingly popular, and we recently saw these amazingly talented athletes compete in the 2014 Winter Olympics. Many of the tricks that these athletes perform are so incredibly complex, such as the "switch nose butter triple cork 1620°" that was performed for the first time ever in the 2013 Winter X-Games Big Air event. These athletes continue to push the limits of human physics, and to explore these mechanisms to promote the safety of the athletes is at the very least a justice to human biomechanics.

ACKNOWLEDGEMENTS

This work was supported by the McNair Scholars program (U.S. Dept. of Education grant #P217A130148)

REFERENCES

- 1. **Brooks, M.** Evaluation of skiing and snowboarding injuries sustained in terrain parks versus traditional slopes. *Injury Prevention: Journal of the International Society for Child and Adolescent Injury Prevention* 2010; **16**: 119-122.
- 2. **Boehm, Harald.** Safety in big umps: relationship between landing shape and impact energy determined by computer simulation. *Skiing Trauma and Safety* 2009; 165-174.
- 3. **Goulet C**, Hagel B. Hamel D. *et. al.* Risk factors associated with serious ski patrol-reported injuries sustained by skiers and snowboarders in snow-parks and on other slopes. *Can J Public Health* 2007; **98**: 402-6.
- 4. Hagel B. Skiing and snowboarding injuries. *Med Sport Sci* 2005; **48**: 74-119.
- Torjussen J, Bahr R. Injuries among competitive snowboarders at the national elite level.
 Am J Sports Med 2005; 33: 370-7
- 6. **Hagel BE,** Pless IB, Goulet C, et. al. Effectiveness of helmets in skiers and snowboarders: case-control and case crossover study. *BMJ* 2005; **330**: 281.
- 7. **Levy AS,** Hawkes AP, Rossie GV. Helmets for skiers and snowboarders: an injury prevention program. *Health Promot Pract* 2007; **8**:257-65.
- 8. **Zygmuntowicz M,** Czerwinski E. The causes of injuries in freestyle snowboarding. *Med Sport* 2007; 11:102-4.
- 9. **Tarazi F,** Dvorak MF, Wing PC. Spinal injuries in skiers and snowboarders. *Am J Sports Med* 1999; **27**: 177-80

Conference of the International Journal of Arts & Sciences, CD-ROM. ISSN: 1943-6114:: 07(02):305–309 (2014) Copyright © 2014 by UniversityPublications.net



A TEST OF THE EFFECTIVENESS OF THE UNDILUTED BLEACH METHOD IN DEFLESHING HUMAN REMAINS

Michael Ruiz

Montana State University, USA

The process of removing soft tissue from the remains of a decedent to reveal demographics that are obscured from the view of the anthropologist is known as maceration. Historically there have been a number of acceptable methods of loosening and removing soft tissue including immersion in water, boiling, removing with various chemical solutions, dermestid beetles, and manual removal with a sharp instrument. Each of these methods has demonstrable drawbacks in time, safety, the potential to damage the remains and required workspace. This methodological report presents the findings of an alternative safe and effective bleaching method for removing soft tissue introduced in 2012 by Mann and Berryman using undiluted household bleach at 8.25% concentration (sodium hypochlorite).

Keywords: Forensic science, Forensic anthropology, Bleaching, Human remains, Human bones.

Introduction

The ability to effectively remove soft tissue from the skeleton without compromising surface morphology or overall bone integrity is essential to a thorough and complete analysis by a forensic anthropologist. There is no agreement among forensic anthropologists regarding the best method for defleshing skeletal remains. Choosing the most appropriate method for defleshing remains and exposing the unique features of the individual must be done with consideration of the forensic context of the remains. The use of undiluted household bleach, as a means of defleshing cadavers is notably controversial inthe forensic science literature. Specifically, when bleach is introduced to forensically significant skeletal material, the potential for cortical exfoliation due to the corrosive nature of bleach (sodium hypochlorite) poses a significant threat to the integrity of the outer cortex of the bone. Bleach cleans and whitens bones, which may be appropriate for museum display; in the forensic context it is an adverse product of the process. No single method is a panacea for all situations. Maceration is an invaluable procedure in a forensic context, although not all maceration techniques are applicable to medico-legal cases. Anthropological assessment of the technique's usability often involves the length and ease of the process, the resulting bone quality and color, and the relative odor (1). Removal of the soft tissue can reveal subtle nuances of trauma that may otherwise be obscured or masked by the presence of flesh (2).

Maceration techniques have been shown to reduce the potential for DNA extraction following maceration (1). As discussed by Mann and Berryman (2), the bleach attacks and oxidizes the protein bonds in the bone, effectively destroying the potential to harvest any mtDNA and Nuclear DNA. Thus, if possible, in cases where identity is in question mtDNA and Nuclear DNA should be harvested prior to using this particular method of cleaning.

Methodology

The current study focuses on whether the method presented by Mann and Berryman for defleshing remains, illustrated using the chest plate of a stabbing victim post- autopsy, can safely and effectively remove soft tissues from recently deceased partially skeletonized remains. The specimens used in this study are non-human, cattle of the family *Bovidae*. Bovine skeletal materialhas demonstrated biocompatibility with living human bones in various biomedical surgical procedures(3)and more recently as a biochemical osteointegratable bone grafting mediumin humans (4). Thus, for the purposes of this experiment, bovine material is as near to an ideal medium as possible. The two specimens consisted of an articulated distal end of a femur and proximal end of a tibia.

We obtained the remains from a local slaughterhouse; they were not treated with any chemicals and were dismembered using industry standard blades designed for animal dismemberment. Some of the decedent's external layers of flesh had already been removed from the femur and tibia leaving the tendons, ligaments, and some muscles intact (Fig.1). Approximately 48 hours post-mortem, the first specimen, containing a distal femur and proximal tibia wasimmersed in 8.25 % sodium hypochlorite concentration of household bleach under a fume hood. This concentration is +2.75% than the concentration used in Mann and Berryman's experiment (2). The bleach attacks and oxidizes the protein bonds adhering the soft tissue to the bones causing the soft tissue to break apart and fall away from the bones at a much quicker rate than other methods. When the specimen is immersed the bleach will quickly begin to bubble and heat up indicating that the soft tissue is being chemically removed. The solution is emptied and replaced every twenty minutes as prescribed by Mann and Berryman. This process continues for two hours. Visual examination indicated a rapid disintegration of the adhering soft tissue. The skeletal remains were examined for signs of "whitening" and chalkiness (deposits of hydroxyapatite) carefully at each time interval to determine if significant alterations to the cortex of the bone were occurring (Fig. 2).

A great deal of the soft tissue remains intact leaving the synovial joint encased in flesh following the first experiment and therefore, required the manual removal of several layers of tissue prior to the immersion of the second specimen. For the second experiment, I manually removed superficial layers of tissue mostly composed of adipose and muscle to reveal the underlying ligaments of the synovial joint of the knee. Deciding only to use the distal femur of the second specimen, I cut the surrounding ligaments to disarticulate the joint (Fig. 3). The original experiment utilized the chest plate of a stabbing victim with little soft tissue, post- autopsy, given the size and delicate nature of the bones of the sternum the remains are immersed in bleach for only twenty minutes. The morphological differences in the robusticity of tissue and of long bones in contrast to the bones and tissues of the sternum required an increased time interval. For this experimentintervals are increased and the specimen is monitored at 40-minute intervals under a fume hood. Therapid disintegration of tissue continues for three and a half hours, inspected at



Figure 1. Distal Femur and Proximal Tibia 48 Hours Postmortem.



Figure 2. Tibia following the first immersion in bleach.



Figure 3. Disarticulated femur in bleach solution

forty-minute intervals to ensure the integrity of the remains. As prescribed by Mann and Berryman (2) the solution is replaced with a new 700 mL of bleach (sodium hypochlorite) at each forty-minute interval or when a heavy film forms at the surface of the solution. When complete skeletonization is accomplished the remains are immediately immersed in tap water for twenty minutes to cease the reaction. The distal femur is allowed to dry for 48 hours before thoroughly examining the bone.

Results and Discussion

The effectiveness of the maceration technique is measured and scored using the Steadman et al maceration scoring system (1). Table 1 describes the variables observed and the scoring procedure. Three variables: odor, texture of the tissue, and the ease of flesh removal were considered during qualitative examination. The determination of scores are as follows: Odor is a 3 with little to no smell, a slight odor possible around or under the fume hood; Soft-tissue texture is between 2-3, with larger specimens less malleable than smaller cross-sections; Ease of flesh removal score is a 2, adherence to bone is moderately strong although large portions can be easily removed; the core of flesh close to the bone is still adherent; Bone quality is a 5, strong normal bone texture and quality (Fig. 4). Overall, two samples displaying four transecting cuts produced by a blade class consistent with that of high-power mechanical saw have been used for direct observation. The medium has been impacted with sharp force trauma to determine the



Figure 4. Femur following revised maceration procedure.

Table 1. Maceration Scoring System (1).

Odor

- 1. Strong smell that permeates the entire lab space
- 2. Moderate smell in the immediate vicinity of the experiment
- 3. Little to no smell; a slight odor possible around or under the fume hood

Soft-tissue texture

- Soft tissue is firm and/or quite solid; may feel tougher or more rubbery than when first submerged
- 2. Soft tissue is as malleable as when originally observed
- 3. Soft tissue is considerably softer and looser than when the experiment began; very malleable
- Soft tissue is nearly liquefied and floats on the surface with little or no connection to bone

Ease of flesh removal

- Adherence to bone is quite strong with little or no flesh removal possible without damaging the bone
- Adherence to bone is moderately strong although large portions can be easily removed; the core of flesh close to the bone is still adherent
- Adherence is minimal to bone as flesh falls off as bones are removed from solution or easily removed with fingertips

Bone quality

- 1. Brittle, fragile, easily broken
- 2. No cortical erosion but bone is lighter in weight and porous
- 3. Softer, more pliable than normal bone but no cortical damage
- 4. Cortex eroding and/or flaking but bone will not easily fracture
- 5. Strong, normal bone texture and quality

reliability of the bleaching method to preserve both the integrity of the bone and forensically significant trauma. Although an exhaustive discussion of trauma is beyond the scope of this project, it is important to discuss the fundamental principles guiding the use of maceration. In the course of an investigation, law enforcement officials are interested in the sequence of events leading up to the cause of death and treatment of the individual following their death by a perpetrator. It has been argued that the data available to forensic anthropologists rarely allows for the reconstruction of the physiological events that caused death (5). It is more probable that the remains will provide clues to manner of death rather than cause of death in a case where skeletonized remains are present at the scene. Although a murder weapon must pass through the soft tissues first, it is often the hard tissues that best record and preserve the

impression of the weapon; indeed, they will be the only record after decomposition. While one cannot, with complete confidence, demonstrate what exactly initiated a chain of physiological events that resulted in the cessation of life, it is often possible to reveal evidence that suggests death was by homicide, suicide, accident, or was natural. Upon visual examination, post-maceration, these remains displayed traits consistent with other authors' descriptions of post-mortem injury to bone, using a blade class of saw with high power, including but not limited to the morphology of the kerf marks (6), the general appearance of striae at the site of impact (6, 7) and the lack of indications of osteogenic regeneration (8). The information from the set of remains fits the context in which they were retrieved. Thus, it is our conclusion that the undiluted bleach method, with respect to unique qualifying circumstances (i.e. to isolate stab wounds, post-mortem dismemberment, when identity is not in question, etc.), when done properly is a quick, safe, and effective method for exposing and examining the skeleton.

Acknowledgements

I would like to thank John W. Fisher, Ph.D for his guidance and strong support in this project. Shelly Hogan, Ph.D –Director of the Ronald E. McNair Scholars Program at Montana State University, The National Science Foundation, and the Engineering Minorities Program in the College of Engineering at Montana State University for their support in this endeavor. I also wish to express gratitude to the Department of Chemistry and Biochemistry at Montana State University for sharing lab space to conduct this work.

References

- 1. Steadman DW, DiAntonio LL, Wilson JJ, Sheridan KE, Tammariello SP. The Effects of Chemical and Heat Maceration Techniques on the Recovery of Nuclear and Mitochondrial DNA from Bone*. Journal of forensic sciences. 2006;51(1):11-7.
- 2. Mann RW, Berryman HE. A Method for Defleshing Human Remains Using Household Bleach. Journal of Forensic Sciences. 2012;57(2):440-2.
- 3. Taniguchi Y, Tamaki T, Oura H, Hashizume H, Minamide A. Sintered bone implantation for the treatment of benign bone tumours in the hand. Journal of Hand Surgery (British and European Volume). 1999;24(1):109-12.
- 4. Laird DF, Mucalo MR, Dias GJ. Vacuum assisted infiltration of chitosan or polycaprolactone as a structural reinforcement for sintered cancellous bovine bone graft. Journal of Biomedical Materials Research Part A. 2012;100(10):2581-92.
- 5. Sauer N, Simson L. Clarifying the role of forensic anthropologists in death investigations. Journal of forensic sciences. 1984;29(4):1081.
- 6. Reichs KJ, Bass WM. Forensic osteology: advances in the identification of human remains: Charles C. Thomas Springfield, IL, 1998.
- 7. Bonte W. Tool marks in bones and cartilage. Journal of forensic sciences. 1975;20(2):315.
- 8. Alison Galloway PhD D, Zephro L. Skeletal trauma analysis of the lower extremity. Forensic medicine of the lower extremity: Springer; 2005;253-77.

1

Characterization of a High Temperature Chlorosilane Corrosion System for Improved Polysilicon Production

Kelly Walls, Mechanical Engineering
Paul Gannon, Associate Professor & McNair Research Mentor
Josh Aller, PhD Candidate, Mechanical Engineering
Department of Chemical and Biological Engineering
Montana State University

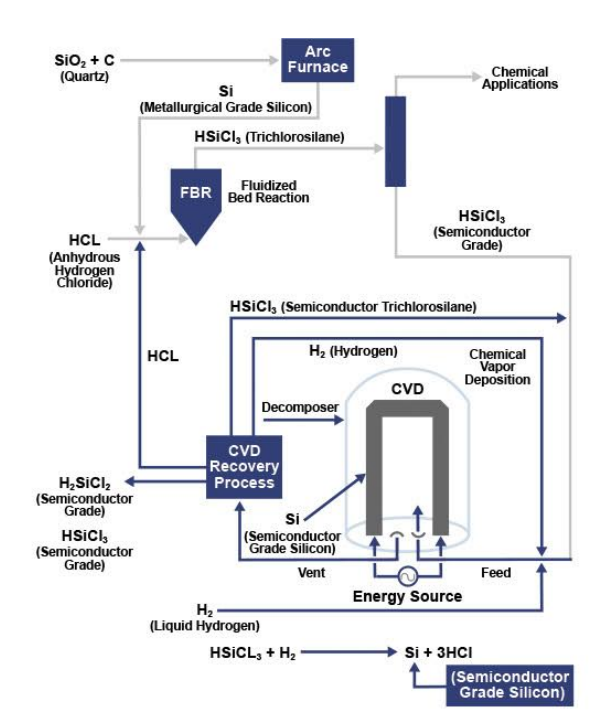
Abstract

Poly-crystalline Silicon (polysilicon) is a high quality product manufactured for use in many real world applications, most commonly in solar panels. Polysilicon is produced in large pressure vessels using a vapor deposition process which requires high temperature chlorosilane gas streams flowing through them. Chlorosilane gas is made of hydrogen (H₂), silicon (Si) and chlorine (Cl) and it is known that many metals form silicide and chloride compounds. In a high temperature environment, the presence of chlorine and silicon creates a unique corrosion environment dependent on time, temperature, and material composition. Thus, a high temperature chlorosilane corrosion environment was created to replicate industrial processes in order to understand the corrosion interaction of this gas with certain metals. In this study, temperature dependence on corrosion of 316L stainless steel was investigated. Specifically, this 316L stainless steel was subjected to four different temperatures above 500C with the same starting chlorosilane gas composition. It was observed that mass gains increased exponentially with temperature increase. The results, conclusions and characterization of this test system are discussed further in this paper.

Introduction

Chlorosilane gas streams at 500°C are used in the refining and manufacturing of many industrial products, to include poly-crystalline silicon (polysilicon). In the polysilicon manufacturing process, this stream typically contains silicon tetrachloride (SiCl₄, STC), trichlorosilane (HSiCl₃, TCS), dichlorosilane (H₂SiCl₂, DCS), silane (SiH₄), hydrogen chloride (HCl), and hydrogen (H₂). [3] This gas stream is pumped into large pressure vessels that contain rods of pure silicon in order to allow the rods to grow to a certain diameter in a process known as chemical vapor deposition. Figure 1.0 illustrates the process by which polysilicon is manufactured and this process is explained in more detail below.

The manufacturing process starts out with silicon tetra-chloride (STC). The silicon tetra-chloride is combined with metallurgical grade silicon, hydrogen gas and hydrogen chloride to produce trichlorosilane (TCS). This TCS is purified and



2

Figure 1.0: Diagram of polysilicon manufacturing process

pumped into reactors containing high quality silicon rods and heated and allowed to grow the silicon rods to a given diameter. STC is a by-product of this deposition process. This STC is then refined to make TCS and the process begins again. The rods that are produced from this process are the polysilicon rods that are further refined to make solar panels [2]. A few problems arise when the chlorosilane gas stream described above is subjected to high temperatures. Most metals can form chloride and silicide compounds, which creates a unique corrosion environment. These corrosive processes are known as chlorination and silicidation respectively. It is known that chloride formation is more detrimental in industrial uses because chlorine has a high vapor pressure which causes it to readily evaporate depending on the temperature of its surroundings. Silicidation is not as large of a concern due to the fact that silicides form on the surface of the metals which can sometimes have a protective effect. [3] The reactors that contain the silicon rods are constantly subjected to this corrosion environment, causing either mass loss due to chlorination or mass gain due to silicidation [1]. The chlorosilane environments seen in the polysilicon industry need to be understood in order to lower the manufacturing cost of the polysilicon and ultimately reduce the cost of the products that use it, such as solar panels. It is important to note that chlorosilane environments vary based on time of exposure, temperature, and sample composition. In this paper, the effects of temperature on a chlorosilane corrosion environment will be studied. More specifically, previous results showed a variability with location in a high temperature corrosion environment. Two hypotheses could explain this phenomenon. The first is that the gas species within the testing environment had reached chemical equilibrium, and the second is that there was an uneven temperature distribution within the hot zone of the test system. The later was investigated in

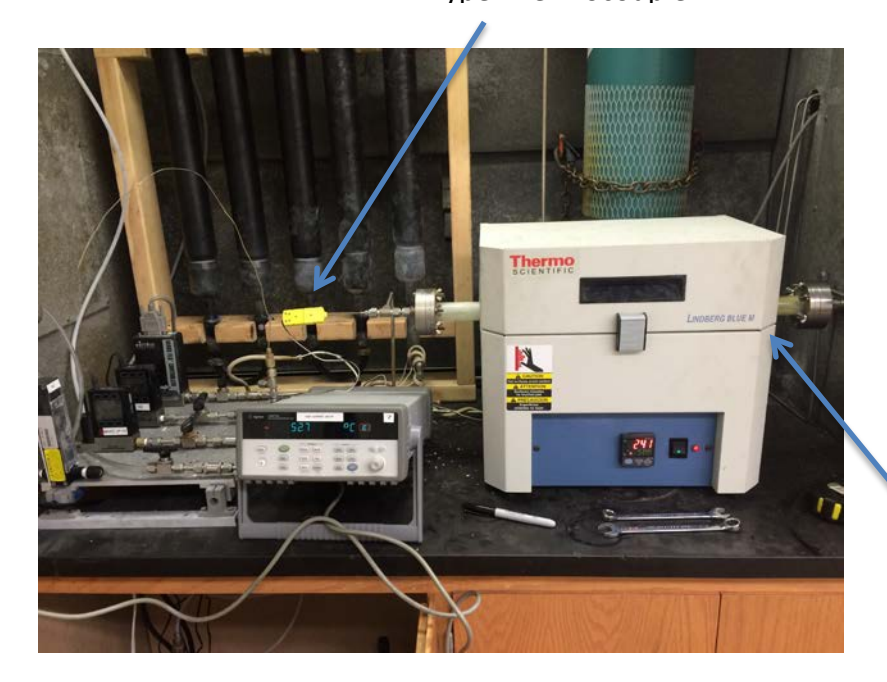
this paper by conducting a temperature profile of the test system in order to characterize the system and have it more accurately reflect the systems used in industry today.

To date, formal temperature profiles have not been published for a unique cholorosilane environment used to test the effects of chlorosilane on 316L Stainless steel. This environment consists of a tube furnace that heats chlorosilane gas flowing over 316L Stainless steel samples.

Methods

In order to measure the temperature within the tube furnace while operating like it would during a run on given samples, a thermocouple had to be inserted into the tube furnace without causing gas to leak. To do this, the swagelok connections were set up in the manner shown in figure 1.1. A data acquisition machine was fitted with a thermocouple reader and a K type welled thermocouple was inserted into the reader. The thermocouple was placed in the same location as the thermocouple of the furnace as shown in order to determine a possible temperature difference between the two thermocouples. The crucible was placed into the tube and was placed into the furnace and secured using the swagelok connections. The thermocouple was inserted into the tube via the swagelok T setup until the tip of it was just visible from the rightmost side of the furnace. This was the datum from which all distances were taken. Nitrogen gas was flowed through the furnace at a rate that corresponded to the ball of the rotameter being near the top of the meter. Nitrogen gas was a much safer alternative to SiCl₄ in case of a possible gas leak. The furnace was set to 500 °C and allowed to equilibrate. Once the thermocouple temperature displayed on the data acquisition machine stabilized, that temperature was recorded for a distance of 0 cm. The thermocouple was then pulled out a distance of 2 cm and the process was repeated until the tip of the thermocouple was just visible to the leftmost side of the furnace. This was the final data point collected at 32 cm from the datum. This process was repeated for both 600 and 700°C, since those are the temperature ranges that are commonly used for high temperature environments.

K Type Thermocouple



Rightmost side of furnace

Figure 1.1 Thermocouple setup

Results

The data collected is displayed in table 1.1. This raw data was then graphed, as shown in figure 1.2. In order to see a more clear representation of consistency or inconsistency in the temperature profile, the data was then normalized by taking the value obtained using the K type thermocouple and dividing it by the temperature that the thermostat of the furnace displayed. This data is shown in figure 1.3. The K type thermocouple did read between 20-30°C higher than the furnaces thermocouple.

Distance (cm)	Temperature			Normalized Data		
	500C	600C	700C	500C	600C	700C
0	292.7	349.7	428.2	0.5854	0.5828	0.61171
2	360.0	459.8	568.0	0.7200	0.7663	0.81143
4	446.1	542.3	633.4	0.8922	0.9038	0.90486

6	495.5	575.5	670.2	0.9910	0.9592	0.95743
8	511.9	598.2	691.8	1.0238	0.9970	0.98829
10	521.5	609.9	705.3	1.0430	1.0165	1.00757
12	528.3	619.2	716.0	1.0566	1.0320	1.02286
14	530.5	623.5	721.0	1.0610	1.0392	1.03000
16	530.4	624.1	722.6	1.0608	1.0402	1.03229
18	530.8	624.0	722.3	1.0616	1.0400	1.03186
20	527.6	618.9	717.6	1.0552	1.0315	1.02514
22	520.8	611.7	707.4	1.0416	1.0195	1.01057
24	507.6	596.4	693.5	1.0152	0.9940	0.99071
26	481.4	574.0	672.5	0.9628	0.9567	0.96071
28	438.7	513.0	631.7	0.8774	0.8550	0.90243
30	318.0	465.9	542.6	0.6360	0.7765	0.77514
32	250.7	262.6	394.5	0.5014	0.4377	0.56357

Table 1.1: Raw and normalized data for furnace temperature distribution

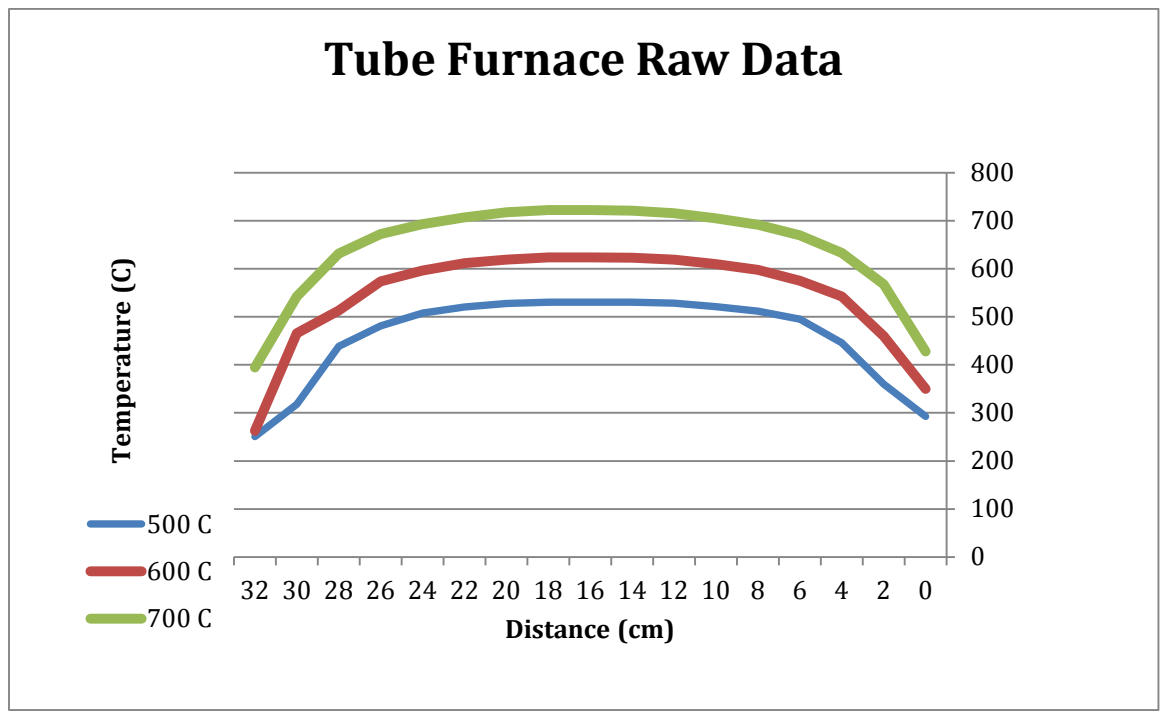


Figure 1.2: Plot of raw furnace temperature data

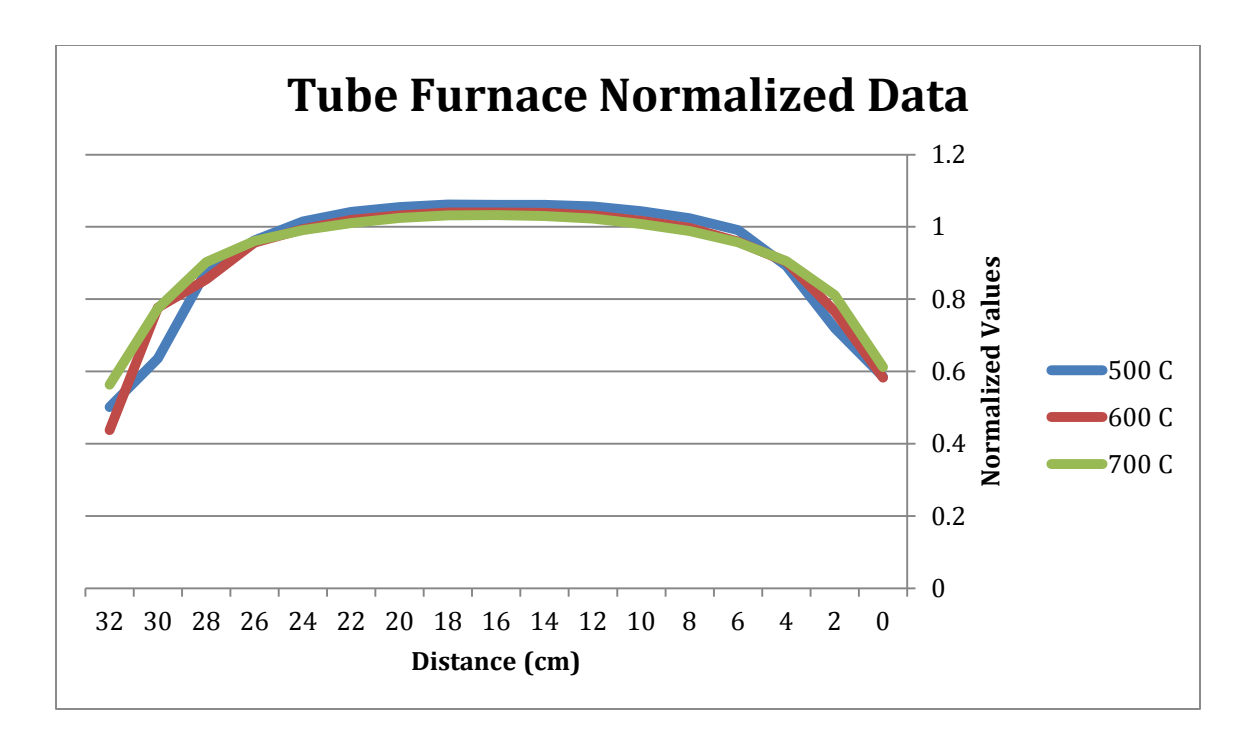


Figure 1.3: Plot of normalized furnace temperature data

Conclusions

After conducting the temperature distribution, it was found that the temperature remained consistent throughout the hot zone. The K type thermocouple did read on average 20-30°C higher than the thermocouple inside the furnace. This could be attributed to the fact that the K type thermocouple was exposed to the air inside the crucible as opposed to the crucible surface itself. Due to the fact that the temperature remained consistent throughout the hot zone of the furnace, it can be assumed that gaseous compositional change did not occur due to uneven heating of the crucible.

Acknowledgements

I would like to thank everyone in the Montana State University High Temperature Materials Laboratory for providing the corrosion system to analyze and the Image and Chemical Analysis Laboratory for providing the surface analysis technology. This work was supported in part by the McNair Scholars Program (U.S. Dept. of Education grant #P217A130148).

References

[1] J. L. Aller, P. White, J. Gum, B. Clark, P. E. Gannon, "High Temperature Corrosion of AISI 316L in Chlorosilane Environments at 550°C", ECS Transactions, vol. 64, no. 26, pp. 161-171, 2015

[2] GT Advanced Technologies. *Polysilicon Manufacturing Plant for Solar Cells, Semi Conductors*. GT Advanced Technologies, 4 Aug. 2011. MP4.

Jacques-Louis David: Classical Forms and Iconography from Rome and Paris

Amanda Nichole Williams

Professor Todd Larkin, McNair Mentor November 22nd, 2014

Jacques-Louis David, perhaps the most notable painter of the late eighteenth and early nineteenth centuries, specialized in moralizing historical scenes and is thought to have perfected neoclassical painting. Early in his career he refused to believe that he could ever be swayed from his rococo aesthetic. However after visiting Rome even his steadfastness waivered and soon he looked back to classical Greece and Rome for subject matter as well as stylistic inspiration¹. It is extremely important to note that David specifically searched for classical references to include within his paintings, for neoclassicism was not his invention; he merely brought the movement to its peak and did so by utilizing authentic classical objects as a sort of archeological evidence. Indeed, David studied under one the preceding first generation neoclassical painters, Vien, although David did also deeply admire his distant relative, Boucher, and was thoroughly influenced by both of them². Although Vien was considered to work with the classical aesthetic, it was more of an interpretation of classical forms, rather than a replication and appropriation of the antique. This, in combination with David's admiration for the *Premier Peintre du Roi*³, Boucher, seems to account for his early works, which in comparison to what he would later paint seemed quite frilly. The soft pastels of Boucher and Vien would be largely abandoned for a seemingly more stark and monochromatic scheme. Where Vien and others had painted subjects after the classical fashion, David studied and utilized exact classical forms within his oeuvres in order to create a sense of authenticity.

¹ David Schnapper, *David*, (New York: Alpine Fine Arts Collection, 1982), 37. David is quoted "the antique isn't going to seduce me, it lacks life, it leaves you cold." This statement is quite ironic in consideration that David is to become the most notable of all neoclassical painters.

² Warren Roberts, *Jacques-Louis David: Revolutionary Artist,* (Chapel Hill: The University of North Carolina Press, 1989), 11. Although Boucher was a distant relative and David deeply admired his work in the rococo style for the monarchy, Boucher was not able to accept David as a student due to his growing age. Boucher recommended that David study under Vien, even though his style was considered to be a little "cold".

³ Michael Levey, Rococo to Revolution, (New York: Frederick A Praeger Publishers, 1966), 45.

David's Andromache Mourning Hector, created in 1783 (Fig. 1) and Paris and Helen, created 1788-1789 (Fig. 2), are two such paintings which reference antiquity with this archeological approach, although occasionally his original rococo aesthetic is utilized when necessary. Both paintings are depictions of ancient mythological scenes; each portrays the classical past differently, in terms of objects and setting, which evoke different emotional reactions in response to the atmosphere which is conveyed. To strengthen his classical ties, David borrowed from the sketches which he created while on his Prix de Rome⁴ for composition as well as specific details to more accurately portray the subject. These sketches of antique objects included architecture and sculpture which he was able to view during his three-year stay. When David's archive of sketches did not suffice in subject matter, detail, or mood, he had the entirety of the Louvre's collections to reference⁵, which included treasures from the antique world, especially those of Rome (considering the recent discovery of Pompeii), as well as other relatively more modern masterpieces which referenced these classical cultures in their forms. By using both resources David was able to create the authentic and somber atmosphere of ancient Rome for Andromache Mourning Hector, (although technically the myth is of Greek origin), while also being able to invent a romantic and idealized version of classical Greece for the painting Paris and Helen, in a somewhat similar fashion to how his predecessors would have- although he did indeed utilize some Roman objects for reference rather than Greek.

⁴ Simon Lee, *David*, (Paris: Phaidon Press Limited, 2002), 21-24. The French Academy, founded 1648, gave the *Prix de Rome* (tour of Rome), to the winning applicant. David was turned away from the Prix five years in a row, mainly due to the Academy's emphasis on the anatomy of the human body, which David struggled very much with. It was not until 1773 that David achieved the Prix de Rome. David returned from his tour of Rome with completely new artistic inspiration and aesthetics.

⁵ Warren Roberts, *Jacques-Louis David: Revolutionary Artist,* (Chapel Hill, The University of North Carolina Press, 1989), 15. After painting the *Belisarius* David received lodging within the Louvre itself, allowing him to envelope himself in the richness of art and architecture.

Andromache Mourning Hector, David's morceau de reception⁶, depicts Andromache as a dutiful wife crying out in agony over the loss of her late husband, whilst their son clings to her waist. The image in general seems quite dense to the viewer, with large bulky furniture and sturdy bodies, draped in volumes of fabric (Fig. 1). In contrast, the painting Paris and Helen portrays the graceful and sumptuous forms of Helen of Troy leaning towards her seated lover, Paris, in a moment of affection. This amorous mood appears to be reflected in the objects around the couple, creating a setting of decadence and romanticism from the culturally different items which David chose. The lovely and morally void painting was not received well by the public. By this time David had already presented multiple paintings which were sensationalized because of their severe neoclassical style. The public was eager for a political change as well as visual change, which called for meaningful art. The severity and symbolism of Roman civic duty and fraternity satisfied this need. In comparison to works such as Andromache Mourning Hector, and David's famed Oath of the Horatti, the frivolous Paris and Helen seemed to be symbolic of prodigal royalty, which had indeed commissioned the painting, specifically Louis XVI's brother⁷. The French populace had tolerated too much of the monarchy's nonsense and flagrant disregard for the well-being of its citizens. As a result, *Paris and Helen* ended up being largely ignored until much later when art historians began to analyze the scene for its erotic allusions as well as the archeological objects painted within it. The sheer amount of

⁶ Antoine Schnapper, *David*, (New York: Alpine Fine Arts Collection, 1980), 68. *Andromache Mourning Hector* was the painting which David submitted to the academy, and consequently earned his admission.

⁷ Anita Brookner, *Jacques-Louis David*, (New York: Harper & Row Publishers, 1980), 87. King Louis XVI's brother, the future Charles X, commissioned *Paris and Helen* on the eve of the French Revolution. While the monarchy was still in place, the decadent forms attributed to rococo where no longer attractive to the general public which was about to revolt. While *Paris and Helen* is not technically of the rococo genre, it possesses colors, sumptuous forms, as well as a subject which is referencing back towards the nobilities artistic sensibilities.

classical references within the painting makes it a supreme example of how David chose discerningly from an array of classical and neoclassical objects in order to create subtle aesthetic differences to match the mood of the scene which he was portraying.

In the case of Andromache Mourning Hector, the composition was largely based on ancient Roman friezes such as the Death of Meleager (Fig. 3) and the Tabula Iliaca (Fig. 4), both Roman scenes of death and grieving⁸. When comparing the *Death of Meleager* to David's Andromache Mourning Hector, it is immediately apparent that the compositions are strikingly similar. While there are a few differences between the two, such as the presence of attendants and Andromache turning away from her husband in grief, the likenesses are many. Hector has been placed upon a sofa; dense drapings cover him waist down. His helmet rests on the floor near the bed, a reminder that this man was a brave warrior. In each representation the wife is seated, visibly distressed. And in both there is the presence of a colonnade in the background firmly placing the event in a classical period. The compositional similarities are many; when one considers that Death of Meleager is housed in the Museé du Louvre, it is not a stretch to assume that this is an object which David might have easily seen and studied. If not this particular piece, it may have been one of the many others depicting a similar scene, such as the Iliad Sarcophagus, also housed at the Museé du Louvre (Fig. 5). The relief on the sarcophagus is much the same as the Death of Meleager, with the exception of the form of the wife. She, like Andromache in David's version, is seated towards her husband. Both women are depicted with an arm reached out in grief, with their hair falling loosely to their shoulders, unlike the

⁸ Steven Z. Levine, Sacrifice of the Hero: The Roman Years: A Classical Frieze by Jaques-Louis David by Seymour Howard, The Art Bulletin, Vol. 59, No. 3, (Sept. 1977), 444-447.

depiction of the wife in the *Death of Meleager*. Whether or not it is Andromache and Hector, the scene of a wife mourning her dead husband can be found as "type" throughout the art of classical Rome, so much so that David readily appropriated the "type" for his composition in order to emphasize the severity and seriousness of the scene. Original compositional sketches of David's can be found in which he plays with variations of these Roman friezes⁹, specifically those of the death of Meleager. It is clear that he is trying to reformat the sculptures into a way that could work for his paintings, although he does eventually edit out many of the details which were included in his sketches and the original Roman friezes, in favor for a stark and hollow feeling setting.

Borrowing compositions from the antique is not unique to Andromache Mourning

Hector; David employed classical originals for a base to work from for Paris and Helen as well. In
this case, it is also a "type"- that of a seated male figure which David used for the Paris figure.

This particular form can be traced back to Greek origins. A vase depicting Apollo (Fig. 6), from

Sir William Hamilton's collection of Greek vases¹⁰, seems to be a direct influence on David. Sir
William Hamilton made such vases readily available to the public in hopes that artists might
have better access to the antique for their artworks and revise their styles¹¹. These are items

⁹ Arlette Sérullaz, *Inventaire Général des Dessins École Française : Dessins de Jacques-Louis David 1748- 1825,* (Paris : Éditions de la Réunion des Musées Nationaux, 1991), 86-90.

¹⁰ Étienne Coche de la Ferté and Julien Guey, *Analyse Archéologique et Psychologique d'un Tableau de David :* <<*Les Amours de Parîs et d'Hélène>>,* Revue Archéologique, Sixième Série, T. 40 (Juilliet- Decembre 1952), 129-161.

¹¹ Viccy Coltman, *Sir Williams Hamilton's Vase Publications (1766-1766): A Case Study in the Reproduction and Dissemination of Antiquity,* Journal of Design History, Vol. 14, No.1 (2001), 1-16. Sir William Hamilton was a Scottish diplomat who had an extreme interest in archeology. He had quite an extensive collection of Greek, Etruscan and Roman antiques, however perhaps his most impressive set were his Greek vases. From this collection comes a vase which is one of the earlier depictions of the seated Paris "type", although it is believed that it is Apollo who is shown on the vase. Sir William Hamilton made his collections readily available to the public in hopes that artists might be able to use them to better access the antique for their works.

which David viewed; a drawing in an album proves that he viewed this particular antique from the Anthology of Etruscan, Greek, and Roman Antiquities in Mr. Hamilton's Collection. 12 In both David's and the Greek version, the male figure is depicted seated, semi-reclined, with one arm stabilizing his body, his head turned behind him, and he wears the Phrygian Cap, which symbolizes freedom. Another possible source, but clearly a descendent of the seated male "type", is a Bronze Coin (Fig. 7) depicting Marcus Aurelius, perhaps as Mars, struck in 145 AD13. Once again, this coin depicts a man reclined, nearly in the exact same position as in the Greek Vase from Sir William Hamilton's collection; however this time the "type" seems to have progressed and evolved a bit. A spear is now present in the hand of Marcus Aurelius, alluding to the divinity of the ruler by relating him to Mars. There is also a woman behind him, whom he is gazing at. Otherwise the composition is quite similar, the young man is still reclined, stabilizing himself with one arm, and he is still wearing the Phrygian Cap. This particular representation evokes a sense of love, a relationship, rather than simply a pleasant composition of a nude god, which is an important addition to the already reclined male form. This gives weight to the evidence that David chose these specific classical antiques because they presented a vulnerable and intimate position of the male form, which was initially depicted on the Greek vase. It is dynamic, draws interest, but also provides the tone for an amorous setting. It is apparent that the Greek version lends itself to a scene of lovers, and that the Roman coin seems to copy this intimate form for the same reasons that David was drawn to it.

¹² Antoine Schnapper, *David*, (New York: Alpine Fine Arts Collection, 1980), 89.

¹³ Étienne Coche de La Ferté and Julien Guey, *Analyse Archéologique et psychologique d'un Tableau de David :* <<*Les Amours de Pâris et d'Hélène>>,* Revue Archéologique, Sixième Série, T. 40 (Juilliet- Décembre 1952), 129-161. A Roman relief is also utilized in the argument, it has much the same composition of the coin, and is quite similar to the depiction of Apollo on the Greek Vase which is referenced earlier on.

Once David's composition was set, which clearly took a generous amount of thought and research, he needed to pick objects that would actualize the classical themes. While his decision to base the composition on antique objects provided the simplicity of a shallow middle ground and background as well as relief-like contrast in his figures, not every viewer would recognize that the composition is meant to be classical based solely upon this, especially without any other iconographical clues. This is where David enriches the scene with objects which personalize the scenes and identify them as classical in nature; this would include furniture as well as personal objects, such as armor, to the compositions. For example, the helmet which David includes in his finished product near the feet of Andromache clearly was influenced by the appearance of a helmet in both ancient reliefs Death of Meleager and the *Iliad Sarcophagus;* however the helmets which appear in those compositions are relatively simple and lack intricate details, which is problematic. Although David's critics called his work cold and stark, David did indeed pay much attention to the details in the objects which he deemed important enough to include; without this, the paintings could become too idealized and simplistic. It is evident that the aesthetic of the armor was important to him due to his studies of ancient helmets, based on various images he found while in Rome at the Trophies of Marius¹⁴. David more than likely recognized that it would have been vital for each element of the painting to be detailed and believably Roman, given the grand scale of the painting and that objects like the helmet would be closest to the viewer's eyes, receiving much scrutiny. At the

¹⁴Arlette Sérullaz, *Inventaire Général des Dessins École Française : Dessins de Jacques-Louis David 1748- 1825,* (*Paris :* Éditions de la Réunion des Musées Nationaux, 1991), 86-87. David's sketches were based off of images which he found at the fountain Trophies of Marius, which was built around 222 AD in the Villa of Emperor Alexander Severus

same time, David would not want the viewers paying too much attention to objects which were present for mere aesthetic and contextual purposes. For example, to add to the stark Roman atmosphere David incorporated a marble candelabrum, which seems to be slightly more simplified than the Roman antiques, such as the 4th century AD marble candelabrum base which is in the Louvre's possession¹⁵. While clearly the candelabrum is a part of Roman culture that is pulling away from its origins and is heading towards Christianity, David saw potential in sturdy form. David is further reappropriating objects from various cultures to fit into his work; he is painting a Greek scene through a Roman aesthetic, but in this case it suits him better to use an antique that is near the fall of the Roman empire, rather than the height when the myth of Andromache and Hector would have been most relevant. David is not looking for exact archeological representation; he is looking for archeological interpretation which is believable and effective in communicating the gravity of the scene- which the dense and bulky nature of early Christian Roman art is well suited for. But even the weighty nature of this object did not seem entirely effective to David, for he did not want too much detail distracting the eyes of the viewer from his actual subject, so he simplified or edited out much of the vegetal details on the candelabrum, and incorporated text instead.

No element was considered too small to deserve thorough consideration, including the leg of the chair which Andromache is seated upon. The chair leg seems to be strikingly similar in form to one which can be found in David's sketch books from Rome. ¹⁶ In this sketch David even

¹⁵ Cécile Giroire and Daniel Roger, *Roman Art from the Louvre*, (Manchester: Hudson Hills Press, 2007), 155.

¹⁶ Arlette Sérullaz, *Inventaire Général des Dessins École Française : Dessins de Jacques-Louis David 1748- 1825,* (Paris : Éditions de la Réunion des Musées Nationaux, 1991), 113. The study of the chair leg can be found on the same page as a study on the helmeted god Mars.

added the drapings of classical clothing of whoever might be occupying the seat. David also utilized sketches from his time spent in Rome for the couch upon which Hector's body is laid, although it is now unclear where David would have been able to find a furniture item such as this 17. While it is entirely possible that his direct source may be lost to our modern world, it is equally possible that this could have been David's way of gleaning stylistic information from many sources and fragments in a sort of cannibalization of the various parts to create his concept of what a whole would have looked like. For example, the couch which is within the Iliad Sarcophagus does indeed have similar qualities to the couch in David's sketches, especially in the forms of the legs and the head rest, but nothing is exact. Another source which David surely would have been aware of are the two lectisternia, which are dining couches featured in Johann Winckelmann's Letter and Report on the Discoveries at Herculaneum, which had been published in 1764 and became widely read 18. Without a doubt these dining couches would have been known to David, and surely he would have regarded them for reference, although the couches themselves are not as bulky as those in David's Roman albums. However it is apparent that the sketch of the couch is later utilized in his compositional sketches of *Andromache* Mourning Hector¹⁹ and when studying both the original sketch of the couch from his Roman albums, it becomes apparent that he used this sketch as a base for the couch within Paris and Helen as well. The soft curve at the head is especially reminiscent; however it is known that David commissioned ébéniste Jacob to construct a neoclassical version that would be more

¹⁷ Jacques Louis David, *Jacques-Louis David*, *1748-1825* (Paris: Eds. de la Réunion des musées nationaux, 1989), 81. ¹⁸ Johann Winckelmann, *Letter and Report on the Discoveries at Herculaneum*, (Los Angeles: Getty Publications, 2011), 190. Fig. 138.

¹⁹ Jacques Louis David, *Jacques-Louis David, 1748-1825* (Paris: Eds. de la Réunion des musées nationaux, 1989), 149.

fitting for the romantic needs of *Paris and Helen*²⁰. In comparison to the sketches, the couch in *Paris and Helen* is more delicate and thin than the bulkier versions which also appear in *Andromache Mourning Hector*, an entire section of the couch has been edited out, where there is sculptural relief depicting a heroic scene on the side. The revision of this element creates a delicate neoclassical sofa, rather than an immense Roman bed (reminiscent of a coffin), allowing for believable and romanticized classical details for the scene of the enamored couple.

It is important to note that David softened his choices aesthetically in nearly every way for *Paris and Helen*; where there was a hefty bed for a corpse, there now is a graceful sofa for the lovers. *Andromache Mourning Hector* is nearly monochromatic and stark in coloring, whereas Paris *and Helen* is rosy- It does not quite harken back to the pastels of rococo, but there is something reminiscent of the style preferred by the monarchy. Where Andromache is enveloped in volumes of thick fabric, Helen is sliding out of her shimmering clothing, which is portrayed in the Hellenistic style in order to emphasize her voluptuous form²¹. The entire painting is encrusted with classical references, but David chooses these references wisely; they might be smaller Roman objects, Greek forms, or even French interpretations of classical objects reinterpreted by David. The caryatids in the background of the painting present

²⁰ Yvonne Korshak, *Paris and Helen by Jacques Louis David: Choice and Judgement on the Eve of the French Revolution,* The Art Bulletin, Vol. 69, No. 1 (Mar., 1987), 109. David frequently commissioned works from *ébéniste* Jacob, perhaps one of the most talented artisans of the time. Much of this furniture was designed by David after Roman objects he had seen while abroad. David even had a set made specifically for his home, and was known to utilize these on occasion for his paintings, or would commission works according to his specifications as is the case with the sofa from *Paris and Helen*.

²¹ Warren Roberts, *Jacques-Louis David: Revolutionary Artist*, (Chapel Hill, The University of North Carolina Press, 1989), 44. It is during the Hellenistic period that the female form fully emerges in nudes, and is incredibly visible through clothing if the figure is wearing any. At times it appears that the figure has been doused in water in order to get the clothing to cling to the body and create an illusion of transparency.

themselves as a perfect example. There is absolutely no doubt that the origins of these caryatids are the *Salle des Caryatids*²² (Fig. 8) by Jean Goujon in 1550. There truly is no way that David could have lived in the Louvre, and not have been aware of this reinterpretation of the caryatids on the *Erechtheion (Fig. 9)* in Athens. The figures in Goujon's versions tend to be a bit more sinewy, with more emphasis on the sway of the female figure's hips. His also utilizes a different way of draping the clothing on the women, a method which involves a knot near the womb, which may suggest the fertility of the female form- which makes Goujon's figures more fitting for David's composition than the *Erechtheion's* caryatids.

Although David did modify elements such as the couch, or chose neoclassical representations such as the *Salle des Caryatids*, David did use Roman antiques also, but he did so with great discretion. What he did select tended to have characteristics that would blend well with the romanticized objects already in place; antiques from Rome which possessed graceful lines, and were not to grand of scale. Perhaps the object that is most notable to the viewer is the bronze tripod brazier in the background on the right side, which is an exact match for one of the numerous braziers found at Herculaneum²³ (Fig. 10). These braziers were perhaps some of the most popular items to be reinterpreted into neoclassical forms use within the home, and would come to their height of style underneath the Empire of Napoleon, but here, David has recognized the aesthetic qualities which popularized the braziers, and appropriated it for his painting before the trend had fully caught on. Once again, if not elsewhere, David surely would have been able to view some of these braziers in Johann

²² Étienne Coche de La Ferté and Julien Guey, *Analyse Archéologique et psychologique d'un Tableau de David :* <<*Les Amours de Pâris et d'Hélène>>,* Revue Archéologique, Sixième Série, T. 40 (Juilliet- Décembre 1952), 156.

²³ Walter Friedlaender, *David to Delacroix*, (Cambridge: Harvard University Press, 1952), 18.

Winckelmann's *Letter and Report on the Discoveries at Herculaneum*²⁴. It seems that perhaps the only liberty which David took in the representation of the ancient brazier is with its color. It seems to gleam a more golden hue than bronze, which seems to reflect upon the sumptuous nature of the scene more appropriately than the original material might have. Yet another archeologically exact antique employed by David is an item of furniture known as the *Curule Seat (Fig. 11)*, which Paris is seated upon. The seat, once again, can be easily found in Johann Winckelmann's *Letter and Report on the Discoveries of Herculaneum*²⁵, and would have been known to David without any doubt. The lines which the seat creates are sturdy, yet gently curved, much like Helen who was Spartan. Although the seat is of Roman origins, David adapts it to reflect upon the nature of the figures. He does adapt the seat somewhat by incorporating a cushion which is of the similar soft colorings which he utilized for the scene, perhaps with the intention of softening the robust nature of Roman furniture.

It is apparent that French neoclassicism of the 18th century was seen through a Romanist lens. David's and many other artists' treatment of Greek mythological scenes were largely serious in tone, which led them to utilize Roman forms a majority of the time. It is logical that aesthetically artists would have attached to Rome as an inspiration because of the recent discoveries of Herculaneum and Pompeii. The political situation also lends itself to Romanist ideals, the French public was growing increasingly restless with the monarchy's lack of morals and frivolity. The strong presence of the concepts of civic duty, fraternity, and moral obligations

²⁴ Johann Winckelmann, *Letter and Report on the Discoveries at Herculaneum*, (Los Angeles: Getty Publications, 2011), 105. Fig. 74.

²⁵ Johann Winckelmann, *Letter and Report on the Discoveries at Herculaneum,* (Los Angeles: Getty Publications, 2011), 115. Fig. 91. In the text the seat is represented by a sketch by Williams Clark, pen and ink.

in Roman culture and art became increasingly appealing for this reason; the forms of Roman art lend themselves to the serious nature of the moral society that it belonged to, and to the society which France was yearning for. David was able to communicate a true sense of seriousness and sorrow in his painting *Andromache Mourning Hector* with these Roman influences, and yet he also had the sensibility to select antique forms from other sources when Roman objects did not suit the mood for his painting *Paris and Helen*.

When taking inventory of all the antique and neoclassical objects present in *Paris and Helen,* it does seem slightly convoluted that David would find forms from Greece, Rome, and France in order to paint a Greek myth. However, when considering his the amorous atmosphere which he was striving to create, it is truly impressive to see how various works were appropriated and collaged together for his use. In order to execute the work effectively David was required to venture into a lengthy academic pursuit in order to find the correct forms, before ever actually painting.



Figure 1. Jacques-Louis David, *Andromache Mourning Hector*, 1783. Paris Musee du Louvre.



Figure 2. Jacques-Louis David, *Paris and Helen*, 1788-1789. Paris, Museé du Louvre.



Figure 3. Rome, *Death of Meleager*, 2nd Century CE. Paris, Musée du Louvre.



Figure 4. Rome, *Tabula Iliaca*, 1st Century CE. New York, The Metropolitan Museum of Art.



Figure 5. Rome, *Iliad Sarcophagus, 2nd Century CE. Ostia,* Museo Archeologico Ostiense.



Figure 6. Greece, Seated Apollo on Vase, Hamilton Collection



Figure 7. Rome, *Bronze Coin Marcus Aurelius*



Figure 8. Jean Goujon, Salle des Caryatids, 1550. Paris, Musée du Louvre.



Figure 9.Greece, *Erectheion Caryatids*, 421-405 BC. Athens, Acropolis.



Figure 10. Roman, Bronze Tripod Brazier, 1st Century BC. Museo archeologico Nazionale di Napoli.

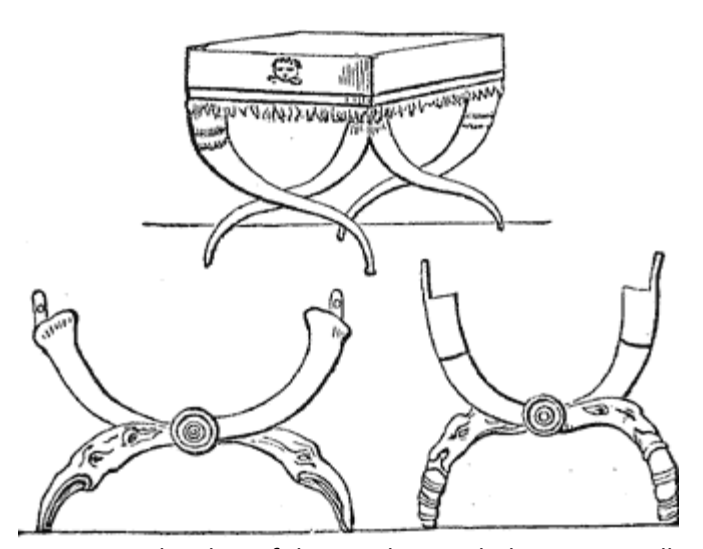


Figure 11. *Sketches of the Curule Seat,* belonging to sellae curules, preserved in Museo Borbonico, Naples.

Bibliography

Brookner, Anita. Jacques-Louis David, (New York: Harper & Row Publishers, 1980), 87

Coche de La Ferté, Étienne and Julien Guey. *Analyse Archéologique et psychologique d'un Tableau de David : <<Les Amours de Pâris et d'Hélène>>,* Revue Archéologique, Sixième Série, T. 40 (Juilliet- Décembre 1952), 129-161.

Coltman, Viccy. Sir Williams Hamilton's Vase Publications (1766-1766): A Case Study in the Reproduction and Dissemination of Antiquity, Journal of Design History, Vol. 14, No.1 (2001), 1-16.

David, Jacques-Louis. *Jacques-Louis David*, 1748-1825 (Paris: Eds. de la Réunion des musées nationaux, 1989), 81.

Friedlaender, Walter. David to Delacroix, (Cambridge: Harvard University Press, 1952), 18.

Giroire, Cécile and Daniel Roger. *Roman Art from the Louvre,* (Manchester: Hudson Hills Press, 2007), 155.

Korshak, Yvonne. Paris and Helen by Jacques Louis David: Choice and Judgement on the Eve of the French Revolution, The Art Bulletin, Vol. 69, No. 1 (Mar., 1987), 109

Lee, Simon . David, (Paris: Phaidon Press Limited, 2002), 21-24.

Levey, Michael. Rococo to Revolution, (New York: Frederick A Praeger Publishers, 1966), 45.

Levine, Steven Z. . Sacrifice of the Hero: The Roman Years: A Classical Frieze by Jaques-Louis David by Seymour Howard, The Art Bulletin, Vol. 59, No. 3, (Sept. 1977), 444-447.

Roberts, Warren. *Jacques-Louis David: Revolutionary Artist,* (Chapel Hill: The University of North Carolina Press, 1989), 11.

Schnapper, David. David, (New York: Alpine Fine Arts Collection, 1982), 37.

Sérullaz, Arlette. *Inventaire Général des Dessins École Française : Dessins de Jacques-Louis David 1748-1825, (Paris :* Éditions de la Réunion des Musées Nationaux, 1991), 86-90.

Winckelmann, Johann. *Letter and Report on the Discoveries at Herculaneum*, (Los Angeles: Getty Publications, 2011), 190. Fig. 138.